UNIVERSITÀ DI MILANO

FACOLTÀ DI MEDICINA E CHIRURGIA

DIPARTIMENTO DI SCIENZE E TECNOLOGIE BIOMEDICHE

CORSO DI DOTTORATO DI RICERCA IN

MEDICINA MOLECOLARE ciclo XXIII

Indirizzo: Medicina Molecolare delle Reazioni Immuni ed Infiammatorie

TESI DI DOTTORATO DI RICERCA

DENDRITIC CELLS IN A MURINE MODEL OF BREAST CANCER: FUNCTIONAL AND PHENOTYPIC EVALUATION USING NANOPARTICLES

Settore MED/04 – Patologia Generale

TESI DI:
Dott.ssa Manuela Borelli
Matricola R07683

TUTORE Chiar.mo Prof. Mario Clerici

CO-TUTORE Chiar.ma Prof.ssa Trabattoni

COORDINATORE: Chiar.ma Prof.ssa Maria Luisa Villa

ANNO ACCADEMICO 2009/2010

A mamy e papino, è anche grazie ai loro “per saperne di piu’”,
a Maurizio, per sempre!

INDEX

LIST OF ABBREVIATIONS

Ab: Antibody
Ag: Antigen
APCs: Antigen Presenting Cells
ASICs: Application Specific Integrated Circuits
BM-DC: Bone-Marrow-derived Dendritic Cell
BP-1 Binding Protein 1
BSA: Bovin Serum Albumin
$CD4^+$: Lymphocytes T CD4 positive
$CD8^+$: Lymphocytes T CD8 positive
CFDASE: CarboxyFluorescein Diacetate Succinimidyl Ester
CLRs: C-Type Lectin Receptors
CpG: Cytidine Phosphate-Guanosine
CT: Computerized Tomography
CTL: Cytotoxic T-Cell
DCs: Dendritic Cells
ENC: Equivalent Noise Charge
ER: Endoplasmic Reticulum
ERAAP: Aminopeptidase Associated with Antigen Processing in the Endoplasmic Reticulum
^{18}F -FDG: ^{18}F-FluoroDeoxyGlucose
FBS: Fetal Bovine Serum
FcR: Fc Receptors
FDA: Food and Drug Administration
fDCs: Follicular Dendritic Cells
FID: Free Induction Decay
FLASH: Gradient Echo Sequence
FL: Fluorescence
FLI: Fluorescence Imaging
FOV : Field of View
FSC: Forward Scatter Channel
GFP: Green Fluorescence Protein
GM-CSF: Granulocyte Macrophage – Colony Stimulating Factor
HEVs: High Endothelial Venules
[^{3}H]Thymidine: Tritiated Deoxythymide
hRas: MMTV-v-Ha-Ras
HSPs: Heat Shock Proteins
HSV: Herpes Simplex Virus
i.d.: intradermic
i.l.: intralymphatic
i.n: intranodal
i.v.: intravenous
iDC: immature DC
Ig: Immunoglobulin
^{111}In-oxine: ^{111}Indium-oxine
IFN: Interferon
IL: Interleukin
LFA-1: Lymphocyte Function-Associated Antigen 1
LN: Lymphnode
LPS: Lipopolysaccharide
mDC: mature DC
MFI: Mean Intensity Fluorescence
MHC: Major Histocompatibility Complex
MIN: Mammary Neoplasia
MMTV-v-Ha-Ras: Mammary Murine Tumour Virus – human Ras transgenic mice
MMR: Mannose Receptor
MNPs: Magnetic NanoParticles
MRI: Magnetic Resonance Imaging
MSME: Spin Echo Sequence
NLRs: Nucleotide Oligomerization Domain-Like Receptors
NMR: Nuclear Magnetic Resonance
NOD: Nucleotide Oligomerization Domain

PAMPs: Pathogen-Associated Molecular Patterns
PBS: Phosphate Buffer Saline
PET: Positron Emission Tomography
pDCs Plasmacytoid Dendritic Cells
PFA: Paraformaldehyde
PHA: Phytohaemagglutinin
PI: Propidium Iodide
PMA: Phorbol Myristate Acetate
PMT: Photomultiplier Tube
PRRs: Pathogen Recognition Receptors
QE: Quantum Efficiency
RF: Radiofrequency
RLRs: Retinoic Acid Inducible Gene-I-Like Receptors
s.c.: Subcutaneous
SDC: Syndecans
SDD: Silicon Drift Detector
SE: Spin-Echo
SEB: Staphilococcal Enterotoxin B
SPET: Single Photon Emission Tomography
SPECT: Single Photon Emission Computed Tomography
SPIO: SuperParamagnetic Iron Oxide
SRs: Scavenger Receptors
SSC: Side Scatter Channel
STAT3: Signal Transducer and Activator of Transcription-3
T: Tesla
T2: Time of Loss of Transversal Magnetization
TAA: Tumor-Associated Antigens
TAP: Transporter Associated with Antigen Processing
TCR: T-Cell Receptor
TEM: Transmission Electron Microscopy
TGF-β: Transforming Growth Factor-β
Th1: T helper type 1
Th2: T helper type 2
TLRs: Toll-Like Receptors
TNF-α: Tumor Necrosis Factor alpha
Treg: Regulatory T cell
TSA: Tumor-Specific Antigens
USPIO: Ultra small SuperParamagnetic Iron Oxide

Abstract

Dendritic cells play a pivotal role in antigen presentation and adaptive immune response activation. Studies on mice models reported that tumoral antigens-loaded DCs can induce therapeutic and protective anti-tumour immune response, both in vitro and in vivo. These results provide an evidence of the possible use of DCs as vaccines. However, the efficacy of such therapeutic vaccination was recently questioned due to the limited degree of actual tumour regression in some clinical trials. Thus, it is necessary to better characterize immunological and clinical parameters of DCs immunization to increase the therapeutic efficay of the vaccines. In vivo imaging tecniques, as magnetic resonance imaging (MRI) and single photon emission tomography (SPET), are used to study cell trafficking mechanisms in vivo and state anti-tumoral treatments efficacy, allowing an accurate assessment.

In this work we initially set the optimal culture conditions to obtain functional immature DCs. Evaluations based on DCs number, cell viability and immature DCs percentage led to establish day 6 as the one in which the highest number of functionally active immature DCs can be achieved. We then set a DCs labelling protocol with commercial SPIO (Endorem®) evaluating Iron content using Perl's staining and relassometry. Time and dose-response kinetic evaluations allowed to define as optimal labelling conditions the use of 200 µg Iron of Endorem®/ ml of culture for 16 hours. Cell viability and phenotypic markers analysis proved that SPIO labelling had no influence on immature DCs viability or activation status. Images acquired by transmission electron microscopy showed that Endorem® were inside cells, in particular inside lysosomes, and were taken up by endocytosis mechanisms. We then focused on DCs antigens loading. Tumoral antigens were obtained lysing neoplastic masses extracted from a mammary tumour mouse model (MMTV-Ha-Ras). DCs pulsed with different antigen concentrations resulted mature by means of high levels of activation and maturation markers. Moreover, such cells were able to stimulate T lymphocytes extracted from MMTV-Ha-Ras spleens. [3H]-thymidine and CFSE proliferation assays, together with IFN-γ production measured by ELISA, showed an increase in T lymphocytes activation when co-cultured with antigen-pulsed DCs. Cytokines production assessed by flow cytometry and ELISA allowed us to verify that tumoral antigen-pulsed DCs were able to elicit a specific T-lymphocyte response toward a Th1 type. Indeed, high amounts of IFN-γ were produced by T lymphocytes, high levels of IL-12 were produced by DCs and low levels of IL-10 were detectable. In vitro migration showed that tumoral antigen-pulsed DCs displayed migratory abilities toward MIP3β and 6Ckine chemockines, responsible in vivo of mature DCs attraction. Flow cytometric analysis confirmed that migrated cells displayed a mature phenotype and expressed high levels of CCR7.

We then performed in vivo experiments in MMTV-Ha-Ras mice bearing neoplastic lesions and in control mice without tumours. MRI showed that Endorem®-labelled DCs pulsed with tumour antigens are able to migrate to the draining lymph site in vivo. Histological analysis on ex vivo lymph nodes showed the presence of Iron-labelled cells in the cortical area. Immunohistochemistry reveals co-localization of Iron-containing cells with CD208-labelled DCs, but not with macrophages. In vivo SPET migration of antigen-pulsed DCs labelled with ^{111}In-oxine showed specific radiotracer presence in the lymph nodes omolateral to injection site; γ-counter analysis of ex-vivo organs confirmed such results.

Taken together, these results suggest that this protocol could candidate for experimental use on animal models for in vivo tumour immunotherapy efficacy imaging.

Sommario

Le cellule dendritiche (DC) svolgono un ruolo fondamentale nella presentazione degli antigeni e nell'attivazione della risposta immunitaria adattativa. Studi condotti su modelli murini hanno riportato che le DC caricate con antigeni tumorali possono indurre immunita' anti-tumorale terapeutica e protettiva in vitro ed in vivo: cio' fornisce una prova della possibile efficacia del loro utilizzo come vaccino. La validita' di tale vaccinazione terapeutica e' stata pero' recentemente messa in discussione a causa del limitato grado di effettiva regressione tumorale osservata in alcuni studi clinici. Risulta dunque necessario definire meglio i parametri immunologici e clinici dell'immunizzazione con DC per aumentarne l'efficacia. Tecniche di imaging in vivo come la risonanza magnetica (MRI) e la tomografia di emissione a singolo fotone (SPET), sono impiegate per studiare i meccanismi di trafficking cellulare in vivo e stabilire la validità dei trattamenti anti-tumorali, permettendone una valutazione accurata.

In questo lavoro abbiamo inizialmente settato le condizioni ottimali di coltura per ottenere DC immature (iDC) funzionali. La valutazione del numero di DC, della vitalità cellulare e della percentuale delle iDC ha permesso di stabilire il giorno 6 come quello in cui si ottiene il maggior numero di iDC funzionalmente attive. Successivamente abbiamo messo a punto il protocollo di marcatura delle iDC con SPIO commerciali (Endorem®) valutando l'incorporazione del ferro tramite colorazione di Perl ed analisi rilassometrica. La valutazione della cinetica tempo e dose-risposta ha permesso di definire come condizioni ottimali di marcatura con Endorem® l'incubazione con 200 µg Fe di Endorem®/ ml di coltura per 16 ore. La valutazione della vitalità cellulare e l'analisi dei marcatori fenotipici hanno inoltre dimostrato che la marcatura con SPIO non influenza in alcun modo la vitalità e lo stato di attivazione delle DC immature. Immagini ottenute con il microscopio elettronico a trasmissione hanno dimostrato che le Endorem® vengono incorporate dalle cellule tramite un processo endocitico e sono contenute all'interno dei lisosomi. Ci siamo occupati poi del caricamento delle DC con antigeni tumorali ottenuti mediante lisi della neoplasia estratta da modello murino di carcinoma mammario (MMTV-Ha-Ras). Le diverse concentrazioni antigeniche con cui le DC sono state caricate hanno tutte determinato la maturazione delle cellule in termini di aumento dei marcatori di attivazione e maturazione. Tali cellule sono risultate capaci di stimolare linfociti T separati da milza di topi MMTV-Ha-Ras. L'analisi dell'attivazione dei linfociti T mediante test di proliferazione con [3H]-timidina e CFSE, insieme alla valutazione della produzione di IFN-γ tramite saggio ELISA, ci ha permesso di individuare un aumento dell'attivazione dei linfociti in co-coltura con le DC caricate con antigeni tumorali. La produzione di citochine, valutata mediante citometria a flusso e test ELISA, ci ha permesso di verificare che le DC maturate con antigene tumorale sono in grado di stimolare una risposta linfocitaria specifica in senso Th1. E' stata infatti riscontrata un'elevata produzione di IFN-γ da parte dei linfociti T, alti livelli di IL-12 da parte delle DC e bassa produzione di IL-10. Il test di migrazione in vitro ha mostrato che le DC caricate con antigeni tumorali presentano capacità migratorie in risposta alle chemochine MIP3β e 6Ckine, responsabili in vivo della chemoattrazione delle DC mature. L'analisi citofluorimetrica delle cellule migrate ne ha confermato il fenotipo maturo ed un' alta espressione di CCR7. Abbiamo quindi condotto esperimenti in vivo su topi MMTV-Ha-Ras presentanti lesioni tumorali e su controlli privi di tumore. Gli esperimenti tramite risonanza magnetica hanno dimostarto che le DC differenziate e caricate con Endorem® ed antigeni tumorali sono in grado di migrare nella stazione linfonodale drenante il tumore. Le analisi istologiche dei linfonodi prelevati ex vivo hanno mostrato la presenza di cellule marcate con ferro nella zona corticale dei linfonodi e le analisi immunoistochimiche hanno evidenziato co-localizzazione del ferro con le cellule dendritiche marcate con CD208 e non con i macrofagi.

La migrazione in vivo tramite SPET delle DC differenziate e marcate con ^{111}In-oxina hanno mostrato la presenza specifica del tracciante nei linfonodi omolaterali al sito di iniezione e le analisi al γ-counter degli organi prelevati ex-vivo hanno confermato tali risultati.

Sulla base dei risultati fino ad ora ottenuti possiamo suggerire che questo protocollo potrebbe candidarsi all'applicazione su modelli sperimentali animali per la visualizzazione in vivo dell'efficacia dell'immunoterapia dei tumori.

Introduction

1. DENDRITIC CELLS

1.1 Overview on Dendritic Cells

Dendritic Cells are professional antigen-presenting cells (APC) present in trace numbers in virtually all organs [1]. “Professional” means that DC have unique abilities to induce a first efficient activation of naïve antigen specific T cells in the periphery [2], their proliferation and differentiation into antigen-specific T effector cells [3]. Dendritic Cells (DCs) arise from CD34+ progenitors in the bone marrow through yet non-fully characterized intermediates [4].Even in the absence of inflammatory processes, immature DCs or their precursors are constantly recruited from the blood into peripheral tissues [5], such as skin, mucosal surfaces and spleen, where they reside as immature DCs. Immature DCs have a high capacity to sense, sample, and process incoming antigens, but a poor ability to stimulate T cells [6]. The extraordinary ability of immature DCs to capture antigens is related not only to their high endocytic capacity, but also to the fact that they are strategically localized at anatomic sites with high antigenic exposure [7]. This steady-state dynamic is markedly modified during the course of an ongoing infection, when immature DCs and/or committed bone marrow precursors are quickly recruited from the blood into the damaged site, peaking about 2 hours after inflammatory challenge [8]. Notably, this recruitment of DCs is as fast as the one observed for neutrophils during the course of acute inflammatory reactions [9]. Stimuli responsible for the local recruitment of DCs include chemokines, complement cleavage products and bacterial peptides [10]. Upon maturation, DCs become capable to trigger adaptive immunity by inducing the activation of naïve T cells and directing the differentiation of newly activated T lymphocytes into effector T cells [11].

1.2 Not Simply One Family

The ability to induce a T cells response is strictly dependent on the type of DCs and their state of maturation [12]. DCs population comprises a large collection of subpopulations located in both lymphoid and non-lymphoid tissues, that can be distinguished by the expression of specific surface markers and by functional properties, perhaps reflecting a selective specialization in their response to antigens [13]. In steady state, DCs are found in lymphoid tissues and in a dense network at body surfaces like the skin, pharynx, upper oesophagus, vagina, ectocervix and anus, as well as at internal mucosal surfaces such as the respiratory and gastrointestinal systems [14]. Together they ensure immunity against invading pathogens and maintain tolerance against autologous structures. DCs also circulate in the blood, ready to migrate into tissues to enhance antimicrobial immunity.

Although DCs in mice and man differ in many aspects, a much better understanding of the DCs system is constantly growing as a whole when studying mice. In general, on the basis of functional properties, it is possible to differentiate between the “classical DCs” and the migratory DCs.

Migratory DCs act as sentinels in peripheral tissues and migrate to the lymph nodes (LNs) through the lymphatic vessels, bearing the antigens collected in the periphery [15]. A classical example of this type of DCs are Langerhans cells and interstitial DCs, which migrate from the skin to the LNs, where they exhibit a mature phenotype. Migratory DCs transfer antigen to a lymph node-resident DCs population and do not directly activate T cells [16]. In this assumption, migratory DCs act as transporters and in the draining LNs they do transfer antigens to the resident “classical” DCs for an effective presentation. The advantages of this antigen transfer may include potentially inhibiting spread signal, helps to enhance the number and lifespan of presenting DCs and prolongs the process of antigen presentation [17].

“Classical” DCs are lymphoid tissue-resident DCs that do not migrate into lymphoid organs from lymphatics and peripheral tissues, they rather collect and present antigens in the lymphoid organ itself. Lymphoid tissue-resident DCs have an immature phenotype and are active in antigen uptake [18].

On the basis of surface-receptor expression or according to their origin/ tissue of residence, DCs in mice can be divided in myeloid DCs ($CD11c^+CD11b^+CD8\alpha^-$), lymphoid DCs ($CD11c^+CD11b^-CD8\alpha^+$), and plasmacytoid DCs ($CD11c^+B220^+Gr\text{-}1^+$) [19]. Typical myeloid DCs are Langherans cells and dermal DCs [20]. The former are found in the epidermis, while the latter are found in the dermis. Both populations are able to capture and process antigens in the immature state and they show low levels of MHC and costimulatory molecules. After antigen uptake, upon arrival at the LNs, Langherans cells mobilize to the deep paracortex of the T-cell zone, while dermal DCs reside near B-cell follicles [21]. This distinct localization probably permits these different DCs populations to carry out non-overlapping roles in immune responses [19]. Murine lymphoid DCs are very diverse, with the thymus containing predominantly $CD8\alpha^+$ $DEC205^+$ $CD11b^-$ DCs, resembling DCs from other tissues but retaining their unique expression of binding protein 1 (BP-1) [22]. Because of their anatomical location, DCs in the spleen are involved with blood-born antigens. Their presence in the spleen is a result of migration of the precursors via a hematogenous route, as they develop into two major populations of immature DCs: $CD8\alpha^+$ and $CD8\alpha^-$ [23]. The population of DCs in the LNs is similar to that in the spleen, including $CD8\alpha^-$ and $CD8\alpha^+$ DCs. Unlike the spleen, most DCs enter LNs via afferent lymph. However, this idea needs revisions since there is mounting evidence demonstrating that $CD8\alpha^+$ DCs enter the LNs through the blood by crossing the high endothelial venules (HEVs) [19].

Plasmacytoid DCs (pDCs) are also known as type I interferons (IFNs)-producing cells with plasma cell morphology [24], as they secrete large quantities of IFNs after viral stimulation [25]. pDCs are generated in the bone marrow, then circulate and reside in the secondary lymphoid tissues [26]. Unlike myeloid DCs, pDCs migrate to the LNs through blood and HEV pathways [24]. pDCs are pre-DCs in the steady-state condition [23], thus, they express low levels of MHC class II and costimulatory molecules, and are incapable of stimulating antigen-specific T-cell proliferation. In addition, pDCs are poor at taking up exogenous microbes, suggesting that they are more specialized in presenting viral antigens and endogenous self-antigens [24]. pDCs can be distinguished from other DCs subsets by the expression of CD123 and blood dendritic cell antigen 2 (BDCA2). Moreover, pDCs selectively express Toll-like receptors (TLRs) 7 and 9, which enable them to sense single stranded RNA and DNA viruses, respectively [27,28]. Recently, it was demonstrated that the subset of CCR9 pDC is tolerogenic and is able to induce T cells with suppressive activity [29]. However, the exact functional features of pDCs in induction and regulation of T-cell immunity as well as defined differentiation states of pDCs are open questions of investigation.
Another type of DCs, follicular DCs (fDCs), resides in the follicle area. The cellular origin of fDCs and the conditions for their development are poorly understood. A precursor of fDCs has not yet been identified, but fDCs are not derived from bone marrow and are not related to bone-marrow-derived DCs. They are not migratory and reside in the germinal centers of lymphoid follicles in the spleen and LNs [30]. fDCs neither internalize nor present antigens in the context of MHC, but present intact antigen–antibody complexes via Fc receptors to B-lymphocytes.

1.3 Sampling the Environment

Immature DCs reside at sites of potential antigen entry in a physiologic stage that is specialized for antigen capture. In this state, they efficiently and continuously sample the antigenic content of their environment by high-volume fluid phase macropinocytosis [31], receptor-mediated endocytosis [32], phagocytosis of particulates [33] and direct contact with apoptotic or virally infected cells [34].
Macropinocytosis refers to the formation of large (1-3 μm) primary endocytic vesicles by the closure of lamellipodia generated at ruffling membrane domains. Immature DCs constitutively macropinocytose extracellular fluid [35], taking up a very large volume of extracellular fluid (40% of the cell volume every hour) in order to sample efficiently the antigens in the surrounding. Macropinocytosis appears to play an important role not only in the presentation of peptides from exogenous antigens by MHC class II molecules, but also in the cross-presentation of exogenous soluble antigens by MHC class I molecules [36]. Exposure of immature DCs to inflammatory cytokines such as TNF-α or microbial products such as LPS leads to an initial and transient stimulation of macropinocytosis, favouring antigen capture. This transient stimulation is followed by a dramatic inhibition of macropinocytosis, concomitant with the up-regulation of maturation markers such as CD80, CD86 and MHC class II molecules [37].
Receptor mediated endocytosis allows the uptake of macromolecules through specialized regions of the plasma membrane, termed coated pits. Like many other cell types, DCs recognize pathogens by conserved pathogen-associated molecular patterns (PAMPs). At least four families of pathogen recognition receptors (PRRs) exist: Toll-like receptors (TLR), cell surface C-type lectin receptors (CLRs), intracytoplasmatic nucleotide oligomerization domain (NOD)-like receptors (NLRs) and intracellular retinoic acid inducible gene-I-like receptors (RLRs) [38]. Depending on the contact site with the microorganism, the PRR is located on the cell surface or within cells. The recognition of PAMPs, inflammatory cytokines and/ or other stress signals may lead to the maturation of DCs [39]. Toll-like Receptors usually recognize molecular patterns leading to the activation of signalling cascades that result in the activation of DCs and the production of inflammatory cytokines [40]. TLRs detect a variety number of distinct bacterial products including peptidoglycan, LPS cytidine phosphate-guanosine (CpG) motifs, viral genomes, bacterial flagellin and double-stranded RNA. Studies in animals have demonstrated that the activation of TLRs stimulates the migration of antigen-activated DCs to T-lymphoid areas of the lymphoid tissue [41].
Receptors for viral RNA like the RLRs or for cytoplasmatic Gram-positive bacteria like the NLRs are found intracellularly. Interestingly, receptors for double- or single-stranded RNA (TLR3, TLR7/TLR8) or DNA (TLR9) are confined to endosomes. The endosomal location prevents unwanted activation of DCs by free RNA or DNA derived from necrotic cells yet allows for activation of DCs by ligands derived from phagocytosed microbial pathogens.
C-Type Lectin Receptors are responsible for the recognition of carbohydrate structures on pathogens and bind ligands in a Ca^{++}-dependent manner. Distinct subpopulations of DCs express different patterns of CLRs, that include macrophage mannose receptor (MMR, CD206) [38], DEC-205 (CD205) [42] and dendritic cell-specific ICAM3-grabbing nonintegrin (DC-SIGN, CD209) [43].
Moreover, mouse immature DCs express receptors for the Fc portion of Ig (FcR): FcγRI (CD64), FcγRII (CD32) and FcγRIII (CD16) [44]. Interestingly, the internalization of immune complexes by FcγR not only triggers the maturation of DCs but also efficiently targets the antigen to the cytosol promoting presentation by MHC class I molecules by cross-presentation [45].

Immature DCs express also receptors for activated components of complement such as CR3 (CD11b/CD18) and CR4 (CD11c/ CD18) [46] which play a role not only in the recognition of opsonized antigens and pathogens but also in the uptake of apoptotic cells [47].
Scavenger receptors (SRs) are cell surface glycoproteins defined by their potential to bind polyanionic ligands. As a result of their binding properties, SRs display a broad array of functions, including clearance of lipoproteins and uptake of pathogens. DCs express class-A scavenger receptors (SRA) [48], CD36 (class B-SR) [49], and LOX-1 [50] .
Phagocytosis and Macropinocytosis are involved in the efficient internalization of particulate and soluble antigens respectively. Both process are actin dependent, require membrane ruffling and result in the formation of large intracellular vacuoles. Phagocytosis is generally receptor mediated, whereas macropinocytosis is a cytoskeleton-dependent type of fluid phase endocytosis. Phagocytosis of opsonized microorganisms involves the participation of FcR and complement receptors, while unopsonized microorganisms are internalized by different receptors, such as the MMR [51], DCSIGN [45], CD36 [51] and the SR-PSOX/CXC chemokine ligand 16 [52].
Stress stimuli Studies of the mechanisms involved in the regulation of DCs activity are mostly restricted to the action of cytokines, chemokines and microbial products. However, other stress signals generated during the course of dangerous processes have also shown to stimulate the activation of DCs.
DCs are able to sense extracellular acidosis as a danger signal thus enhancing endocytosis, the acquisition of extracellular antigens for MHC class I-restricted presentation and the ability of antigen-pulsed DCs to prime CD8+ CTL responses [53]. Oxidative stress has also been shown to induce the activation and the production of cytokines by DCs [54], while fever-like temperature stimulated the maturation of DCs through the induction of Heat Shock Protein-90 (HSP-90) [55].
Together, these observation suggest the existence of multiple pathways by which the activation of DCs can be induced, supporting the view that this multiplicity of pathways enable immature DCs to efficiently sense a variety of danger signals at the onset of infection (Figure 1).

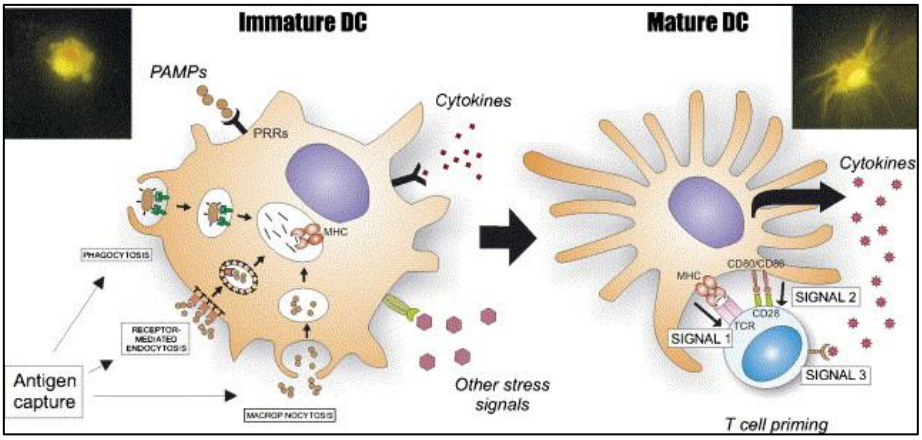

Figure 1. *Functional profile of immature and mature DCs. Immature DCs efficiently sample antigens from the surrounding environment by macropinocytosis, receptor-mediated endocytosis and phagocytosis. They also express a high diversity receptors which enable them to recognize PAMPs, cytokines, chemokines and other stress signals. Upon maturation, they become capable to activate T cells, promoting their differentiation into effector cells.*

1.4 Antigen Presentation

Unlike B-cells and macrophages, DCs can present complex protein fragments, carbohydrates, and lipid antigens [56]. Therefore, DCs represent one of the most unique APCs, able to process and present endogenous and exogenous antigens.
After internalization of exogenous antigens, the phagosomes or endocytic vesicles fuse with lysosomes, which contain an abundant number of hydrolytic enzymes, notably cathepsin, that function in breaking down the antigen into peptides. The cleaved peptides bind to MHC class II molecules by fusion of the endoplasmic reticulum (ER), where MHC class II are assembled and synthesized.
While the presentation of extracellular antigens is exclusive to DCs, presentation of endogenous protein antigens is possible for all nucleate cells. Viruses, intracellular microbes, and cytoplasmic proteins are tagged with ubiquitin in the cytoplasm and processed through the proteasome, where the protein is cleaved into peptides. The newly cleaved peptides are then transported into the endoplasmic reticulum via a heterodimer of the transporter associated with antigen processing (TAP1 and TAP2), located in the ER. TAP translocates peptides of 6–15 aminoacids with hydrophobic or basic C-termini into the ER lumen. Since the binding groove of MHC-I can accommodate short peptides from 8–9 aminoacids, peptides processed by TAP are further tailored to shorter fragments by the aminopeptidase associated with antigen processing in

the ER (ERAAP). The selective peptide sequence is then transported to the ER for binding to MHC class I molecules. The peptide-presenting MHC class I molecules are transported to the cell surface, and MHC-I/ peptide complexes on the cell surface are monitored by $CD8^+$ T-cells for foreign or mutated peptides.
Cross presentation is a third presentation mechanism to maintain cell growth, development and homeostasis. Exogenous antigens in the endosome/ lysosome compartment can gain access to the cytoplasm through an unknown mechanism and be processed through the MHC class I pathway, eventually leading to the activation of antigen-specific $CD8^+$ T-cells [57]. CD1 molecules that are quite similar to MHC class I are specialized to present lipid antigens [58].

1.5 Maturation

The concept of DC maturation, first proposed by Steinman and co-workers 20 years ago [59], refers to a complex differentiation pathway mainly triggered by pathogens and inflammatory cytokines, whereby DCs become capable to trigger the activation of T cells. *In vitro* studies have shown that a variety of inflammatory stimuli are able to trigger the activation of DCs. These signals direct all changes in phenotype, morphology and migratory behavior of DCs, leading to a rapid production of inflammatory cytokines such as type I IFNs, IL-1, IL-6 and TNF-α [9]. At this stage, DCs down-regulate their antigen-uptake machinery, which restricts the specificity of T-cell stimulation to those antigens encountered in peripheral tissues [9]; they increase and stabilize the expression of MHC-peptide complexes on the cell surface to achieve 10/ 100 times the density found on monocytes or B cells [9]. Moreover, DCs up-regulate the expression of CD40, the integrin lymphocyte function-associated antigen 1 (LFA-1) and the co-stimulatory molecules CD80 and CD86 [9]; they go through the *de novo* synthesis and secretion of a number of cytokines and chemokines [9] and migrate to T-cell areas in lymphoid tissues (Figure 2).

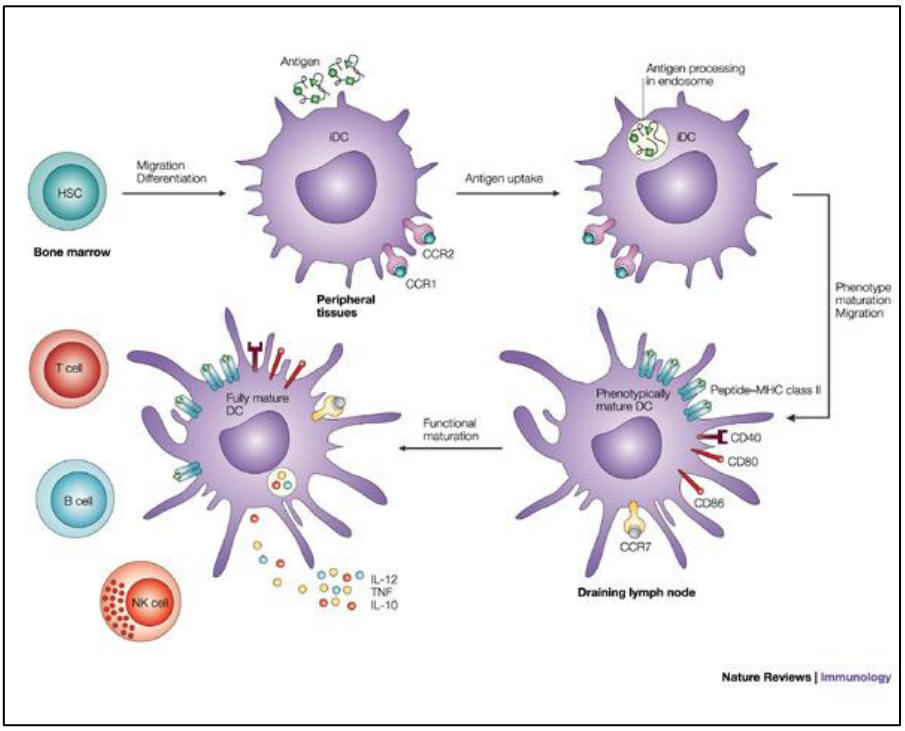

Figure 2. *After antigen capture, DCs migrate to the draining lymphoid tissue and mature phenotypically, up-regulating the expression of CD40, CD80, CD86, MHC class II molecules and CCR7. In the draining lymphoid tissue, they present antigens on the cell surface in association with MHC class I or II molecules to lymphocytes and produce pro-inflammatory cytokines.*

To emigrate from the periphery towards the draining lymph nodes, DCs rapidly change their repertoire of chemokine receptor and adhesion molecules and the expression of many other migration-related proteins, such as matrix metalloproteases and cytoskeletal proteins.
Chemokines receptors The dominant mediator in the mobilization of DCs to lymph nodes via lymphatics is CCR7 [60]. Constitutive expression of its ligands CCL19 (ELC, MIP-3β) and CCL21 (SLC, 6-Ckine) is found at the luminal site of high HEVs and in the T-cell-rich areas of secondary lymphoid tissues, such as tonsil, spleen and lymph nodes [61]. 6-Ckine is also expressed on lymphatic vessels in the peripheral tissues and its expression is increased during inflammation [62]. The expression of CCR7 is essential for both the entry of DCs into lymphatic vessels at peripheral sites and the entry into T-cell-rich areas of lymphoid tissues in steady-state or under inflammatory conditions [63]. The expression of CCR7, however, appears to be not

sufficient for DCs migration: inflammatory mediators such as PgE2 and the ADPribosyl cyclase CD38 are required to sensitize CCR7 to MIP-3β and 6-Ckine [64].
Besides CCR7 several other chemokine receptors play a role in DC homing from the periphery to draining lymph nodes, as CCR5 [65], CCR8 [66] and CCXCR3 [67], but appear less important. Parallel to up-regulation of CCR7, in mature DCs there is a down-regulation of CCR1, CCR5 and CCR6, whose ligands are RANTES, MIP1α and MIP1β that are expressed in the peripheric tissues [68].
Adhesion molecules Adhesion molecules play a pivotal role in successive steps of migration. Therefore, their expression profile is tightly controlled. A switch in adhesion molecule expression profile is required to allow detachment of resident DCs from existing interactions and to enable migration through the lymphatic system and into the lymph nodes. Thus, so far no extensive analysis of the molecules implicated in trans-endothelial migration of DCs into the lymphatic system has been carried out [69], but a variety of adhesion molecules seems to be involved in the emigration of DCs through extracellular matrix. Integrins [70], intercellular adhesion molecule 1 (ICAM-1) and leukocyte function-associated molecule 1 (LFA-1) [71] are found to play a significant role in DCs migration. Also non-integrins are regulated during DCs migration and maturation. In mice CD44 is described as an adhesion molecule that binds to hyaluronic acid that is expressed on the leading edge of migrating cells [72]. Another example of adhesion molecules regulated during DCs migration are the syndecans (SDC), a family of transmembrane proteoglycans, which have been implicated in the migration of LC in human skin explants [73].

1.6 T Cell Programming

Maturation determines the functional diversity of DCs, which on one hand enables the induction of efficient immune responses against pathogens of all kinds and on the other hand induces tolerance to self-antigens and aid the resolution of inflammation by giving a negative feedback to effector cells [74].
In order to generate an efficient immune response, three signals are needed: 1) antigen presentation, 2) co-stimulatory molecules presence, 3) production of polarizing cytokines.
In the T-cell areas of lymph nodes, to recognize antigens T cells need to establish contact with DCs by forming an immunological synapse, with the cross-linking of T-cell receptor (TCR) triggered by the appropriate peptide-MHC complex presented on DCs (Signal 1). Co-stimulation (Signal 2) is mainly induced through CD28 as a consequence of its interaction with the co-stimulatory molecules CD80 and CD86 expressed by DCs. A serial TCR triggering by peptide-MHC complexes initiates a signalling cascade, the magnitude and duration of which determines the entry of naïve T cells into the cell cycle [75]. The amount of the signal that T cells receive is dependent on the level of peptide-MHC complexes that initiate signal transduction, on the level of co-stimulatory molecules that amplify the signalling process and on the stability of the synapse that determines for how long the signalling process is sustained [76].
In absence of costimulation, naïve T cells can be activated only by extremely high, non-physiologic doses of antigens and required a prolonged stimulation. In contrast, in presence of co-stimulatory molecules, they can respond to almost 100 fold lower doses of antigen and also more rapidly.
Once committed to the first division, T cells proliferate rapidly in response to IL-2, which is produced by activated T cells and can act in autocrine and paracrine fashions [75]. There is a growing evidence that the duration of TCR stimulation together with polarizing cytokines, determines the progressive differentiation of CD4+ and CD8+ T cells leading to the generation of terminally differentiated effector cells as well as intermediates [77].
DCs can differently orient the T cell responses, from thymic negative selection to the generation of effector and memory cells as well as to the induction of peripheral tolerance. The plasticity of DCs functions is regulated by cytokines (Signal 3) that can either promote immunity (Figure 3) or favor the induction of tolerance.

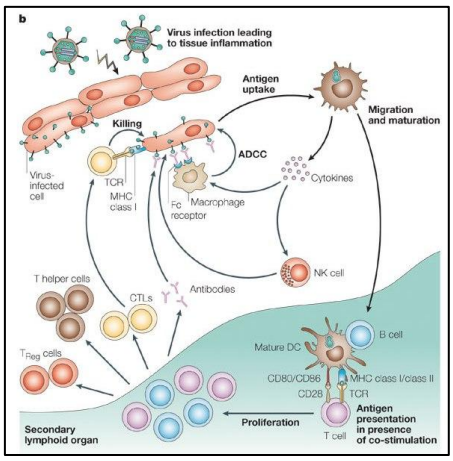

Figure 3. *Mature DCs induce immunity, leading to antigen-specific lymphocytes proliferation*

By producing IL-12, IL-18 and IFN-α, mature DCs promote the differentiation of TCD4+ lymphocytes into Th1 cells, producing IFN-γ, as well as the differentiation of T CD8+ lymphocytes into cytotoxic cells [78]. Alternatively, by selectively expressing members of the Jagged family of Notch ligands, DCs seem to promote the differentiation of T CD4+ lymphocytes into Th2 cells, producing IL-4, IL-5 and IL-13, cytokines which are silenced in the Th1 lineage [79]. Th1 cells are crucial for cellular immunity against intracellular pathogens while Th2 cells are essential in humoral immunity and in defence against nematode parasitic infections [78, 79] (Figure 4).
Th17 cells represent a third type of T-effector cell population that preferentially produces IL-17, IL-21 and IL-22 [80]. Th17 cells are important for the clearance of certain pathogens such as *Candida* or Gram-negative bacteria [81] and they play a role in the pathogenesis of autoimmune diseases [82]. The exact requirements for efficient programming of Th17 by DCs are still incompletely understood.

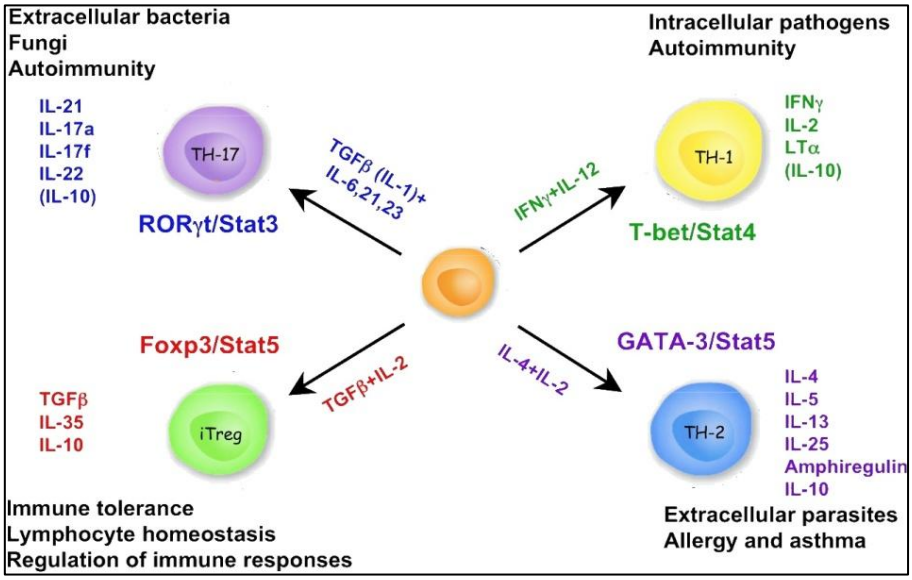

Figure 4. *T-Cell Subsets on the basis of their different cytokine products.*

DCs can induce and maintain both central and peripheral immune tolerance [83]. Central tolerance depends on mature thymic DCs, which are essential for the deletion of newly generated T cells with a TCR that recognizes self-components [84]. Many self-antigens might not have access to the thymus and others are only expressed later in life, so there is a requirement for peripheral tolerance, which occurs in lymphoid organs and is mediated by immature DCs. In the absence of inflammatory signals, resident tissue specific DCs remain in an immature or resting state, characterized by low expression of co-stimulatory molecules and cytokines [85] leading to peripheral tolerance. Tolerance induction by immature DCs includes several mechanisms: silencing of differentiated antigen-specific T cells, T-cell anergy or deletion [83], transfer of regulatory properties to effector T cells [86], activation and expansion of naturally occurring regulatory T cells (Tregs) [87], and the differentiation of naïve CD4+ T cells into regulatory T cells [88] (Figure 5). The most robust method for detection of Treg cells is on the basis of CD25 and FoxP3 expression. Tregs silence peripheral autoreactive T lymphocytes through the activities of TGF-β [89], IL-10 [90], CTLA-4 [91], or through accumulation of IL-2 via expression of CD25 [92].

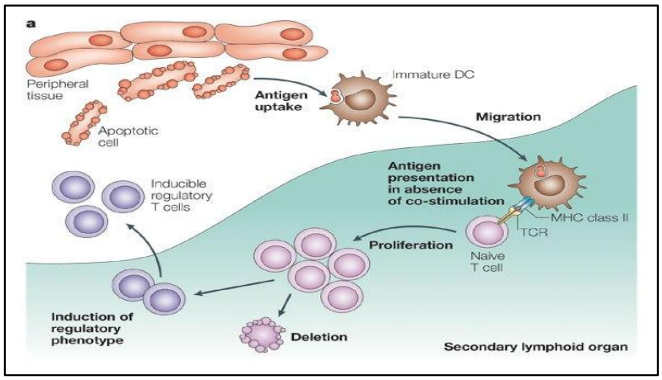

Figura 5: *Immature DCs induce tolerance. In absence of inflammation, immature DCs present antigens without co-stimulation, leading to deletion of reactive T cells or the generation of Treg cells.*

2.TUMOURS

2.1 A Step into History

The concept of tumor recognition and elimination by the immune system was first advanced by Ehrlich in 1909 [93] and later formalized by Burnet [94] and Thomas [95] as the theory of immune surveillance. Since then, a large body of evidence has indicated the existence of both humoral and cell-mediated tumor-specific immune responses in cancer patients, both systemic and at the tumor site [96,97].
According to the immune surveillance hypothesis, tumor cells can be recognized and eliminated by the immune system before the manifestation of clinical symptoms [103]. Thus, it is reasonable to speculate that cancer vaccines might be useful throughout the spectrum of cancer development. Recent sophisticated studies in murine models provided support for this hypothesis, revealing the critical roles of IFN-γ and lymphoid populations in cancer immunosurveillance [98]. However, IFN-γ and lymphoid cells were also shown to alter the tumour itself by decreasing immunogenicity and facilitating growth in immunocompetent animals. In an effort to incorporate the tumour-modulating effects of the immune system into the original immunosurveillance hypothesis, Schreiber and colleagues introduced the concept of cancer immunoediting, which encompasses the processes of elimination, equilibrium, and escape [99]. During the elimination phase, which corresponds to immunosurveillance, innate lymphoid cells recognize and eliminate accumulated transformed cells. This protective response exerts a selective pressure on genetically unstable transformed cells, allowing them to evolve and persist in a dynamic equilibrium with the immune response. The equilibrium phase may last for many years until transformed cells acquire the ability to evade and escape the immune response and manifest as clinically evident disease. A growing body of evidence suggests that genomic instability provides tumors with the ability to produce immunomodulatory factors that can inhibit immunosurveillance (Figure 6).

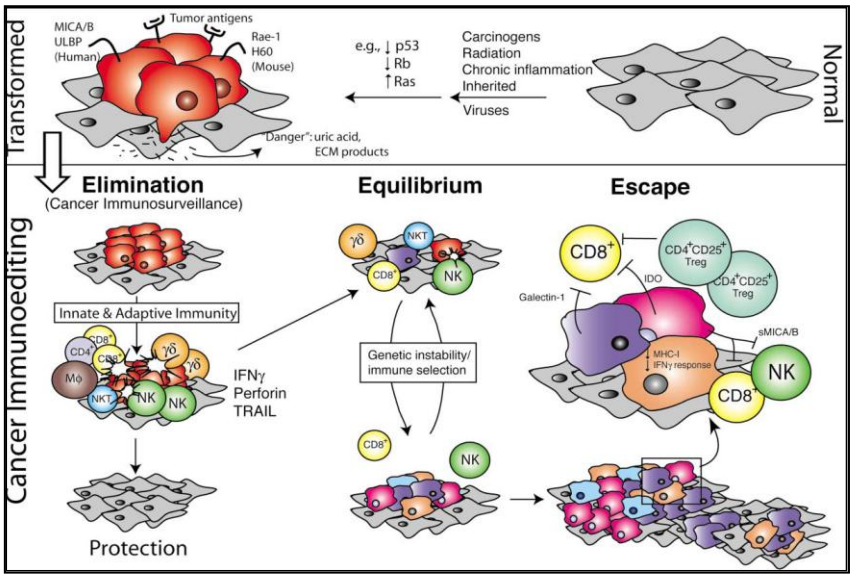

Figure 6: *Immunoediting process*

Over the last two decades, important progress has been made in tumour biology, especially to understand the immune response elicited by tumour cells. The role of immunity in the rejection of tumours had already been suggested a long time ago based on the observation of spontaneous tumour regression following infectious episodes [100]. Such events are very rare in humans and most tumours have been shown in mice to be weakly or not immunogenic [101]. These regressions are considered as the result of a naturally occurring anti-tumour immune responses [102]. The observation of higher cancer incidence in chronically immunosuppressed, organ-transplanted patients [103], the possibility to mediate tumour regression in patients by reinfusing *in vitro* stimulated T lymphocytes isolated from melanoma patients [104], and the existence of a graft-versus-leukaemia effect of allogeneic bone marrow transplantation [105] further supports that immune effector cells can kill cancer cells. Based on these elements, the search for molecular determinants of this anti-tumour immune response began. In 1982, Van Pel and Boon provided the first evidence of the existence of tumour antigens by showing that chemically or ultraviolet-induced mouse fibrosarcomas could induce strong immune responses able to protect against a subsequent tumour challenge, and by the identification of specific T lymphocytes in the spleen of these mice [106] . However, in most instances this natural anti-tumour immune response is unable to reject the tumour.

The recent progress in immunology has revealed the crucial role of dendritic cells in the generation of a protective immune response against both infectious diseases and tumours [107], due to the unique ability of these cells to prime naïve T and B cells and, thus, to link innate and adaptive immunity [1].

2.2 Tumour Features

Tumors develop as a result of a complex deregulation of proto-oncogenes, tumour suppressor and genome stability genes, leading to uncontrolled cell cycle progression and immunosubversion [108]. However, accumulating evidence indicates that the immune system could keep in check a minimal residual disease [109] or contribute to the therapeutic success of compounds that induce cell death [110].
The first identification of a tumour antigen was made using a method called mixed lymphocyte/ tumour culture, combined with DNA cloning and transfection. Tumour specific cytotoxic T-cell clones were derived from blood lymphocytes or tumour-infiltrating lymphocytes of melanoma patients, were cultured *in vitro* with autologous irradiated tumour cells and then used to identify tumour antigens thanks to recognition of gene transfectants by the CTLs [111]. This method, together with biochemical purification of MHC class I binding peptides [112], reverse immunology [113] and serological analysis of cDNA expression libraries (SEREX) [114], led to the identification of several types of tumour antigens recognized by T lymphocytes: tumour-specific shared antigens (TSA), antigens encoded by mutated genes, differentiation antigens, over-expressed or ubiquitously expressed proteins (all together named Tumour-Associated Antigens; TAA) and viral antigens.
Classic TSA are often generated by mutated proteins and are expressed only by tumour cells. The term 'shared' comes from the observation that these antigens are expressed in a variety of tumour types [115]. As a consequence of genomic instability in tumour cells, each new mutant gene product represents a putative tumor-specific antigen that may be recognized by the immune system.
TAA are often aberrantly expressed endogenous proteins that are otherwise normal (ERBB2/HER2/neu).
Several mutated genes in the "genomic landscape" of cancer contribute to the transformed phenotype of tumour cells, reinforcing their potential desirability as therapeutic targets, whereas other such genes have less apparent roles in tumorigenesis [116]. Epigenetic instability can unveil antigens that were previously inactive, as the oncofetal antigens, or minimally expressed in normal tissues, as melanoma antigen (MAGE) [117]. Gene products with differential over-expression (HER2) or post-translational modifications (MUC1) may compose abundant TAA that, although genotypically wild-type, can invoke an immune response [118].
Expression of the genes that encode for tumour-specific antigens has been observed in the testis, placenta and in the fetal ovary [119], but in germline cells that do not express MHC class I molecules and thus with no antigen presentation capabilities [120]. Examples of such antigens are found in the MAGE gene families for which several epitopes recognized by T cells have been identified [121].
Tumour antigens encoded by mutated genes or as consequence of chromosomal translocations are neo antigens, totally specific for a single or very few different tumours. As such, they should not lead to side effects, but their high specificity, being often linked to one individual, prevents them from building a broad approach for immunotherapy. Example of mutated tumour antigens are CDK4 [122] and Caspase-8 [123].
Differentiation antigens derive from proteins specific to the cell lineage from which the cancer is derived [114]. Examples of differentiation antigens are gp100, tyrosinase and Melan-A [124,125] in melanocytic lineage, but also the prostate-specific antigen (PSA) in the prostate, and the carcino-embryonic antigen (CEA) in the gut. Targeting such antigens may lead to side effects in the normal tissue, such as vitiligo when the target is expressed in skin and is thus only acceptable when this affects non-essential organs.
The best-known example of an over-expressed tumour antigen is Her2 [126]. Although such over-expressed antigens could be a target for immunotherapy, their low levels of expression in normal tissue could endanger such development.

2.3 Tumour Escape

Malignant tumour cells develop mechanisms to escape elimination by immune responses and possess mechanisms to tolerize the immune system, leading to tumor establishment.
Tumour cells that escape elimination can persist in equilibrium with the immune system until the balance between the immune response and the tumour tilts towards tumour growth due to the outgrowth of poorly immunogenic tumour cells (immunoediting) and suppression of the immune system [127]. Tumour escape is believed to be a multifactorial process [128]. Down-modulation of T cell activity and CTL tumour cell lysis can depend on secretion by tumoral cells of immunosuppressive factors, such as TGF-β and IL-10.
TGF-β is has profound immunosuppressive activity, including inhibition of DCs maturation and T-cell proliferation and activation, and also promotes the accumulation of Treg cells [89].
IL-10 can activate signal transducer and activator of transcription-3 (STAT3), resulting in the accumulation of immature DCs and Tregs in the tumor microenvironment [129]. STAT3 is constitutively expressed by many solid tumours and results in the further inhibiting antitumour immunity [129]. Tumour escape also may be facilitated by the selection of tumour escape variants, characterized by loss of expression of TAA and down-regulation of MHC/ co-stimulatory molecules.

3. IMMUNOTHERAPY

Cancer immunotherapy aims at re-activating the immune system to destroy tumour cells [130] and to induce specific and long lasting immunity to protect against recurrent disease [1]. Immunotherapy represents a valuable approach, complementary to standard therapies for the treatment of cancer, based on its specificity and limited associated toxicity [131].

In spite of the significant progress achieved in understanding the basic immunologic mechanisms responsible for the antitumour efficacy of immunotherapy in animal models, there has been a poor translation into the clinical setting and currently no vaccination regimen is indicated as a standard anticancer therapy [132]. In fact, although the immune response in patients can play a significant role in controlling tumour growth, as suggested by the correlation between clinical outcome and tumour infiltration by T cells [133], tumour cells tend to evade the immune system.

Over the last decade many studies have led to the design of novel strategies capable of breaking tumour-induced tolerance, thus improving the immunological and clinical response to cancer immunotherapy. These approaches, which included depletion of Tregs [134] and blockade of the negative signaling receptor CTLA4 [135], have shown considerable toxicity in terms of autoimmune or autoinflammatory side effects. The decisive role of dendritic cells in inducing immunity and tolerance has boosted both fundamental and translational research to understand and exploit their unique immune-modulatory capacity for cancer [136,137]. DC vaccines are safe, feasible, with minimal side effects and effective in some patients, particularly if the DCs have been appropriately matured and activated [138,139].

Although immunological responses are observed in most studies, clinical responses are limited to a minority of patients [140,141].Several of the early studies published were inadequate in their design and interpretation, as immature rather than mature DCs were used [149]. This may have affected the immunological and clinical outcome of the vaccine protocols. In fact, comparative studies with immature or mature DCs have shown that only mature DCs stimulate T-cell responses [142] and enhance homing to draining lymph nodes, the sites where therapeutic T-cell responses must be initiated [143].

Opportunities for improvement the clinical outcome lie in a number of variables, such as DCs subsets and culture methods used for the generation of DCs, antigen loading, route of administration, dose and frequency of DCs administrations [139]. In pilot clinical trials in which non-Hodgkin's lymphoma [144] and melanoma patients [145] received DCs vaccinations, induction of specific humoral and cellular-immune responses and tumour regression have been documented. The most advanced DC-based immunotherapy nowadays is being developed by Dendreon and uses autologous DCs, expanded *ex vivo* and then pulsed with a prostatic acid phosphatase fusion protein. This therapy is called Provenge® (Dendreon Corp.). Two different Phase III trials were initiated to evaluate Provenge® versus placebo in 127 and 98 patients with asymptomatic, metastatic androgen-independent prostate cancer [146]. Although both trials failed to meet their primary end point, an integrated analysis combining the data of both trials suggests a statistically significant increase in overall survival with 23.2 months in the Provenge® group versus 18.9 months in the placebo group [147].

Of note, the majority of studies investigates the therapeutic effects of DCs vaccines in late-stage cancer patients with metastasis. The stage of the disease affect the efficacy of any cancer vaccine. Cancer vaccination strategies used after the appearance of malignant lesions generally have been unsuccessful in inducing tumour regression and improving survival [148]. A possible explanation for this failure is the prominent tumour-derived immunosuppression observed in patients with advanced disease. Indeed, even best immune response might ultimately succumb to an overwhelming tumour. These considerations warrant the testing of cancer vaccines in the adjuvant setting, where relapse-free and overall survival are the key determinants of efficacy [149]. In this perspective, research should primarily focus on cancer vaccination strategies to prevent disease. Whether or not a vaccine can mount an effective antitumour response ultimately depends on the functionality of the immune response in the developing microenvironment of the tumour.

3.1 Preparation of Dendritic Cells

Clinical trials of DC vaccination have been made possible by the development of methods for obtaining large numbers of human DCs. DCs comprise less than 1% of mononuclear cells in the peripheral blood [150]. In human two general approaches have been exploited: (*a*) the purification of immature DCs precursors from peripheral blood and (*b*) the *in vitro* differentiation of DCs from peripheral blood monocytes or CD34+ hematopoietic progenitor cells.

The former approach represents the most direct method of DCs isolation and the first to be utilized in clinical studies of DCs vaccination. Circulating immature DC precursors can be isolated from T-cell- and monocyte-depleted peripheral blood cells and cultured in the absence of cytokines. DC precursors undergo maturation and acquire a low buoyant density, which allows their purification by density-gradient centrifugation [151]. DCs isolated this way possess potent allostimulatory activity and the ability to prime naïve $CD4^+$ T helper cells [152] and CD8+ CTLs [153] to exogenous antigen *in vitro*. Yields of 5×10^6 DCs are typically obtained from the PBMC products of a single leukapheresis procedure.

Large numbers of DCs can also be generated by *in vitro* culture of monocytes or CD34+ progenitor by treating cells with granulocyte macrophage-colony stimulating factor (GMCSF) plus interleukin-4 (IL-4) [154], or with IL-13. After a variable number of days, the culture results in the generation of cells possessing the characteristics of DCs, including stellate morphology, high-level expression of MHC, adhesion and co-stimulatory molecules, loss of CD14, and powerful T cell stimulatory capacity [155].
DC precursors may be enriched from peripheral blood mononuclear cells by techniques such as plastic adherence, density gradient centrifugation, positive selection of CD14+ cells, negative selection of B and T cells, and/ or elutriation.
DC with potent antigen-presenting capacity may also be generated from CD34+ precursors [156], that can be collected from umbilical cord blood through positive selection using CD34 monoclonal antibodies and goat anti-mouse IgG-coated microbeads.
In the mouse system it is inconvenient to isolate DCs subpopulations or precursors directly from peripheral blood or tissues due to the small sample size. Therefore, DCs are mostly generated from bone marrow precursors. Bone marrow contains various stem cells that can be used *in vitro* to generate B cells, polymorphonuclear neutrophiles, macrophages and DC by using different cytokines and growth factors. As in the human situation, GM-CSF and IL-4 are essential for the generation of DCs from bone marrow precursors. The standard protocol for generating large quantities of highly pure dendritic cells from whole bone marrow precursors has been described by Lutz et al. in 1999 [157].

3.2 Antigen Delivery

There are a number of techniques currently available to prime DCs with tumour antigens, either undefined (with the use of whole tumour cells, tumour cell lysates of tumour antigen-enriched fractions) or well characterised (tumour-specific antigens aiming at eliciting a specific T-cell response).
Whole tumour Methods that take advantage of the complete protein content of the tumour cell, thereby broadening the induced immune response and avoiding tumour escape, have been developed. Anticancer immunotherapies based on autologous tumour cells have the advantage of targeting multiple antigens and presenting the antigens in a patient-specific manner, in the context of patient-matched MHC [158]. However, this kind of approach suffers from its technical feasibility issues, with a requirement for the patient's tumour to be resectable and for the *in vitro* culture of the cells before administration to the patient.
Tumour Cell Lysate represent the whole protein content of lysed tumour cells. The advantage of using tumour lysate lies in the fact that the multiple antigens that can sensitize T-cells may be heterogeneously expressed on growing tumours, especially those that do not have molecularly defined TAA [159]. Cellular stress induced by lisation processes can elicit a number of adaptive mechanisms, including the expression of heat shock protein (HSPs), which can be released from dead cells after primary or secondary necrosis [160].There are numbers of mechanisms through which HSPs can enhance immunogenicity. On the one hand they may improve the recognition and uptake of dying cells by DCs when they are present on the cell surface; on the other hand, tumour-derived antigenic peptides may bind to HSPs and may be recycled for antigenic presentation in a particularly efficient fashion [161].
Tumour Specific Antigens, Peptide/Protein approach The protocol most commonly used for loading antigens onto DCs is pulsing with synthetic peptides. Synthetic peptides are easy and cheap to manufacture, do not require immunological processing and allow ready control of the dose and route of administration [162]. However, there are several weaknesses in the use of peptide for cancer immunotherapy. First, the need for identification of TAA epitopes, low affinity binding of self-derived peptides and lack of $CD4^+$ T-cell help, since only a limited number of CD4 epitopes are known [163]. Moreover, when injected alone, peptides are likely to have a very short *in vivo* half-life in the circulation and usually do not induce measurable immune responses [164]. In addition, as peptides are restricted to a particular HLA molecule, the immune response they can elicit is limited to a particular T-cell repertoire and the target patient population is narrowed to the patients expressing the adequate HLA molecules. Furthermore, tumour cells also present shared self antigens, which could give rise to unwanted autoimmune responses [165].
Purified whole TAA proteins have also been used for loading DCs [166]. This method has the advantage of being independent of the knowledge of the MHC haplotype of each patient and of prior identification of defined TAA-derived peptide epitopes.
Tumour Specific Antigens, Genetic approach Advantages of gene-based delivery of TAA into DCs are the ease of cloning genetic constructs and the possibility to include sequences for improving antigen presentation in both MHC class I and class II. DNA and mRNA can be delivered as naked strands, but transfection efficiencies are enhanced by lipid-mediated transfection or electroporation. Transfection of DCs with DNA has not met with great success and important concerns can be raised regarding safety, because DNA can integrate into the host genome [167]. mRNA delivery to DCs proved to be more effective and safe and is surrounded by significantly less safety issues, because mRNA is only transiently expressed in the cells and does not integrate into the genome.
Another strategy to stimulate the immune response against a tumour consists of a genetic modification of the autologous tumour cells to secrete GM-CSF. The dendritic cell recruitment and activation properties of GM-

CSF are envisioned to enhance the immune response at the injection site, a step considered to be critical for an optimal response to any immunotherapy product [168].

3.3 Vaccine Administration

One important aspect of cell-based immunotherapy is the accurate delivery of the vaccine. DCs must closely encounter and interact with T cells to exert their action and lead to a positive clinical outcome. Therefore, DCs must reach the secondary lymphoid tissues and enter the T-cell-rich areas. It has now been generally accepted that the site at which T cell priming occurs significantly influences the homing characteristics of the effector cells. For the delivery of DCs three different options can be distinguished: intradermal (i.d.) or subcutaneous s.c in peripheral tissue, such as skin and mucosa; intralymphatic (i.l.) or intranodal (i.n.) into the lymphatic system; and intra venous (i.v.) administration.
Vaccine delivery and distribution after injection has been studied injecting DCs radiolabeled with ^{111}Indium or ^{99}Technetium. The distribution after injection was imaged and quantified by scintigraphic imaging. In mice, after i.v. injections, DCs reached the liver and spleen after a short accumulation in the lungs, and in some studies very low amounts of DCs were detected in mesenteric and mediastinal nodes [169]. This is consistent with the finding that myeloid DCs in the peripheral blood do not enter lymph nodes via the HEVs but first migrate to peripheral tissues and subsequently to draining LNs via the afferent lymphatics [170]. To target peripheral lymph nodes, DCs can be injected into the skin or directly into the skin-draining lymphatics or LN. In mice, s.c. injection is effective in both targeting DCs to draining LN and inducing immune responses [171]. In human, no [172] or little [173] migration of DCs to skin-draining lymph nodes was found after s.c. injection of DC. Intradermal injection is more effective although the number of DCs that reach the regional LNs do not exceed 4% [174]. Alternatively, DCs can also be injected directly into lymph nodes or lymphatic vessels draining the skin, as a result of which all cells will be targeted to the draining lymph nodes [175].

3.4 Combining DCs and other therapies

Studies in the late 1970s and early 1980s showed that in animal models cytostatic drugs, as cyclophosphamide, facilitate adoptive immunotherapy for tumours as they can eliminate Tregs [176]. Recent data that show improved outcomes of vaccination with DCs in myeloablated animals [177] reinforce this concept and indicate that controlled 'immune ablation' might improve the clinical efficacy of DCs vaccines administered to patients with cancer. As well as the elimination of Treg cells, the mechanism might also involve the elimination of pre-existing memory T cells, which might not be of the most effective phenotype.
It has become increasingly evident that adjuvants generally act through the induction of cytokines, which are the key mediators of the immune response. This fact has raised the question of whether the direct use of certain selected cytokines as natural adjuvants could be of some advantage with respect to the conventional adjuvants. Studies in mice show that pre-injection of TNF-α at the site of vaccination with DCs greatly improves the migration of DCs to the draining lymphoid tissue and the magnitude of the resultant immune response. Concomitant administration of other cytokines, for example IFN-α, could improve the efficacy of the DC vaccine [178] and possibly protecting it from tumour-derived inhibitory factors.
The delivery of recombinant IFN-α or IL-2 after vaccination with DCs could protect the elicited T cells from the immunosuppressive tumour environment, thereby improving vaccination efficacy [179].
In general, this cytokine-conditioned milieu promotes the recruitment and activation of DCs and macrophages and induction of Th1 responses within a few days of treatment and leads to apoptosis of cancer cells and their substitution by a mononuclear cell infiltrate within 2 weeks [180].

3.5 MMTV-v-Ha-ras Model

Mouse mammary tumor virus (MMTV) mouse models are informative models for human breast cancer despite morphological, hormonal and lifestyle differences between mice and humans. MMTV is an onco-RNA-virus of the *Retroviridae* family, which causes breast tumors once activated [181]. Efficient replication of MMTV occurs predominantly in the alveolar epithelial cells of the mammary gland. During lactation, MMTV expression markedly increases under the influence of steroid hormones. Activating mutations in the *Ras* oncogenes are found in approximately 30% of human malignancies [182]. Mutant H-*Ras* occur in varying frequencies in different tumour types, for reasons that are not completely understood. MMTV-*Ras* mice have been created by placing an activated v-Ha-*Ras* under the control of the MMTVLTR [183]. Approximately 20% of MMTV-v-Ha-*Ras* transgenic mice develop bilateral exophthalmos that is the result of progressive enlargement of the Harderian glands. Malignant tumours arise stochastically among transgenic mice between 6 and 12 months and histological examination consistently reveals the presence of mammary adenocarcinomas. Both male and female MMTV-*Ras* transgenics develop mammary and salivary gland tumours [183]. Human breast cancer models using MMTV-LTR mice have often been created in the FVB strain due to its high productiveness of pups.

4. IMAGING IN CELLULAR IMMUNOTHERAPY

4.1 In vivo Imaging

In vivo imaging is an essential component of basic and clinical cancer research. Molecular and cellular imaging can be defined as the noninvasive repetitive imaging in living organisms of targeted macromolecules and cells, and of biological and cellular processes respectively [184]. The technology behind molecular and cellular imaging embraces two areas: one related to the detection technology and the other related to the contrast agents, tracers and reporter probes. Several techniques for studies in human subjects, including computerized tomography (CT), magnetic resonance imaging (MRI), positron emission tomography (PET), single photon emission tomography (SPET) and ultrasound (US) imaging, have been redesigned for studies in small animals, whereas other techniques initially used for *in vitro* assays, including nuclear magnetic resonance (NMR), bioluminescence (BL) and fluorescence (FL) methods, have been refined for *in vivo* studies [185]. All these technologies differ for spatial and temporal resolution, penetration depth, energy used to generate the image, need or availability of contrast agents, threshold of detection and type of anatomical or functional information provided. Thus, each methodology should be used with different efficiency in relation to the application chosen.

4.2 Imaging DCs in vivo

While it is increasingly recognized that DC-based therapy benefits a number of cancer patients in clinical trials [145, 146], detailed information regarding cellular migration, fate and how DCs interact with other cells in the secondary lymphoid tissue of the host remain a subject of intensive study. Tracking DCs migration by imaging techniques is a compelling approach for future clinical settings. Recently, the emergence of imaging techniques has made possible the first-ever visualization of cell uptake and migration, and how DCs interact with T lymphocytes in the context of presentation in animal models. The dynamic transformation of DCs during the maturation–migration process combined with their distinct interactions with other immune cells and the surrounding environment constitutes a unique phenomenon in DC-based therapy. To fully understand the complex nature of these processes on the basis of their dynamic and tissue-specific characteristics, there is the need to visualize each individual interaction in real time beyond static 'snapshots' of the histological slides. New imaging technologies have just begun to explore these issues. There are two major approaches for imaging DCs *in vivo*: one is to image DC migration in lymph nodes to study the mechanisms and kinetics of T-cell priming by DCs, and the other involves global tracking of the distribution of antigen-activated DCs for cell therapy. At present, the migration of DCs and their interactions with T-lymphocytes in the lymph node microenvironment in animal models are being studied using two-photon microscopy [186]. Meanwhile, global tracking studies seek to advance the application from animal model to human using nuclear and magnetic resonance (MR) imaging. Besides having an advantage with regard to cost, space and time, optical imaging methods used non-ionizing low-energy radiation, have high sensitivity, and allow continuous data acquisition in real time in an intact environment. Nuclear and MR imaging are sensitive and, with the high resolution of the former, they are capable of tracking the migration of DCs in humans in a non-invasive manner. Moreover, the development of new classes of targeted contrast agents already approved for clinical use [187] can easily be used for DCs labelling because of their high phagocytic aptitude [188]. Currently, imaging has not reached the mainstream of clinical DC-based therapy. Some pioneering studies are in progress. Most of these studies focus on imaging preclinical mouse models or mouse models that mimic human diseases so that hypotheses concerning human diseases can be developed and tested. With the availability of robust techniques, imaging of mouse models can be performed in parallel with clinical trials as a supporting modality. For instance, imaging a mouse model helps to optimize the route of DCs distribution, test the selectivity of tumour antigens and determine the kinetics of DCs interactions with other cell types in the lymph nodes.

4.3 Nuclear Imaging

Positron emission tomography (PET) and single photon emission tomography (SPET) are functional radionuclide imaging techniques that differ substantially in the type of radionuclide employed to label the tracer and in the method of data acquisition [189].

Early scintigraphic imaging the biodistribution patterns of DCs in syngeneic and allogeneic mice was demonstrated using gamma-emitting ^{111}In-labelled splenic DCs [190]. At various time intervals after cell transfer, organs were removed for direct measurement of radioactivity in a gamma counter. These data showed that DCs injected intravenously migrate to non-lymphoid and lymphoid tissue, and that the later is regulated partially by T lymphocytes. In contrast, DCs injected in the s.c. footpad migrate to sentinel lymph nodes and are trapped there without migration to the next one. Tracking DCs using ^{111}Indium isotopes has been promptly applied in several clinical trials [191], due to its long half-life compared with other isotopes that allows serial imaging for up to several day. Regardless of the tremendous popularity of gamma scintigraphy in clinical studies, its lack of spatial resolution and anatomical features prompted the development of a hybrid

imaging platform. This approach combines tomographic gamma imaging and CT, thus offering greater improvement of gamma radionuclei imaging [192], such as demonstrated recently in the application of using SPECT/CT for imaging DC migration [193].
Similar to SPECT, the resolution of PET is not advancing at the same pace as that of two-photon microscopy or MR. Its sensitivity is the driving force behind tracking the migration of adaptively transferred DCs *in vivo*. One of the advantages of PET imaging is that the technique allows for quantitative determination of the biodistribution of the probe *in vivo*. With this technique, the migration of bone marrow-derived DCs labelled with *N*-succinimidyl 4-[F-18]-fluorobenzoate (FSB) was tracked from the footpad to the draining popliteal lymph node over the course of nearly 4 hours [194]. As mentioned above, the intrinsic disadvantage of PET imaging lies in its lack of spatial resolution and anatomical correlation. However, the advent of the multimodal approach, which uses PET sensitivity and the superior anatomical features of Computed Tomography (CT), provides superior visualization capabilities unmatched by a single imaging technique.

4.4 Magnetic Resonance Imaging

Imaging the migration of DCs using MRI gives the highest spatial resolution among the non-invasive modalities, with exquisite dynamic information and anatomical contrast. Furthermore, the technique is safe and clinically translatable. A contrast agent is necessary to provide cellular-scale resolution. Currently T2-weighted Iron oxide nanoparticles represent the most sensitive agent used in both animal and human applications. In general, any particle larger than 50 nm is termed a superparamagnetic Iron oxide nanoparticle (SPIO), while particles smaller than 50 nm are called ultra small superparamagnetic Iron oxide (USPIO). Currently, SPIO is the only T2 contrast agent approved by the FDA for MRI and there are several reasons for its popularity. First, the particles are usually non-toxic to cells. In particular, there is no observed adverse effects of SPIO-labelled DCs and the particle is biodegradable *in vivo*. Second, it is a negative contrast probe, so it provides clear contrast to the background of soft tissue such as lymph nodes, which usually has a bright background. Third, the particles can remain inside terminally differentiated DCs throughout their lifetime, thus allowing long-term studies. Fourth, the particles are taken up inside DCs in confined vesicles, which in principle leads to a larger local magnetic field, resulting in higher contrast in MR images than when the contrast agent is distributed throughout the cell volume [195]. Finally, due to its sensitive signal, SPIO-based imaging requires small concentrations, which makes SPIO more suitable for labelling human cells than other contrast agents. To enable MR imaging of DCs migration, the cells are isolated and pulsed with SPIO with or without delivery-assisted reagents. The advantage of this procedure lies in the fact that uptake can be manipulated to enhance access of the particles to the cells. In contrast, *in vivo* labelling of immune cells with SPIO is very demanding since most of the time the uptake of Iron particles by immune cells is not easily achieved in order to provide good images. Quantitative studies have demonstrated that DCs take up about 10 pg of Iron per cell, while with the presence of transfecting reagents, this can become as high as 35 pg Iron/ cell [196].
In a dynamic MRI using SPIO-labelled DCs [197] it was shown that adaptively transferred cells could migrate from the injection site into T-cell areas of the lymph node 24-48 hours post-injection. Furthermore, the migration was dependent on up-regulation of the chemokine receptor CCR7 on the labelled cells. A clinical study laboratory using human DCs showed that immature DCs take up the particles spontaneously over a reasonable incubation time [188]. Interestingly, this work revealed that unsuccessful DCs therapy may not be due to the cell vaccine. Instead, MRIshowed that intranodal injection in clinical tests often failed to distribute the cells into the lymph nodes even with ultrasound guidance. Together with other clinical and preclinical studies [198], this work demonstrated that the imaging of DCs migration through MRI gives the highest spatial resolution among non-invasive modalities, with exquisite dynamic information and anatomical contrast [17].

Aim

Much attention has currently focused on the use of dendritic cells as cellular adjuvants in immune-cell therapy against tumours. DCs are professional antigen-presenting cells playing key roles as immune sentinels and initiators of T-cell responses. Several clinical and pre-clinical studies exploiting DCs features had already been performed, but their efficacy has recently been questioned because of the limited rates of objective tumour regression or recovery observed in some clinical trials. Thus, considerable challenges remain for improving the efficacy of therapeutic immunizations against cancer. Imaging techniques can provide means to dynamically follow in time and space the migration, homing, survival and differentiation of labelled cell populations and therefore help immunization efficacy.
The wide aim of this study is to set a strategy to investigate the biodistribution of dendritic cells in a murine model of breast cancer using *in vivo* imaging tecniques.
With this intention, we focused on:

- the development of an efficient isolation protocol and setting of optimal culture conditions in order to differentiate dendritic cells from bone marrow progenitors with high efficiency and desiderable features. The best maturation strategy for tumour-antigen pulsing was then established, taking into account the ability of pulsed DCs to trigger a T cell response.
- the identification of the optimal DCs labelling procedures with commercial superparamagnetic nanoparticles, considering viability, morphology, cell features and functions.
- cell functionality, migratory ability and DCs role in inducing a specific T-cell response.
- *in vivo* DCs imaging by MRI and SPET. Migration of properly labelled cells was monitored from the injection site to the lymph nodes in a mammary tumour mouse model (MMTV-v-Ha-Ras).
- Immunohistochemistry and histological analysis to confirm specific DCs migration to the draining lymph nodes.

Materials and Methods

1. *Dendritic Cells Isolation*

Femurs and tibias of 5-8 weeks old female wild type FVB mice (Charles River Laboratories, Calco, Italy) were removed and purified from the surrounding muscle tissue. Intact bones were then left in pure Ethanol (Merck, Darmstadt, Germany) for 2–5 min for disinfection and washed with sterile PBS (Phosphate Buffer Saline, PBI international, Milan, Italy). Then both ends were cut with scissors and bone marrows flushed with pure ISCOVE (Euroclone, Siziano, Pavia) using a Syringe with a $26^1/_2$ diameter needle (Sigma-Aldrich, St. Louis, MO, USA). Clusters within the marrow suspension were disintegrated by vigorous pipetting. After one wash in ISCOVE (Euroclone), cells were counted using an automated cell counter. About $30*10^6$ cells were obtained per mouse. Cells were then seeded in a 6-wells plate (CELLSTAR, Greiner Bio-one, Northbrook, Illinois) at $1,5*10^6$ cells/ml in 5ml complete medium per well. Complete culture medium was as follows: ISCOVE (Euroclone) supplemented with 10% FBS (Fetal Bovine Serum, PBI International), 100 U/ ml Penicillin, 100 U/ml Streptomycin, 2 mM L-Glutamine (Biological Industries, Israel) and 25 ng/ ml Amphotericin (Sigma Aldrich). A specific cytokine cocktail containing 3000 U/ ml rmGM-CSF (Granulocyte Macrophage – Colony Stimulating Factor; R&D System, Minneapolis, MN) to support DCs differentiation and survival, and 900 U/ ml rmIL-4 (Interleukin 4, R&D Systems), to inhibit macrophage formation, were added to the culture medium. Cell cultures were performed for 6 days at 37°C with 5% CO_2. On day 3 cells were gently resuspended and splitted 1:2 ratio in fresh complete medium supplemented with GM-CSF and IL-4 (R&D Systems).

2. Cell Count

Cell count was performed with the automated cell counter ADAM-MC (Digital Bio, NanoEnTek Inc, Corea). Adam system provides two kinds of staining solutions: AccuStain Solution T for total cell counting, composed of Propidium Iodide (PI) and lysis solution, and AccuStain Solution N for non-viable cell counting, composed of PI and PBS. Cells were treated with AccuStain Solution T that disrupted the plasma membranes and allows nuclei staining with PI to measure the total concentration of cells. In AccuStain Solution N, live cells remained intact and were not stained. Only the non-viable cells were stained and detected. After treatment, the prepared cells were loaded into a chip and inserted into ADAM for cells counting. A 532nm green laser was automatically focused onto the chip and cells that had been stained were recorded by a sensitive CCD camera. The image results were automatically processed generating the cell count which was displayed on the front of the instrument.

3. DC Immunophenotyping

Flow cytometric analysis was performed staining $0,5*10^6$ cells for 15 minutes with fluorescent directly labelled surface antibodies: CD11c PECy7, CD11c PECy5, MHCII PECy5, CD86 PE, CCR7 PE, CD80 FITC and CD83 FITC (eBioscience, San Diego, CA, USA). Cells stained with the appropriate isotype-matched Ig were used as negative controls. After staining, cells were then fixed in 1% Paraformaldehyde (PFA, Sigma-Aldrich). Cytometric analysis was performed on 20,000 events, using a FC500 cytometer (Beckman Coulter, Hialeah, FL, USA) equipped with a double 15-mW argon ion laser operating at 456 and 488 interfaced with Intercorp computer. Flow data were analyzed by means of forward and side scatters and then on CD11c positive cells. Green fluorescence from FITC (FL1) was collected through a 525-nm band pass filter, red fluorescence from Phycoerythrin (FL2) was collected through a 575 nm band pass filter, deep-red fluorescence from PECy5 (FL4) was collected through a 670-nm band pass filter and far-red fluorescence from PECy7 (FL5) was collected through a 770-nm band pass filter, using linear amplifiers for forward and side scatter and logarithmic amplifiers for FL1, FL2, FL4 and FL5.

3.1 Principles of Flow Cytometry

Flow cytometry is a powerful technique for the analysis of multiple parameters of individual cells within heterogeneous populations. Cytometers are used in a range of applications from immunophenotyping, to ploidy analysis, to cell counting and GFP expression analysis. The instrument performs this analysis by passing thousands of cells per second through a laser beam and capturing the light that emerges from each cell as it passes through. Flow cytometry uses the principles of light scattering , light excitation, and emission of fluorochrome molecules to generate specific multi-parameter data from particles and cells in the size range of 0.5 μm to 40 μm diameter. The data gathered can be analyzed statistically by a software to report cellular characteristics such as size, complexity, phenotype, and health.
The primary systems of the flow cytometer are:

- the fluidic system, which presents samples to the interrogation point and takes away the waste;
- the lasers, which are the light source for scatter and fluorescence;
- the optics, which gather and direct the light;

- the detectors, which receive the light;
- the electronics and the peripheral computer system, which convert the signals from the detectors into digital data and perform the necessary analyses.

The interrogation point is the heart of the system. This is where the laser and the sample intersect and the optics collect the resulting scatter and fluorescence.

The Fluidic System

When a sample in solution is injected into a flow cytometer, the particles are randomly distributed in three-dimensional space. For accurate data collection, it is important that particles or cells are passed through the laser beam one at a time. This process is managed by the fluidics system by injecting the sample stream containing the cells into a flowing stream of sheath fluid or saline solution. Essentially, the fluidics system consists of a central channel/ core through which the sample is injected, enclosed by an outer sheath that contains faster flowing fluid. As the sheath fluid moves, it creates a massive drag effect on the narrowing central chamber. This alters the velocity of the central fluid whose flow front becomes parabolic with greatest velocity at its centre and zero velocity at the wall. The effect creates a single line of particles and is called hydrodynamic focusing. Under optimal conditions (laminar flow) the fluid in the central chamber will not mix with the sheath fluid. Without hydrodynamic focusing the nozzle of the instrument (typically 70 μM) would become blocked, and it would not be possible to analyze one cell at a time.

The Optical System

As a cell passes through the laser, it will refract or scatter light at all angles. The laser and the arc lamp are the most commonly used light sources in modern flow cytometry. In particular, Argon laser is the most used because of its wavelength (488 nm) that can excite the most common fluorochromes used.

A cell traveling through the laser beam will scatter light at all angles. Light that is scattered in the forward direction, typically up to 20° offset from the laser beam's axis, is collected by a lens known as the forward scatter channel (FSC). The magnitude of forward scatter is roughly proportional to the size of the cell, thus FSC can be used to quantify that parameter. The scattered light received by the detector is translated into a voltage pulse. Because small cells produce a small amount of forward scatter and large cells produce a large amount of forward scatter, the magnitude of the voltage pulse recorded for each cell is proportional to the cell size. If we plot an histogram of these data, smaller cells appear toward the left and larger cells appear toward the right. The one-dimensional histograms do not necessarily show the complexity of the cell populations. For example, what appears to be a single population in the forward scatter histogram is in reality multiple populations that can only be discerned by looking at the data in a second dimension.

Light scattering at larger angles, for example to the side, is caused by granularity and structural complexity inside the cell. This side-scattered light is focused through a lens system and is collected by a separate detector, usually located 90 degrees from the laser's path. The signals collected by the scatter detectors can be plotted on one dimensional histograms. Scattered light is quantified by a detector that converts intensity into voltage. In most cytometers, a blocking bar, called an obscuration bar, is placed in front of the forward scatter detector. The obscuration bar prevents any of the intense laser light from reaching the detector. As a cell crosses the laser, light is scattered around the obscuration bar and is collected by the detector.

All one-parameter histograms have 1024 channels. These channels correspond to the original voltage generated by a specific "light" event detected by the photomultiplier tube (PMT) detector. In a two-dimensional dot or scatter plots, the peaks from the forward and side-scatter histograms correlate with the colored dots in the scatter plot.

Fluorochromes and Light

One of the most common ways to study cellular characteristics using flow cytometry involves the use of fluorescent molecules such as fluorophore-labeled antibodies. Fluorescence is a term used to describe the excitation of a fluorophore to a higher energy level followed by the return of that fluorophore to its ground state with the emission of light. The energy in the emitted light is dependent on the energy level to which the fluorophore is excited. That light has a specific wavelength and, consequently, a specific color. One unique feature of flow cytometry is that it measures fluorescence per cell or particle. This contrasts with spectrophotometry in which the percent absorption and transmission of specific wavelengths of light is measured for a bulk volume of sample. Labelled antibody is added to the cell sample and binds to a specific molecule on the cell surface or inside the cell. When laser light of the right wavelength strikes the fluorophore, a fluorescent signal is emitted and detected by the flow cytometer. The fluorescent light coming from labeled cells as they pass through the laser travels along the same path as the side scatter signal. As the light travels along this path, it is directed through a series of filters and mirrors, so that particular wavelength ranges are delivered to the appropriate detectors, where it is translated into a voltage pulse proportional to the amount of fluorescence emitted. All of the voltage pulses are recorded by optical detectors, called fluorescence (FL-) channels and can be presented graphically. The number of detectors will vary according to the machine and its manufacturer. Detectors are either silicon photodiodes or PMTs. Silicon photodiodes are usually used to measure FSC when the signal is strong. PMTs are more sensitive instruments and are ideal for scatter and fluorescence readings. The specificity of detection is controlled by optical filters, which block certain wavelengths while transmitting (passing) others. There are three major filter types. 'Long pass' filters allow through light above a cut-off wavelength, 'short pass' permit light below a

cut-off wavelength and 'band pass' transmit light within a specified narrow range of wavelengths (termed a band width). When a filter is placed at a 45 degrees angle to the oncoming light it becomes a dichroic filter/ mirror. As the name suggests, this type of filter performs two functions, first, to pass specified wavelengths in the forward direction and, second, to deflect blocked light at a 90 degrees angle. The electrical pulses originating from light detected by the PMTs are then processed by a series of linear and log amplifiers. Logarithmic amplification is most often used to measure fluorescence in cells. This type of amplification expands the scale for weak signals and compresses the scale for "strong" or specific fluorescence signals. Multiple fluorescence parameters are necessary to dissect complex biological systems.

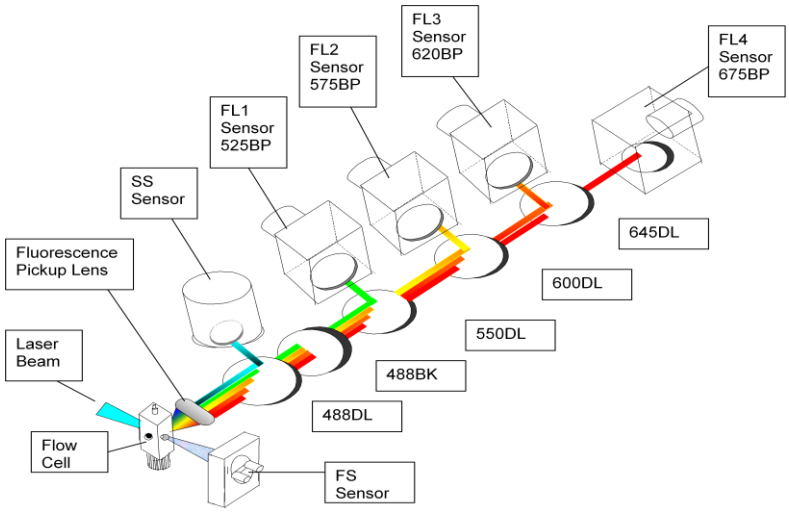

***Figure 7**. The optical system and the optical configuration for a four FL PMT sensors.*

When light hits a photodetector a small current of a few microamperes is generated. Its associated voltage has an amplitude proportional to the total number of light photons received by the detector. This voltage is then amplified by a series of linear or logarithmic amplifiers, and by analog to digital convertors (ADCs), into electrical signals large enough (5–10 volts) to be plotted graphically. Logarithmic amplification is normally used for fluorescence studies because it expands weak signals and compresses strong signals, resulting in a distribution that is easy to display on a histogram. Linear scaling is preferable where there is not such a broad range of signals e.g. in DNA analysis. The measurement from each detector is referred to as a 'parameter' e.g. forward scatter, side scatter or fluorescence. The data acquired in each parameter are known as the 'events' and refer to the number of cells displaying the physical feature or marker of interest.
One consideration to be aware of when performing multicolor fluorescence studies is the possibility of spectral overlap. When two or more fluorochromes are used during a single experiment there is a chance that their emission profiles will coincide, making measurement of the true fluorescence emitted by each difficult. This can be avoided by using fluorochromes at very different ends of the spectrum; however, this is not always practical. Instead, a process called fluorescence compensation is applied during data analysis, which calculates how much interference a fluorochrome will have in a channel that was not assigned specifically to measure it.
One final important point regarding data collection is the use of a threshold. If every single particle passing through the laser caused the instrument to collect data, the data pool would be dominated by information coming from a very large number of minute particles, like platelets and debris. To prevent this, a threshold is set such that a certain forward scatter pulse size must be exceeded for the instrument to collect the data. On the histogram, the blank area represents the small cells and debris that are excluded from analysis by the threshold. This means that the majority of events that the cytometer collects are the cells of interest. It is important to realize that the small particles are still passing through the instrument; they are just being ignored.

4. Dendritic Cells Labelling with Paramagnetic Nanoparticles

BM-DCs were stained with Paramagnetic nanoparticles (MNPs, Endorem®, 11.2 mg Iron/ mL, Guerbet, Roussi, France) added to the culture medium for 24 hours at different concentration: 100-200-400 µg Iron/ ml of culture medium. Plates were then incubated only with 200 µg Iron per ml of culture at 37°C at 5% CO_2 for different times: 6-16-24-48 hours. Cells were washed three times with PBS (PBI International) at 1500 rpm for 10 minutes before any further analysis.
Labelling efficiency was evaluated by microscopy to establish cell Iron content after Iron specific Perl's staining and by relaxometric analysis of T2 reduction.

Labelled cells were analysed also by flow cytometry for CD11c, MHCII, CD86 e CD80 (eBioscience) expression.

5. Perl's Staining

After labelling with Endorem®, cells were harvested and washed three times in order to eliminate free MNPs. After cell counting, $1*10^5$ cells were spun down on microscope slides with a Cytospin centrifuge at 2000 rpm for 10 minutes. Samples were fixed with a fixative solution (JT Baker, Phillipsburg, NJ, USA) at room temperature and then incubated for 45 minutes with Perl's solution: the reaction between Iron oxide and 2% Potassium Ferrocyanide (Merck, Darmstadt, Germany) in 2% HCl (Carlo Erba, Rodano, Milan, Italy) determined the formation of a stained salt, known as Prussian Blue, visible on optical microscopy. Contrast on cellular structure was obtained with 0,1% Safranine staining in acetic acid (Merck and Carlo Erba).

6. Iron Content Evaluation

Iron concentration was measured using a colorimetric method. 300 µl of cell suspension was centrifuged and resuspended in 200 µl HCl 5M. Cells were mineralized by a 24 hours incubation in a water bath at 37°C. After 15 minutes incubation, the absorbance was measured at 630 nm using a Hewlett Packard spectrophotometer. Standard curves were acquired using OD 630 versus the Iron content of HCl-digested Endorem® samples, treated with Perl's reagent. The parameters of the standard curve were taken into account, as well as the number of cells contained in the samples. Since digested unlabeled cell samples have a measurable absorption at 630 nm, a correction taking into account this background value was also performed.

7. Relaxation Time Measurements

After incubation with Endorem®, cells were harvested, washed three times with PBS (PBI International) at 1500 rpm for 10 minutes and counted. The sequence of NMR acquisition was performed at 40°C using a 0.47-T Bruker Minispec mq20 relassometer, with different parameters for control and labelled cells. For samples without MNPs, analysis were performed with the following parameters: 8000 points, 10 sec of delay and tau=1,5. For samples containing MNPs, analysis were performed as follows: 2000 points, 2 sec of delay, 1 scansion, gain=64 and tau=1,5.

7.1 Principles of Nuclear Magnetic Resonance

Nuclear Magnetic Resonance (NMR) deals with the interaction between an oscillating magnetic field and the net magnetization of a sample, which originates from its constituent nuclei in the presence of a static magnetic field. The nuclei at the centre of atoms are electrically charged for the presence of protons. In addition, many atomic nuclei (isotopes or nuclides) possess an angular momentum or spin I, which is caused by the rotation of nucleus about its axis. In principle, the nuclear spin follows the rules of quantum mechanics. A rotating charge (circular current) induces a magnetic dipole (µ); thus, all atomic nuclei with spin I behave as tiny compass needles. As long as no external magnetic fields exist these "compass needles" are statistically oriented in all possible spatial directions. If we subject a substance to a magnetic field (B_0), the magnetic dipoles strive to align themselves along the direction of the magnetic field, and the magnetization precesses along a conical path around the B_0 field direction. According to quantum mechanics, an angular momentum can have only a restricted number of alignments with respect to the magnetic field. Hence, the angular momentum of, for example, the hydrogen nucleus (proton, ^1H), which has spin I = 1/2, can have only two (2I + 1) possible stable orientations relative to the magnetic field B_0: one parallel to the magnetic field, the other anti-parallel to it. The two spin states differ in their energy such that the probability of finding a spin in a certain state is not uniform. A parallel orientation obviously means less energy than an antiparallel direction. The difference in energy ΔE is proportional to the field strength B_0: this means that doubling the field strength entails a doubling of energy difference. There is in addition a temperature effect: at absolute zero all the nuclear spins are aligned along the field direction, whereas at room temperature the thermal energy works against alignment, i.e. temperature interferes with an ordered arrangement. As a result, the two energy levels are not equally populated and there is a slight predominance of vectors in the parallel configuration, according to the Boltzmann's law distribution. At a typical magnetic field strength at room temperature and in thermal equilibrium, for every one million nuclei at the higher energy level one million and six nuclei would exist at the lower energy level. Consequently, a macroscopic magnetization M_z in the magnetic field results as the sum of all microscopic nuclear magnetic dipole moments and this magnetization can be detected. The net magnetization lies along the axis of the main magnetic field, in general defined as z-axis, and is named "Longitudinal Magnetization".

The nuclei of atoms placed in a magnetic field are not exactly aligned along the direction of the lines of force of the field: the magnetic axis of each nucleus tends to be disposed in an oscillating way along the vector of field itself, as with the needle of the compass. This oscillation combines with the motion of spin, giving rise to a complex movement of rotation on a conical surface having its axis along the direction of stable magnetic field. This movement is called precession of the nuclei and is similar to the motion of a gyroscope that oscillates on its axis of rotation due to the gravity field of the earth. The speed of precession is proportional to the magnetic field strength and is different for each atom. The precession rate is called Larmor frequency and, for hydrogen nucleus, is in the range of radiofrequencies.
If we irradiate the sample with radio waves in the MHz frequency range, the proton will absorb the energy and be promoted to the less favourable higher energy state. The precession rate of all nuclei is in the same position of conic surface. This energy absorption is called resonance, because the frequency of the applied radiation and the precession cohincide or resonate.
The resulting effect of the nucleus in phase concordance is the formation of a new magnetization vector along the x-y plane, perpendicular to B_0 vector, named Transverse Magnetization.
When radiofrequency pulse is removed, nuclei start loosing their stored energy, generating radiofrequency waves that can be detected. During this phenomenon, the net magnetization from the xy plane will rotate back until is again aligned with B_0. At the same time all spins will spread out and loose coherence with each other and the x-y component of the magnetization will gradually disappear.
The recovery of longitudinal magnetization occurs with a time constant T1, referred to as T1 o spin lattice relaxation time: the energy is just handed over to their surroundings, the so-called lattice. The gradual loss of transversal magnetization occurs with a time constant T2, referred to as T2 or spin-spin relaxation time. Each nucleus in fact is influenced by the small magnetic fields from neighbouring nuclei, which are somehow characteristics for a tissue. Since the nuclear spin relaxation process depends on the existence of molecular motions to generate a randomly varying magnetic field, from the relaxation rates we can get valuable information about these motions and therefore about the type of tissue.

7.2 Principles of Relassometry

Relassometry can acquire the NMR (nuclear magnetic resonance) signal produced by nuclei in the samples to test. An NMR system is formed by (Figure 8):

- a circular coil, capable of generating an uniform magnetic field;
- a generator;
- a receiver of radiofrequency (RF) pulse and output;
- a computer for processing signals received.

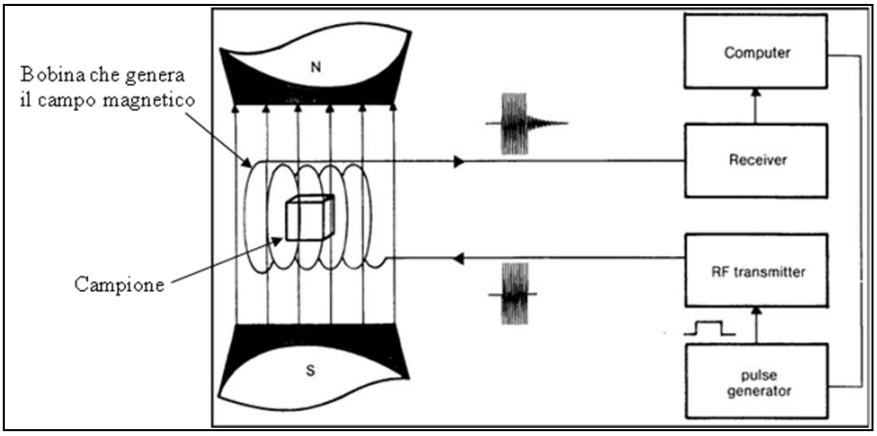

***Figure 8**. Block diagram of an NMR system.*

To obtain measures "weighed" in a selective manner according to the T1 time (recovery of longitudinal magnetisation) or T2 (loss of transversal magnetization), it is essential to use specific sequences of nuclear excitation and collection of signals. It will be possible to have images with desired weighting varying the types of acquisition and/ or regulatory factors of the sequences.
The most common sequence is the Spin-Echo (SE) sequence, which allows to get values weighed in T2 without the interference of the dishomogeneities of the magnetic field. This sequence is also highly flexible and, by varying some acquisition parameters, it is possible to obtain also weighted measures in T1 and proton density. The transverse magnetization is sensitive to the intrinsic dishomogeneities, which are inevitably present in any magnetic field. They would lead to a false interpretation of results, because they determine an apparent more rapid decay of T2, due to the spontaneous dephasing of nuclei of atoms excited. To eliminate this problem, the rephasing signal of nuclear spin after an RT pulse at 180° to the magnetic field is recorded with the Spin-Echo sequence. Each SE sequence is composed of an initial pulse

at 90° to bring the magnetization on the transverse plane. If the signal is measured at this time, a FID signal (Free Induction Decay), the spontaneous fall of the magnetization in the absence of other pulses, can be collected. Then a pulse at 180° is applied. Since the magnetization vector is currently on the transverse plane, this impulse has the effect of "flip" the orientation of the spin direction. In this way, after a time equal to twice the time elapsed between the pulse at 90° and 180°, the precession of the nuclei back into phase and the transverse magnetization takes a maximum value that is measured by the instrument.
If a whole series of 180° pulses is applied, it results in a continuous rephasing of the nuclei in the opposite direction, with production of a succession of spin-echoes. Because no energy is added at the system, each registration of signal T2 is worth less and less, permitting the record of the fall of the transverse magnetization. This sequence, comprising one 90° pulse followed by a series of 180° pulses, is termed a "Carr-Purcell sequence".
The SE sequence is characterized by three fundamental parameters that must be programmed by the operator, and whose values determine the characteristics of the final images. First, the repetition time of pulse at 180°, namely number of points, that represents a discretisation of the total time of measurement. This is the parameter which decides the length of the sequence and the start of a subsequent phase of acquisition. Secondly, the interval between pulse at 90° to 180° determines the time to echo (π), which is equal to twice this value, since half the time is spent to allow the de-phasing of the precession of protons. The other half, just the same, spends between 180° pulse and collection of eco of spin resulting by rephasing. Finally, the presence of a possible repetition pulse at 180° within a given sequence is determined by the echo number. This repetition allows the collection of late echoes, useful for evaluating the signal deriving from sample test characterized by long T2.

8. Ultrastructural Analysis by Transmission Electron Microscopy (TEM)

DC stained with Endorem® were washed twice in PBS (PBI International) at 1500 rpm 10 minutes. Pellet was fixed in 2.5% buffered Glutaraldehyde for 3 hours at 4°C to block degradation processes, post-fixed in 1% Osmium tetroxide for 2 hours at room temperature to preserve cells membranes, and embedded in Epoxy resin (PolyBed 812 Polysciences Inc. USA). 100 nm ultrathin sections were stained with heavy metals as Uranyl acetate and lead Citrate and examined by means of transmission electron microscopy (TEM). TEM images were obtained by a Zeiss EM-109 microscope (Oberkhochen, Germany) operating at 80 Kv and were used to evaluate the intracellular presence of nanoparticles and study their mechanisms of entry into DCs.

8.1 Principles of Transmission Electron Microscope (TEM)

The transmission electron microscope operates on the same basic principles as the light microscope, but uses electrons instead of light. TEMs uses electrons as "light source" and their much lower wavelength makes it possible to get a resolution a thousand times better than with a light microscope: objects to the order of a few Angstrom can be seen.
In TEM, the transmission of electron beam is highly dependent on the properties of material examined. Such properties include density and composition. For example, porous material will allow more electrons to pass through, while dense material will allow less. As a result, a specimen with a non-uniform density can be examined by this technique. Whatever part is transmitted, it is projected onto a phosphor screen for the user to see.
A TEM contains four parts (Figure 9):

- the electron source;
- the electromagnetic lens system;
- the sample holder;
- the imaging system.

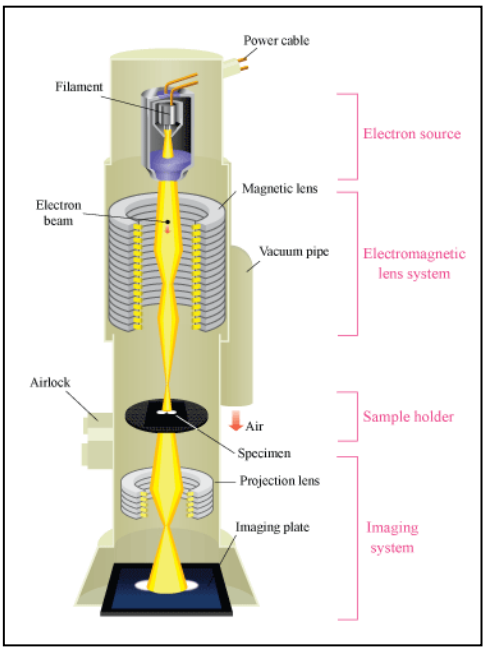

***Figure 9**. The schematic outline of a TEM.*

The Electron Source

The electron source consists of a cathode and an anode. The cathode is a tungsten filament which emits electrons when being heated. A negative cap confines the electrons into a loosely focused beam. The beam is then accelerated towards the specimen by the positive anode. Electrons at the rim of the beam will fall onto the anode, while the others at the center will pass through the small hole of the anode. The electron source works like a cathode ray tube.

The Electromagnetic Lens System

After leaving the electron source, the electron beam is tightly focused using electromagnetic lens and metal apertures. The system allows only electrons within a small energy range to pass through, so the electrons in the electron beam will have a well-defined energy.

Magnetic Lens are circular electro-magnets capable of generating a precise circular magnetic field. The field acts like an optical lens to focus the electrons.

Aperture is a thin disk with a small (2-100 micrometers) circular through-hole. It is used to restrict the electron beam and filter out unwanted electrons before hitting the specimen.

Sample Holder

The sample holder is a platform equipped with a mechanical arm for holding the specimen and controlling its position.

The Imaging System

The imaging system consists of another electromagnetic lens system and a screen. The electromagnetic lens system contains two lens, one for refocusing the electrons after they pass through the specimen and the other for enlarging the image and projecting it onto the screen. The screen has a phosphorescent plate which glows when being hit by electrons. Image forms in a way similar to photography.

9. MMTV-v-Ha-Ras Mouse Model

The murine model of breast cancer MMTV-v-Ha-Ras is characterized by the regulatory element of MMTV (Murine Mammary Tumour Virus) that drives the expression of the v-Ha-Ras p21 (G12R e A59T) oncogene in mammary and salivary glands. All transgenic females develop malignant adenocarcinomas of mammary and salivary glands between the 8^{th} and 16^{th} week of age. At the 8^{th} week of age all transgenic females show low to high grade mammary neoplasia (MIN); at the 12^{th} week of age about 75% of animals show adenomas and/or adenocarcinomas; at the 16^{th} week of age 100% of animals show adenocarcinomas and MIN localized to other areas; from the 20^{th} to 24^{th} week of age most tumours appear. This mouse model is characterized also by lung metastasis, in particular 50% of animal at the 16^{th} week of age, 25% of at the 20^{th} week of age, 0% at the 24^{th} week of age and 25% at the 28^{th} week of age show this kind of lesions.

Male and female MMTV-v-Ha-Ras mice bearing tumour lesions were heterozygous for the hRas transgene and were maintained in a pure FVB background. MMTV-v-Ha-Ras mouse males in the FVB mouse background were bred to wild-type FVB females (Charles River Laboratories, Calco, Italy) to maintain the FVB background. PCR-based mouse screening assay to identify transgenic mice was performed.

10. DNA Extraction

To assess if an animal was transgenic or not we performed a DNA extraction protocol on tail biopsies. Tail biopsies of no longer than about 1 cm were transferred into tubes with 500 μl Lysis Buffer (100 mM Tris.HCl pH 8.5, 5 mM EDTA, 0.2% SDS, 200 mM NaCl, 100 μg Proteinase K/ml; Sigma Aldrich) immediately after cutting or stored at -20°C until treatment. Tail digestion was completed after an overnight incubation at 55°C in agitation. Following complete lysis, tubes were then vortexed and centrifugated for 10 minutes at 13000 rpm. Supernatants were poured into tubes containing 500 μl of Isopropanol. Samples were mixed or swirled until complete precipitation and then centrifuged at 13000 rpm for 15 minutes. Supernatants were discarded and pellets washed with 70% Ethanol (Sigma-Aldrich) at 13000 rpm for 15 min. Supernatants were discarded and when dry, pellets were resuspended in a volume of Water dependant on pellet dimensions.

11. PCR protocol

PCR amplification was carried out in a mix containing a 10X Buffer composed by KCl and $(NH_4)_2SO_4$ with a proprietary formulation and 20 mM $MgCl_2$; 20mM dNTPs; 1,25 U of Dream*Taq* DNA Polymerase (Fermentas, Burlington, Ontario, Canada) and 200 ng/ μl of each primer (Invitrogen Ldt, Pailsey, UK) per 1 μl of genomic DNA template. The couple of primers used for h-Ras amplification was: 5'-CAGGGACCAGCAAGACATC-3' and 5'-CCCTGAACCAGCCATCAAC-3'. The couple of primers used for β-Casein amplification, used as control, include: 5'-GATGTGCTCCAGGCTAAAGTT-3' and 5'-AGAAACGGAATGTTGTTGAGT-3'. After 35 cycles of 45 sec at 94°C, 45 sec at 55°C, and 1 min at 72°C, the products were analyzed on 1% Agarose gel stained with Ethidium Bromide (Sigma-Aldrich).

12. Tumour Lysate Preparation

Mammary tumour lesions from transgenic animal models (MMTV-v-Ha-Ras), characterised by over-expression of h-Ras, were mechanically disaggregated, heated at 42°C in a water bath for 1 hour and then for 2 hours at 37°C in CO_2 5%. Then, tumour cells were digested with 0.02% Trypsin (Euroclone) and washed in PBS (PBI International). Cells were then resuspended at $15x10^6$ cells/ ml and lysed by 3 cycles of freeze-thawing in liquid nitrogen. The preparation was centrifuged at 12000 rpm for 15 minutes and stored in aliquots at -80°C.

12.1 Coomassie Protein Assay

For total protein quantitation of the tumour lysate a Coomassie (Bradford) Protein Assay Kit (Pierce, Rockford, IL, USA) was used. When Coomassie dye binds proteins in an acidic medium, an immediate shift in absorption maximum occurs from 465 nm to 595 nm with a concomitant colour change from brown to blue. 30 μl of sample and each standard, represented by known concentrations of Bovin Serum Albumin (BSA) with a Working Range between 0 and 2000 μg/ml, were incubated with the Coomassie Reagent for 10 minutes at room temperature. The absorbance of all samples was measured with the spectrophotometer (Biorad, Hercules, CA, USA) set to 595 nm. The standard curve was used to determine the protein concentration of each sample.

12.1 Dendritic Cells Antigen Pulsing

Day 6 DCs were incubated with tumour lysates for 24 and 48 hours at different DC to tumour cells equivalent ratios: 1:10; 1:5; 1:2,5; 1:1; 2,5:1; 5:1; 10:1. Unloaded DCs were used as controls. After antigen loading, DCs were collected, stained for CD11cPECy7, MHCIIPECy5, CD86PE and CD80 FITC (eBioscience) expression and analyzed by flow cytometry.

13.In Vitro DCs Migration Test

1 μg of mouse-recombinant chemokines, namely MIP-3β, 6Ckine (R&D System), MIP-1α and MIP-1β (BioSource International, Camarillo, California, USA) were diluted in complete ISCOVE (Euroclone) to a final volume of 600 μl and added to a 24-well transwell tissue culture plate (Corning Coster, Lowell, MA, USA). Transwell culture inserts with 6.5 mm diameter and 5.0 μm pore size were put into each well. $0,5*10^6$ DCs loaded with tumour lysates were seeded in complete medium to the top chamber of each well, at a final volume of 100 μl. Unloaded DCs were used as negative controls. Plates were then incubated at 37°C in 5% CO_2 for 4 hours. After the incubation time, cells migrated in the bottom chamber were recovered, counted and stained with CD11cPECy5, MHCIIPECy5 and CCR7 FITC (eBioscence) for flowcytometric analysis.

14.T Cell Isolation by Immunomagnetic Bead Sorting

Spleens from MMTV-v-Ha-Ras FVB female mice bearing tumour lesions were mechanically disaggregate by using a Cell Strainer with 70 µm pores (BD, Franklin Lakes, NJ, USA). Splenocytes were isolated using a Ficoll-Hypaque gradient (Organon Teknika Corp., Durham, NC) and centrifuged at 2300 rpm for 25 minutes. Cells were collected and washed with PBS (PBI International) at 1900 rpm for 10 minutes. After count, cells were resuspended in complete ISCOVE (Euroclone).
T cells were purified using a Pan T Cell Isolation Kit (Miltenyi Biotec, Bergisch Gladbach, Germany). After magnetic labelling, non-T cells were labelled and depleted by negative selection through paramagnetic columns (LS columns, Miltenyi Biotec) according to manufacturer's instructions. $0{,}5*10^6$ cells were stained with CD3PECy5 (eBioscience) to assess T lymphocytes purity by flow cytometry. T purity of 90-97% was consistently achieved.

14.1 T Cells Proliferation by Tritiated Deoxythymide

$1*10^4$ mouse BM-DCs pulsed with tumour lysate were added to $1*10^5$ T cells in 96-well U-bottomed plates (Corning Coster) at a responder-to-stimulator ratio of 10:1. Cultures were incubated 48; 72; 96 and 120 hours at 37°C with 5% CO_2. 18 hours before being collected, cells were pulsed with [^{3}H]thymidine (1 µCi/ well). At completion, plates were harvested with semi-automated Tomtec cells harvester (Orange, CT) and measured by a Wallac 1205 Betaplate liquid scintillation beta-counter (PerkinElmer, Monza, Italy). Responses were reported as mean cpm ± SEM from triplicate samples.

14.2 T Cells Proliferation by CFDA-SE

The cell-permeant fluorescein-based dye Carboxy-Fluorescein- Diacetate- Succinimidyl –Ester (CFDA-SE or CFSE; Sigma-Aldrich) covalently attaches to cytoplasmic components of cells, resulting in uniform bright fluorescence. Upon cell division, the dye is distributed equally between daughter cells, allowing the resolution of cell division by flow cytometry.
T cells proliferation was analyzed in the following conditions:

- $CD3^+$ T lymphocytes in co-culture at 1:10 ratio with DCs loaded at 1:5 ratio with tumour lysate;
- $CD3^+$ T lymphocytes in co-culture at 1:10 ratio with DCs loaded at 1:10 ratio with tumour lysate;
- $CD3^+$ T lymphocytes in co-culture at 1:10 ratio with unloaded DCs;
- $CD3^+$ T lymphocytes alone stimulated with 5 µg/ ml SEB (Staphilococcal Enterotoxin B) or 12.5 µg/ ml PHA (Phytohaemagglutinin) (Sigma Aldrich).

$30*10^6$ $CD3^+$ T lymphocytes were resuspended in 0,1% PBS/ BSA (PBI International and Sigma-Aldrich) at room temperature and stained with 2.5 µg/ ml CFSE**.** Cells were incubated at 37°C 5% CO_2 for 10 minutes, resuspended in 5 ml complete cold ISCOVE (Euroclone) supplemented with 10% BSA (I10 medium, Sigma-Aldrich) and incubated on ice for 5 minutes. Cells were washed 4 times with I10 medium at 1200 rpm for 7 minutes, resuspended at a final concentration of $3*10^6$ in complete ISCOVE (Euroclone) and seeded in a 24-wells plate (Corning Coster) with or without $3*10^5$ DCs for 7 days.
After that time, cells were resuspended, washed, stained with anti mouse CD3 PECY7 (eBioscience) and analyzed by flow cytometry.
The percentage of proliferated cells was calculated as follows:

$$\frac{\text{number of peak 0 divided cells}}{\text{number of peak 0 divided cells+ number of events in peak 0}}$$

The proliferation index was calculated as follows:

$$\frac{\text{number of total events in a peak}}{\Sigma\ (\text{total events/ replicative cycles})}$$

15. Intracellular Cytokines Production

To evaluate the functional activity of DCs, intracellular cytokines production was assessed by flow cytometry. The following conditions were analyzed:

- DCs loaded with tumour lysate 1:5 ratio for 24 hours;
- Unloaded DCs;
- DCs loaded with tumour lysate 1:5 ratio in co-culture with $CD3^+$ T lymphocytes at 1:10 ratio;
- Unloaded DCs in co-culture with $CD3^+$ T lymphocytes at 1:10 ratio;
- $CD3^+$ T lymphocytes alone stimulated with 5 µg/ ml PMA (Phorbol Myristate Acetate) and 1Mm Ionomycin (Sigma Aldrich).

Each tube (PBI International) was seeded with $3*10^5$ DCs and $3*10^6$ $CD3^+$ T lymphocytes and incubated at 37°C 5% CO_2 for 24,48, 72, 96 and 120 hours. Intracellular cytokines levels were assessed also at day 0.
10 μg/ ml Brefeldin A (Sigma-Aldrich) was added to cell cultures during the last 18 hours to block protein secretion. Cells were then washed in PBS (PBI International) at 1500 rpm for 10 minutes. CD11c PECy5 and CD3 PECy5 (eBioscience) were used to stain DCs and T lymphocytes respectively.
Cells were incubated for 15 minutes at room temperature in the dark, fixed in 1% PFA (Sigma-Aldrich) 15 minutes at 4°C and then washed at 1500 rpm for 10 minutes. Cells were then resuspended in 0,5% Saponin (Sigma-Aldrich); DCs were stained for IL-12 PE and IL-10 FITC, T lymphocytes for IL-10 FITC and IFNγ PECy7 (eBioscience) or proper isotype control. After a 45-min incubation at 4°C in the dark, cells were washed 1500 rpm for 10 minutes and fixed in 1% PFA.

16. Enzymed-Linked Immunosorbent Test Assay (ELISA)

To evaluate the best antigen pulsing ratio the following conditions were analyzed:

- DCs loaded with tumour lysate 1:10; 1:5; 1:2,5; 1:1; 2,5:1; 5:1; 10:1 ratio for 24 hours, each condition in co-culture with $CD3^+$ T lymphocytes at 1:10 ratio;
- DCs loaded with tumour lysate 1:10; 1:5; 1:2,5; 1:1; 2,5:1; 5:1; 10:1 ratio for 48 hours, each condition in co-culture with $CD3^+$ T lymphocytes at 1:10 ratio;
- Unloaded DCs in co-culture with $CD3^+$ T lymphocytes at 1:10 ratio;
- $CD3^+$ T lymphocytes alone stimulated with 5 μg/ ml PMA (Phorbol Myristate Acetate) and Ionomycin 1 mM (Sigma Aldrich).

Each well of a 24-well plate (Corning Coster) was seeded with $1*10^5$ DCs and $1*10^6$ $CD3^+$ T lymphocytes and incubated at 37°C 5% CO_2 for 48, 72, 96 and 120 hours. The plates were then centrifuged at 1000 rpm for 10 minutes and supernatants collected and stored at -20°C.
The INF-γ levels of each condition were analyzed using commercially available kit (R&D Systems) according to manufacturer's instruction. Optical density (OD) at 450 nm of duplicate samples was determined and corrected by a microplate reader, with readings at 570 nm.

To evaluate the ability of DCs of inducing a T lymphocytes response, the following conditions were analyzed:

- DCs loaded with tumour lysate at 1:5 ratio for 24 hours;
- Unloaded DCs;
- DCs loaded with tumour lysate 1:5 ratio in co-culture with $CD3^+$ T lymphocytes at 1:10 ratio;
- Unloaded DCs in co-culture with $CD3^+$ T lymphocytes at 1:10 ratio;
- $CD3^+$ T lymphocytes alone stimulated with 5 μg/ ml PMA and Ionomycin 1 mM (Sigma Aldrich).

Each well of a 24-well plate (Corning Coster) was seeded with $3*10^5$ DCs and $3*10^6$ $CD3^+$ T lymphocytes and incubated at 37°C 5% CO_2 for 48, 72, 96 and 120 hours. The plates were then centrifuged at 1000 rpm for 10 minutes and supernatants collected and stored at -20°C.
IL-4, IL-10, IL-12p40, IL-12p70 and IFN- γ release in the supernatants was analyzed using commercially available kits (R&D Systems) according to manufacturer's instruction. Optical density (OD) at 450 nm of duplicate samples was determined and corrected by a microplate reader, with readings at 570 nm.

17. In Vivo Magnetic Resonance Imaging (MRI)

DCs labelled with Endorem® and pulsed with tumour lysate were injected into the footpad of anterior and/ or posterior limbs, depending on tumour localisation in the MMTV-v-Ha-Ras mouse model using a Syringe with a 27 Gauge diameter needle. The injection sites were pre-treated with 30 ng of TNF-α (R&D System) 24 hours before cell administration and concomitantly with DCs injection in order to create an inflammatory microenvironment which facilitates DCs maturation and migration. $2x10^6$ DCs were used for every injection.
All the animals were visualised on a 7T MRI system (Pharmascan, Bruker Biospin, Billerica, MA, USA) at different time points: 0-4-24-48 hours after cells injection. Animals were anesthetized with Isofluoran gas, positioned prone in the animal bed and inserted in the radiofrequency coil (38 mm) inside the magnet. Scout transverse images were acquired for correct positioning of interest region. Different MR sequences were tried in order to optimize lymph nodes visualization and signal contrast. Spin Echo sequence, named MSME sequence, (FOV (Field of View): 3x3 cm; matrix 256x128; 12 slices of 0.6 mm of thickness); TR/TE: 1500/11 ms; 2 averages; acquisition time: 6' 24'') allows to detect Iron signal with a good morphology of tissues and organs, while Gradient Echo sequence (FLASH sequence, FOV: 3x3 cm; matrix 256x128; 12 slices of 0.6 mm of thickness; TR/TE: 1200/10 ms; 2 averages; acquisition time: 5' 7'') allows to enhance the Iron signal with a decrease on morphology definition. Breath triggering was used only with FLASH sequence in the thoracic area to visualize axillary and brachial lymph nodes.
After last acquisition, animals were sacrificed and tumour draining lymph nodes collected and embedded in Formalin 4% (Sigma-Aldrich) for the subsequent Perl's staining and immunohistochemistry analysis.

17.1 Principles of Magnetic Resonance Imaging (MRI)

The Magnetic Resonance Imaging (MRI) is an image generating technique based on NMR. Hydrogen is the most commonly observed nucleus in MRI, because of its favourable magnetic properties and its abundance. ^{1}H-MR images reflect the density of Hydrogen, main component in tissues as water or fat. MRI signal intensity reflects the number of MR-visible protons in a unit volume of tissue. In other words it reflects the density of mobile Hydrogen nuclei influenced by their chemical environment, which causes magnetic relaxation times T1 and T2.
The main components of an MR imaging system are :

- the main magnet, that generate the magnetic field and polarizes the sample;
- the magnetic field gradients, for spatial reconstruction and localization of signal;
- the radiofrequency coils to transmit and/or receive the MR imaging signal;
- one or more computer and associated signal processing equipment.

The Magnet
The magnet is the largest and most expensive component of the scanner. Its strength is measured in Tesla (T). Clinical magnets generally have a field strength in the range 0.1-3.0 T, with research systems available up to 9.4 T for human use and 21 T for animal systems. The homogeneity of the basic magnetic field over the examination volume should be as high as possible, to ensure low image distortion and high signal homogeneity and achieve good image quality. Also, the homogenous examination volume should be as large as possible. A cylindrical main magnet with the homogeneous volume centred on the central axis fulfills all these requirements and, therefore, represents the most frequent magnet designed today. In general, the magnet is based on the use of superconducting electromagnet. When a Niobium-Titanium or Niobium-Tin alloy is cooled by liquid Helium to −269°C it becomes a superconductor, with low resistance to the flow of electrical current and extremely high field strengths, with very high stability. Helium cooled superconducting magnets are the most common type found in MRI scanners today. Most superconducting magnets have their coils of superconductive wire immersed in liquid Helium, inside a vessel called a cryostat. Despite thermal insulation, ambient heat induces the Helium to slowly boil off. Such magnets, therefore, require regular topping-up with liquid Helium. Generally a cryocooler, also known as coldhead, is used to condense some Helium vapour back into the liquid Helium bath. Several manufacturers now offer 'cryogenless' scanners where, instead of being immersed in liquid Helium, the magnet wire is cooled directly by a cryocooler.
When a sample is placed into the scanner, it creates inhomogeneities in the field. This causes regions without signal and spatial distortion in the acquired images. To restore the field homogeneity, a set of shim coils are included in the scanner. These are resistive coils, usually at room temperature, capable to produce secondary magnetic fields which correct inhomogeneities and errors in the magnetic field strength. This process of “shimming” is usually automated.
The Gradient System
The magnetic field gradients give rise to linear variations of magnetic field strength. In fact, gradient coils are used to spatially encode the positions of protons by varying the magnetic field linearly across the imaging volume. In order to produce an image, 3 gradients in 3 orthogonal orientations are used: one gradient is used to “locate” the level of each plane and is known as “slice gradient”. The other two gradients are used to locate points within each plane and are called “frequency” and “phase encoding” gradients.
Gradient coils are usually resistive electromagnets powered by sophisticated amplifiers which permit rapid and precise adjustments of field strength and direction.
Scan speed depends on the gradient system performance. An optimal system must be able to cover large examination volume in the shortest possible time. In general, the gradient system requirements can be best met with a cylindrical design that fits magnet geometry.
The Radiofrequency System
The radiofrequency (RF) system consists of a RF transmit coil inside the magnet, for selective RF spins excitation and a RF receiver coil system, for picking up the weak RF signal resulting from excited nuclei.
Radiofrequency coils can be constructed with a variety of geometries and they are increasingly built for specific applications; however, large cylindrical volume transmit RF coils with a conductor geometry similar to a birdcage are typically used.
Image Formation
The radiofrequency signal picked up by the receiver at the end of an acquisition doesn’t have an intrinsic spatial information because it is unable to discriminate signals deriving from different points of the sample. Thus it cannot be used to reconstruct an image. The passage between raw signal and the image formation is based on a process of spatial codification, with attribution of a specific frequency and resonance phase for each point of the space, thanks to the application of the gradients.
Each different point of the examined space, identified through a frequency and phase codification, is assigned a numeric value of intensity that is translated in a different intensity of grey scale on the image.
One of the big advantages of MRI over other imaging techniques is its ability to image non-invasively slices of an object at any arbitrary position, thickness and orientation. This is obtained by applying an RF pulse with

a range of frequencies together with a slice magnetic field in the proper orientation. This range of frequencies associated with the RF pulse is referred to as the “bandwidth” and directly determines the slice thickness. Slice thickness can also be altered by changing the slope of the gradient; a very strong gradient allows the reading of thinner slices and vice versa.
An MR image is essentially a two-dimensional representation of the intensity of the magnetic properties of the observed nucleus as a function of its distribution in space.
Many factors affect MR images signal intensity and contrast: intrinsic factors, like proton density, T1 and T2 relaxation times and diffusion, and extrinsic or experimental factors, such as parameters of acquisition.
One of the biggest advantage of MRI is that image contrast can be optimized for specific purposes and the choice of pulse sequences determines the weighting and the quality of the images. A multitude of sequences are available in MRI through conventional Spin Echo and Gradient Echo sequences, fast imaging and ultra fast imaging.

18. Immunohistochemistry

After images acquisitions, animals were sacrificed and draining lymph nodes collected and fixed in 10% neutral buffered Formalin (Sigma Aldrich). The organs were dehydrated, rinsed twice in Xylene and embedded in Paraffin. Thin sections (3-5 µm) were cut by microtome and placed on slides. Then, Haematoxylin and specific Iron Perl’s staining were performed.
Some slides were stained with mAb specific against mouse macrophage (clone RM0029-11H3, AbCam, Cambridge, MA, USA) or CD208 (clone 1010E1.01, Imgenex, San Diego, CA, USA). The detection was performed by Bond™ Polymer Refine Red Detection Kit® (Leica Microsystem) by using the chromogen Fast Red or Diaminobenzidine (DAB), respectively.
Labelled cells had a clear dendritic morphology, having a round nucleus with fine chromatin, a central inconspicuous nucleolus and amoeboid shape. In some slides, it was possible to observe two DCs very close to each other, in the classical conformation of kissing nucleus.
Histologic sections were analyzed in a brigth field microscope, using a 20x, 40x and 100x magnification.

19. DC labelling with ^{111}Indium-oxine and SPET imaging

Antigen loaded DCs were labelled with 30, 60 and150 µBq of ^{111}In-oxine (GE Healthcare, USA) in 0.1 M Tris-HCl pH 7.0 for 15 minutes at room temperature. Cells were washed three times with PBS (PBI International) 1500 rpm for 10 minutes. Labelling efficiency was calculated as the percentage of the activity that remained associated with the cell pellet on total supernatants and pellet discarded measured by a dose calibrator.
DCs migration was followed by *in vivo* planar scintigraphic imaging (matrix of 581x581, corresponding to a Field of View –FOV– of 2,4x2,6 cm, energy window with peak at 170 keV). *In vivo* imaging of the injection depot and the corresponding lymph nodes was performed by a DRAGO prototype γ-camera equipped with medium energy collimators at day 0, 1 and 2 after DCs injection. Being DRAGO a prototype, no standard acquisition sequences were available: for each image timing of acquisition was dependant to the radioactivity of the injected cells.
DCs were loaded with tumor lysate at 1:5 ratio and then labelled with ^{111}In-oxine. The injection sites were pre-treated with 30 ng of TNF-α (R&D System) 24 hours before cell administration and concomitantly with DCs injection. After 48 hours lymph nodes were collected and counted with a gamma counter for 1 minute. The relative amount of radioactivity in the organs was calculated and expressed as counts per gram of tissue (counts/ g) and as a percentage respect to the lymph node opposite to injection site. Lymph nodes were also imaged *ex vivo* with the DRAGO γ-camera.

19.1 Principles of SPECT Imaging

Single Photon Emission Computed Tomography (SPECT) tomograph can detect high energy photons emitted from the subject under examination, following the administration, generally by intravenous injection, of radioactively labelled tracers. After reaching the target organ, the tracers are retained.
The labelled tracers contain an excited nucleus, as a radionuclide, which is unstable and can spontaneously stabilize to a less-excited system. The resulting transformation alters the structure of the nucleus and causes the emission of either a photon or a high-velocity particle with a mass, such as an electron. The radioactive decay is a random process on the atomic level that is impossible to predict, but when a large number of similar atoms is analyzed, the average decay rate is predictable and can be used to image a specific process or cell. One of the main advantages of the nuclear imaging techniques is their very high sensitivity, when compared with other *in vivo* imaging techniques.
SPECT is based on the use of radiotracers labelled with a radionuclide, such as ^{99m}Tc, ^{123}I, ^{125}I, ^{111}In and ^{201}Tl, that decays with emission of single photons with different energy. To locate the source of an emitted photon, its direction of incidence into the detection system needs to be accurately selected and its position of interaction determined in the position sensitive detector.

The principal components that comprise a SPECT imaging system include:

- the collimator;
- a scintillation crystal;
- the position sensitive photo-detector, which is traditionally based on photomultiplier tubes;
- the readout electronic, which is dependent on the type of photo-detector used and gives information about the position of interaction and the energy of each detected gamma photon.

The Collimator

The collimator is a device made of a high-Z material such as lead, which selects gamma rays along particular directions in order to form an image on the sensitive area of the gamma-camera. There are different options for the collimator geometry; one of the most commonly used is the parallel holes. In this case, the holes of the collimator are parallel and allow the passage only of the photons perpendicular to the surface of the photo-detector. The image obtained is thus the projection of the distribution of the radio tracer inside the patient on a plane parallel to the scintillator crystal or the photo-detector. This kind of collimator is the one used during the measurements with the DRAGO Gamma Camera prototype.

The Scintillation Crystal

The scintillation crystal converts the high energy gamma photons into many lower energy photons, usually in the visible range, which can easily be detected by the photo-detector. On the contrary, without a scintillator, the photo-detector would be almost transparent to the gamma radiation and wouldn't provide any useful signals. The gamma photon leaving the patient and impinging on the scintillator is called the primary photon. When the primary photon interacts with the scintillator, it leaves part or all of its energy inside the crystal. With part of the lost energy lower energy photons are generated, called secondary photons. The energy spectrum of the secondary photons generated is usually composed of one or two close lines, depending on the scintillator used. All the secondary photons have the same energy. Due to this and the conservation of energy, the number of secondary photons is proportional to the amount of energy lost by the primary photon inside the scintillator. For example, if we consider only the events in which the primary photon has released all of its energy inside the crystal, i.e. the photopeak in the energy spectrum, the number of secondary photons is proportional to the energy of the photon emitted by the radiotracer.

The way the primary photon looses energy inside the crystal can be described in short as follows: when the gamma photon leaves the patient, it knocks the crystal and looses energy, determining the production of a high energy ionizing electron. The electron generated looses its kinetic energy in the form of thermal energy, light photons or by ionizing other electrons, which will loose their energy inside the crystal through the same mechanisms until all the electrons find a minimal energy state. At the end of the process, part of the energy of the primary photon is converted into many secondary photons, while the rest of the energy is "lost" in thermal energy inside the crystal.

There are two ways in which the primary photons can first interact with the scintillator: the photoelectric effect and the Compton effect. In the first case, all the energy of the gamma photon is lost inside the crystal, generating the photopeak in the energy spectrum, while in the second case only part of the energy remains inside the crystal, because the rest is taken away by the deviated gamma photon.

There are many different kinds of scintillators, but the most common in the gamma cameras are the inorganic scintillators. They are high-Z crystals, so they have a high stopping power for the primary photons, and are transparent to the visible light, in order to let the secondary photons reach the photo-detector. Being one of the most important parts of the gamma cameras, a big amount of research has been done in order to optimize the parameters of the scintillator, so that nowadays many kinds of inorganic scintillators are available. The most common are NaI (Tl), CsI (Tl), used for DRAGO prototype or, more recently, $LaBr_3$ (Ce).

The Position Sensitive Photo-Detector

The secondary photons are detected by the photo-detector, which is placed at the opposite side of the scintillator, with respect to the collimator. Its function is to convert the secondary photons into a proportional electronic signal. One very common photo-detector is the photomultiplier tube (PMT), that has a photocathode to absorbe the visible photons. This process generates free electrons that are subsequently accelerated in a vacuum tube by a sequence of dynodes, having a positive potential increasing proportionally to the distance from photocathode. Along their path inside the tube, the interaction of the electrons with dynodes determines the formation of new electrons, obtaining a signal amplification. At the end of the tube there is the anode, which collects all the electrons and generates an electric signal, whose amplitude is proportional to the number of secondary photons interacting at the photocatode and thus to the total energy released in the scintillator by the gamma photon.

With respect to the simplifies structure described above, some modification have been implemented, in order to add position sensitivity to certain types of PMTs and actually record the image generated by the collimator. More recently, different photo-detectors based on solid-state silicon devices have been proposed, in order to improve performances of the gamma cameras. In particular, silicon devices get better energy performance, spatial resolution, more compactness, lower cost and less sensitivity to magnetic fields, with respect to PMTs. All these solution, however, are under research and the widespread photo-detector for gamma cameras remains the PMT. For example, the DRAGO gamma camera is a research project for

evaluating the use of a very peculiar type of silicon detector, the Silicon Drift Detector (SDD), as the photo-detector in a high resolution gamma camera.

19.2 DRAGO, a prototype of microSPET

DRAGO prototype is an high resolution, small Field Of View (FOV), compact gamma ray imager, based on the Anger camera principle. Thanks to its characteristics, the potential applications of the imager in human medicine are in the field of intra operative probes and of cancer diagnosis, staging and therapy control. Moreover, the probe could be useful in preclinical validation of new drugs carried out with *in vivo* studies on small animals. The most relevant and innovative characteristic of the DRAGO imager is the use of a non-standard silicon photo-detector for scintillation light readout. This detector is the Silicon Drift Detector (SDD) which is characterized by a very low electronic noise, reached without any internal charge multiplication mechanism. Moreover, custom anti reflective coatings have been implemented on the entrance window of the detector, in order to increase the Quantum Efficiency (QE). Thanks to these characteristics, the statistical and noise contributions to the energy resolution in gamma ray spectroscopy are reduced, eventually yielding to an improved image quality.
The DRAGO imaging probe is composed, starting from top, by a collimator, a single scintillator crystal, which covers all the units of the array of photo-detectors and converts the high energy γ-photons into many visible ones, and the photo-detector array, which converts the light into electric signals.
The position of interaction of the gamma photons inside the crystal is obtained by the scintillation light distribution among the elements of the array. The signals of the photo detectors are amplified and filtered by a multi-channel analog readout electronics and then sent to an acquisition board, where they are converted to digital values and sent to a computer. Finally, a digital algorithm reconstructs the position of interaction of the photons in the crystal.
The scintillator is made of CsI : Tl, which has a high light output, but a long decay time constant. The results confirm good performances, such as an energy resolution of 5.38 % on the ^{57}Co peak, indicating that the SDD is an almost noiseless detector in the measured energy range, between 50 KeV and 700 KeV.
The photo-detector is a monolithic array of 77 SDDs, with on-chip JFET, and has an active area of 6.7 cm^2. The array has been characterized, with respect to the parameters relevant for the scintillation light readout, which are, in synthesis, the QE and the Equivalent Noise Charge (ENC). In particular, the second run of production, which solves some charge collection problems of the first, shows very good and uniform performances among all the units, such as an ENC ranging from 8.1 and 14.1 e^- rms, with a mean value of 10.8 e^- rms measured at -10°C. The measured QE is higher than 90 %, for the wavelengths of interest, that is in the range of 400 – 700 nm.
The readout electronics is designed specifically for the DRAGO project and is composed of ten 8-channel ASICs (Application Specific Integrated Circuits). Every single channel features a low noise preamplifier, a 6th order semi-gaussian shaping amplifier with selectable gain and peaking times in the μs range, a peak stretcher and a baseline holder. The 8-channel chip also features an analog multiplexer, registers for threshold programming and some logic, necessary for the multiplexer to work and for interfacing with the rest of the system. The acquisition system converts the peak values of the semi-gaussian shaping amplifiers, shifted out from the multiplexer, with a precision of 13 bits. The converted data are then stored in a FIFO memory for buffering and sent to the host PC, through a high-speed USB interface. Both the control of the acquisition board and the digital processing of the data, for calculating the position of interaction of the gamma photon inside the crystal basing on the Anger logic, is done on the computer.

Results & Discussion

1. Dendritic Cells Isolation and Immunophenotypic Analysis

Bone marrow cells were extracted from FVB female mice and used without depletion of other cell types. Bone marrow cells were then cultured in presence of GM-CSF and IL-4 to enable the differentiation in dendritic cells and inhibit the differentiation of macrophages, respectively.
Flow cytometric analysis of day 6 population showed that all cells had similar granularity and slightly different cell sizes. Increasing cell size correlated with higher amounts of MHC II molecules on the cell surface. On the basis of the low or high surface expression of MHC class II molecules, the suspension could be clearly subdivided into smaller immature and larger mature BM-DCs, both positive for CD11c (Figure 10). Immature and mature DCs were then further characterised by the expression of co-stimulatory molecules (CD86 and CD80) and activation markers (CD83). The analysis of immature DCs showed low levels of MHC class II molecules, CD86, CD80 and CD83, that were instead highly up-regulated in mature DCs.

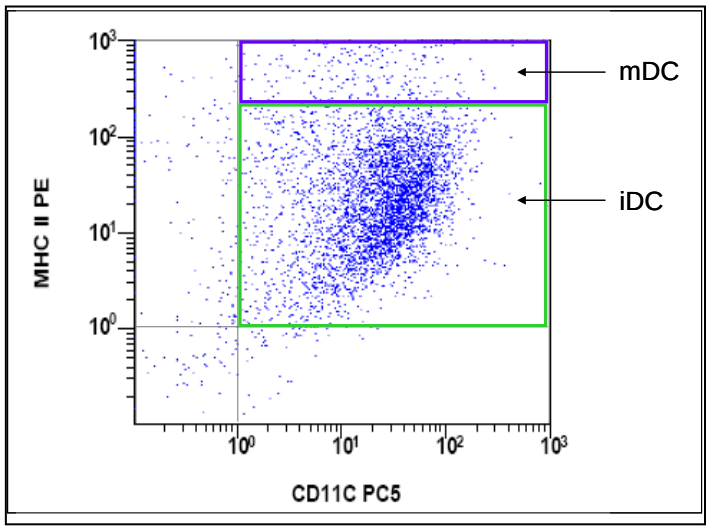

Figure 10. *Flow cytometric analysis (dot plot) of day 6 CD11c$^+$ DCs. Immature DCs express low levels of MHCII (green square), mature DCs express high levels of MHCII (violet square).*

Cell culture was performed for 10 days. Starting from day 3, cell phenotype was evaluated by flow cytometry. The percentage of immature and mature DCs on the total of cells in culture was evaluated during time (Figure 11). The growth curve showed an increase of immature DCs from day 3 to day 7. From day 8 on a decrease in the percentage of the total population could be noted, probably due to cell exhaustion and death of mature DCs [199]. Between day 6 and day 8 the highest production of DCs could be observed.

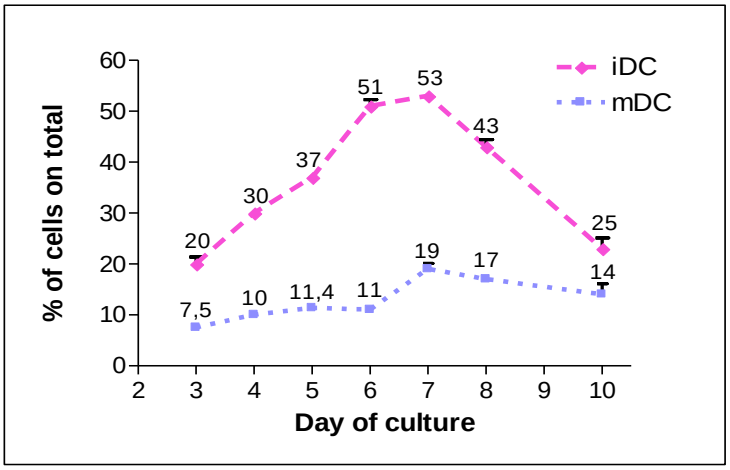

Figure 11*. Growth curve showing immature (iDC) and mature (mDC) percentages from day 3 to day 10 of culture.*

The ratio of immature and mature BM-DCs starting from day 5 to day 10 of culture showed that the highest amount of immature DCs occurred at day 6 (Figure 12), as reported in literature [157].

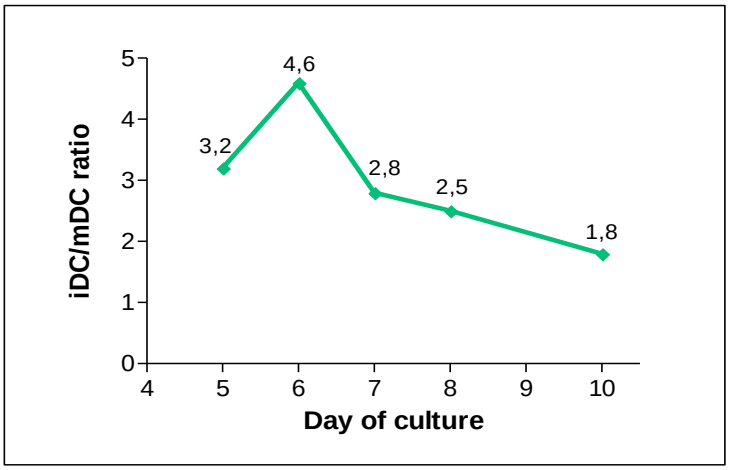

Figure 12. *Immature (iDC) and mature (mDC) dendritic cells ratio from day 5 to day 10 of culture.*

A dose response study was then performed, in order to assess the best concentration of GM-CSF to induce the highest DCs differentiation in presence of standard amounts of IL-4 (900 U/ml). The evaluation at day 6 of the percentage of mature and immature DCs on the total of cells in presence of different quantities of GM-CSF showed that the highest peak of immature DCs occurred using 3000 U GM-CSF (Table 1).

U	ng/ml	% iDC	% mDC	TOTALE DC
10000	28,57	50,7	4,2	54,9
8750	25	57,0	4,2	61,2
3000	8,59	58,2	4,5	62,7
1000	2,85	40,5	7,8	48,3
500	1,43	36,3	9,6	45,9
0	0	30,0	5,7	35,7

Table 1. *GM-CSF dose response study at 6 day of culture.*

2. Dendritic Cells Maturation

To evaluate the ability of BM-DCs to mature after an antigenic stimulus, we pulsed cultured DCs with LPS for 48 hours at different days. The maturation response was evaluated by flow cytometry on the basis of CD11c/ $MHCII^{high}$ expression. Mature DCs percentage was analyzed at basal condition and after LPS treatment each day considered (Figure 13). As shown, LPS enhanced maturation, suggesting that BM-DCs are able to mature after pulsing with a maturation antigen.

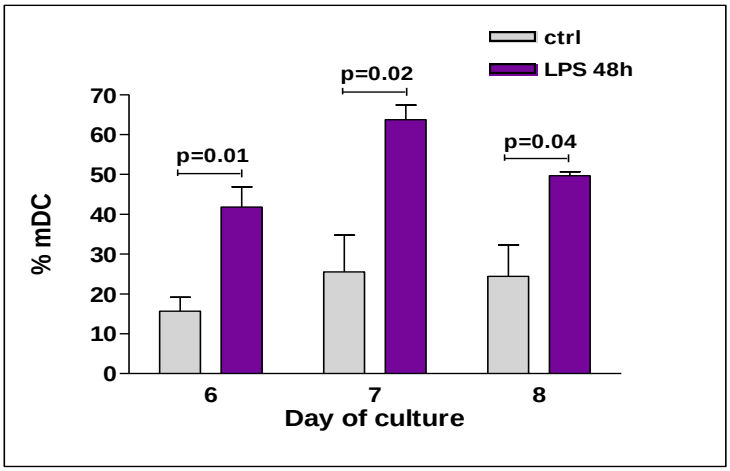

Figure 13. *Evaluation of mature DCs (mDC) percentages at basal condition (ctrl) and after 48 hours of LPS pulsing. Mean values ±SD are indicated.*

Furthermore, the expression of CD80 and CD86 was evaluated as mean intensity fluorescence (MFI) after LPS treatment each day analyzed compared to the mean of the basal controls (Figure 14). LPS-treated BM-DCs displayed a significant up-regulation of both CD86 and CD80 at day 6 and 7 compared to the control, further supporting the idea of a complete functional maturation after antigen pulsing. No significativity was found at day 8, probably due to the high percentage of physiological mature DCs in the culture even in absence of antigenic stimulus.

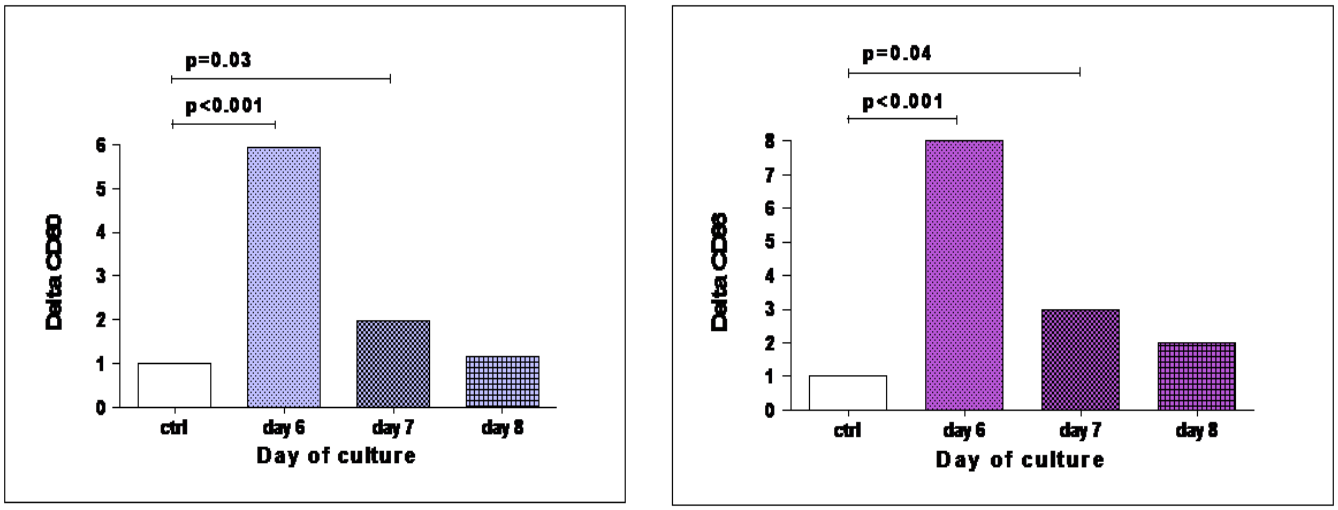

Figure 14. *CD80 and CD86 MFI at day 6, 7 and 8 after LPS treatment compared to untreated cells. Mean values ±SD are indicated.*

3. Dendritic Cells labelling with Magnetic Nanoparticles

BM-DCs were then pulsed with commericial dextran-coated Iron core magnetic nanoparticles called Endorem®, that can be efficiently taken up by immature DCs. Magnetic nanoparticles are contrast agent necessary to monitor DCs distribution *in vivo* by magnetic resonance.
A dose response study was performed at day 6 in order to identify the optimal labelling conditions. 100-200 and 400 µg of Iron Endorem® / ml of culture for 24 hours were thus added to the culture medium and cells analyzed qualitatively and quantitavely.
Labelling efficiency was measured by microscopy after Perl's staining, considering the percentage of cells positive to the Iron-specific labelling on the total of cells in the sample (Figure 15). A qualitative evaluation of the staining revealed an increase in Prussian Blue product proportional to the increase of Iron added to the culture medium. All labelling conditions stained cells efficiently.

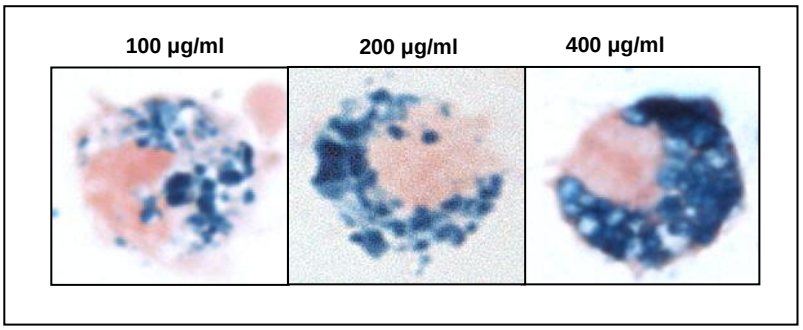

Figure 15. *Perl's staining after Endorem® labelling, dose-response study.*

These data were confirmed also by the fall of relaxation time T2 measured by relassometric assay (Table 2). Such experiment showed quantitatively that labelling with 200 and 400 µg Iron/ ml stained cells efficiently, while 100 µg Iron/ ml generated a signal too low to be detected by magnetic resonance *in vivo*. Data showed a T2 time decrease proportional to the concentration of Iron in the medium, with a R^2 of 0.999 (data not shown).

MNPs	Concentration (ug iron/ml)	T2 (ms)
Control	-	2889
Endorem®	100	480
	200	216
	400	94

***Table 2**. Dose response study, relassometric analysis.*

Cell viability after Endorem® labelling was evaluated using an automated cell counter (Figure 16). A significant decrease in viability occurred staining cells with 400 µg of Iron/ ml of culture medium. This result was confirmed by literature [200].

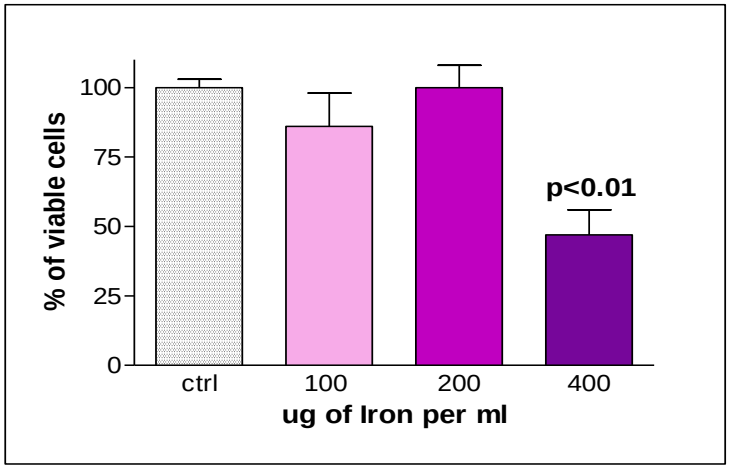

***Figure 16.** Dose response study, viability analysis. Mean values ±SD are indicated.*

Accordingly to the results obtained, 200 µg Iron of Endorem®/ ml of culture was chosen as the best concentration to use for further studies, as confirmed by literature [190].
A kinetic study was then performed incubating day 6 BM-DCs with 200 µg Iron of Endorem®/ ml of culture for different times. Prussian Blue Staining showed that Iron-labelled DCs content increased over time (Figure 17). An optimal qualitative labelling was achieved between 6 to 24 hours, with 48 hours incubation time leading to over-loaded cells.

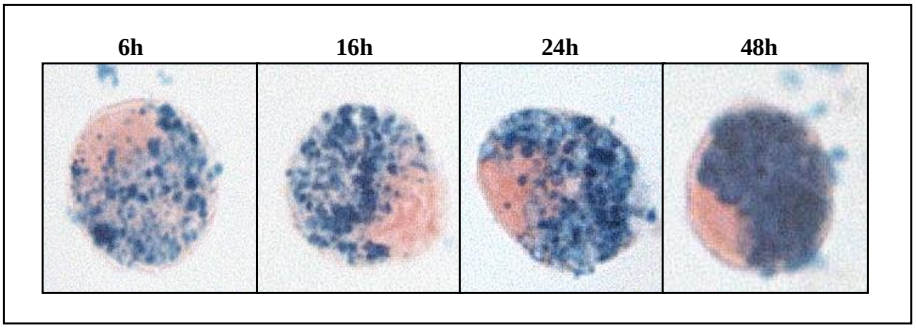

***Figure 17.** Perl's staining after Endorem® labelling, kinetic study.*

Viability assessed by cell counting showed that after 24 hours incubation a significant increase in cell death happened (Figure 18). The fall of relaxation time T2 by relassometric assay confirmed these data (Table 4).

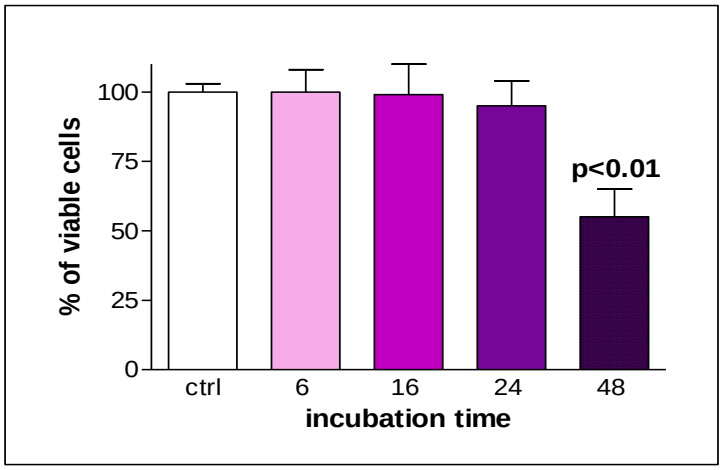

Figure 18. *Incubation time kinetic, viability analysis. Mean values ±SD are indicated.*

MNPs	Incubation time (hours)	T2 (ms)
Control	-	2889
Endorem®	6	377
	16	315
	24	258
	48	364

Table 3. *Incubation time kinetic, relassometric analysis.*

Hence, in order to perform an efficient MNPs labelling protocol and avoid functional alterations, 16 hours incubation with 200 µg Iron of Endorem® / ml of culture was chosen as our standard labelling procedure.
Flow cytometry was used to evaluate any possible influence of MNPs labelling on BM-DCs phenotype. Thus, CD86 and CD83 mean fluorescence intensity was evaluated on DCs after Endorem® labelling and on unlabelled controls (Figure 19). On the basis of co-stimulatory molecules and activation markers expression, no difference in the activation status was observed after DCs labelling with Endorem®, suggesting no interference of MNPs in functional DCs activities.

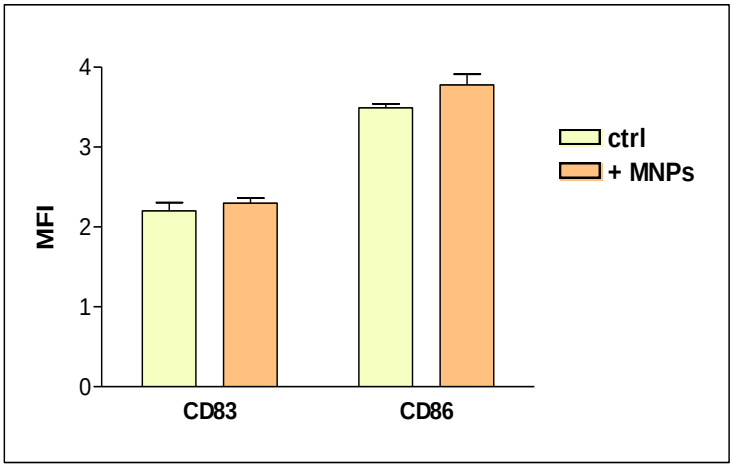

Figure 19. *CD83 and CD86 MFI on MNPs labelled DCs (+ Endorem®) and their controls (- Endorem®). Mean values ±SD are indicated.*

The ability of DCs to mature despite Endorem® was then evaluated after treatment with LPS for 48 hours at different days of culture (Figure 20). Mature DCs percentage was established by flow cytometry on the basis of CD11c/ MHCII^{high} expression. No statistically significant differences were observed in the maturation state after LPS pulsing on MNPs-labelled DCs compared to their control. Dendritic cells maintained their ability to mature after LPS treatment at all the time points evaluated.
In conclusion, labelling with Endorem® did not influence the phenotypical and functional features of labelled DCs.

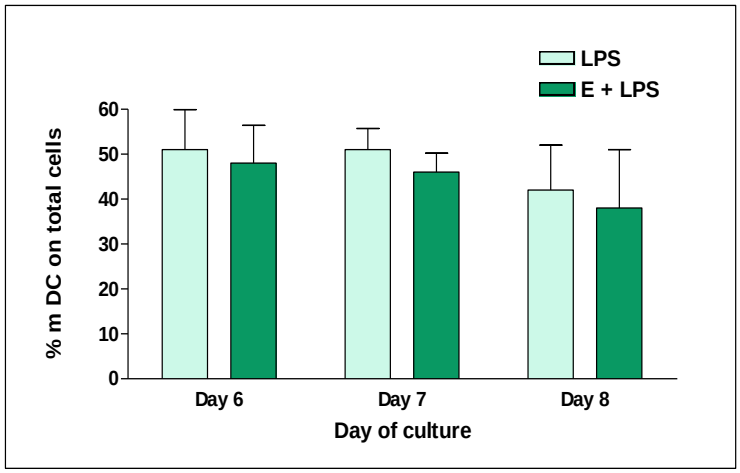

Figure 20. *Mature DCs percentage after treatment with LPS of Endorem® labeled DCs and their controls at different days of culture. Mean values ±SD are indicated.*

4. Ultrastructural Analysis by Transmission Electron Microscopy (TEM)

The intracellular presence of Endorem® was evaluated qualitatively by transmission electron microscopy, investigating their localization with respect to the cells. Day 6 DCs were stained with 100 and 200 µg Iron/ ml of culture for 16 hours (Figure 21). In both staining conditions Iron could be detected inside cells, in particular inside lysosomes. The amount of Iron appeared proportional to the amount of MNPs added to the cell culture.

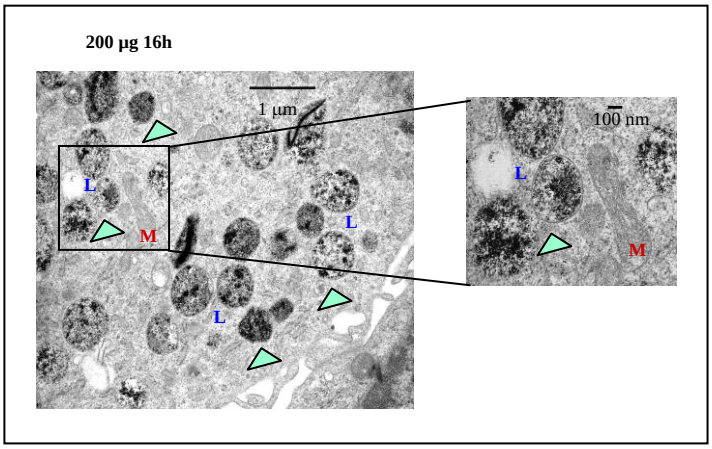

Figure 21. *TEM analysis: DCs after 16 hours incubation with 200 µg Iron MNPs / ml of culture. L=Lysosomes (green arrows); M= Mitochondria.*

Furthermore, TEM allowed to study the mechanisms of Endorem® entry into DCs (Figure 22). For this purpose, DCs were pulsed with 200 µg Iron/ ml of culture for 1-4 and 16 hours. After 1 hour incubation, initial adhesion and extension of plasma membranes around MNPs could be observed by means of a process consistent with vesicle-mediated phagocytosis (Figure 22 A). The amount of Iron increased over incubation time (Figure 22B, 22C). No Iron was detectable in the control culture, where no Endorem® were added.

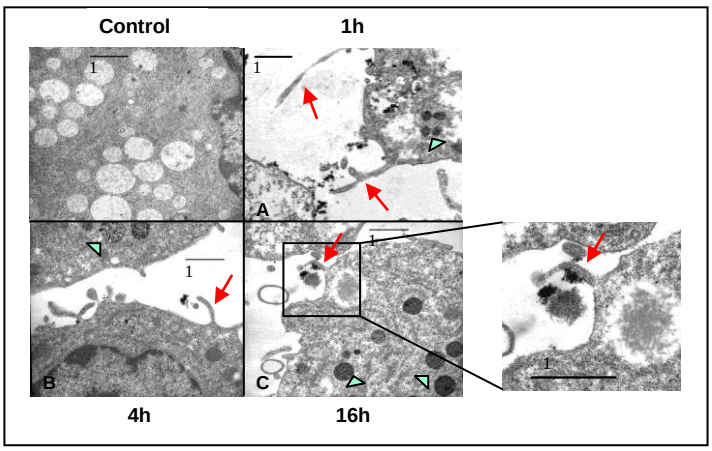

Figure 22. *TEM analysis: MNPs mechanisms of Endorem® entry. Extension of plasma membrane around MNPs (red arrows), iron inside lysosomes (green arrows).*

5. Antigen Loading DCs

Heat-shocked tumour lysates could be used to pulse DCs and elicit a potent specific anti-tumor response. The heat treatment that tumour receives increases the amount of heat shock proteins that act as chaperon proteins and thus enhance the antigens transport to DCs surface [201]. In order to establish the optimal tumour lysate amount to use, day 6 BM-DCs were incubated for 24 hours with different concentrations of antigens, expressed as a ratio between DCs and an equivalent number of tumour cells. The examined conditions were: 1:10;1:5; 1:2,5; 1:1; 2,5:1; 5:1; 10:1. After 24 hours incubation, DCs of every condition were analyzed by flow cytometry for the expression of CD86 and CD11c/ MHCII^{high}. On day 6, 11% of unpulsed DCs used as control presented a mature phenotype. After incubation with tumour lysate, in each condition analyzed, the percentage of mature DCs greatly increased, ranging from 75% to 90% (data not shown). Viability analysis (Figure 23) and cell morphology evaluation with optical microscopy allowed to establish 1:5 and 1:10 ratios as the best conditions for DCs tumour lysate loading, with a viability around 100% in both conditions.

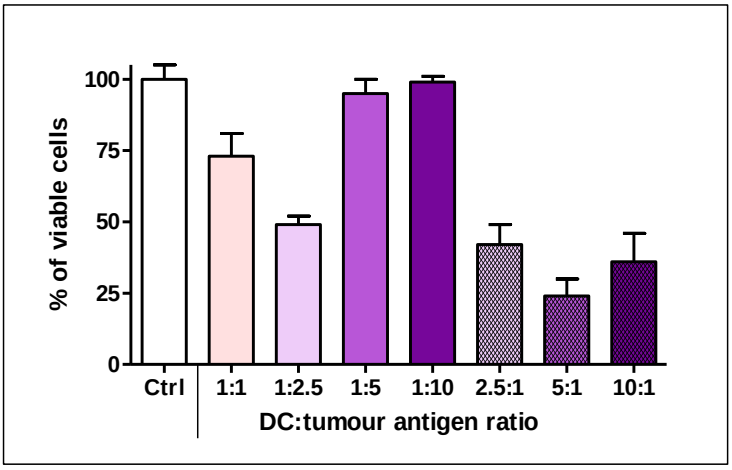

Figure 23. *Viability of mature DCs after 24 hours incubations with different concentrations of tumoral antigens. Mean values ±SD are indicated.*

To evaluate the best antigen pulsing ratio we then analyzed the ability of 1:5 and 1:10 pulsed DCs to activate a T cell response, measured as the kinetic of IFN-γ production in each condition (Figure 24).
Based on the magnitude of the T cells response, we could state that antigen-loaded DCs were able to trigger a specific response, especially when pulsed with 1:5 ratio. Of note, high levels of IFN-γ could be achieved after 5 days stimulation, indicating that T lymphocytes needed a prolonged DCs stimulation to give rise to a proper response.

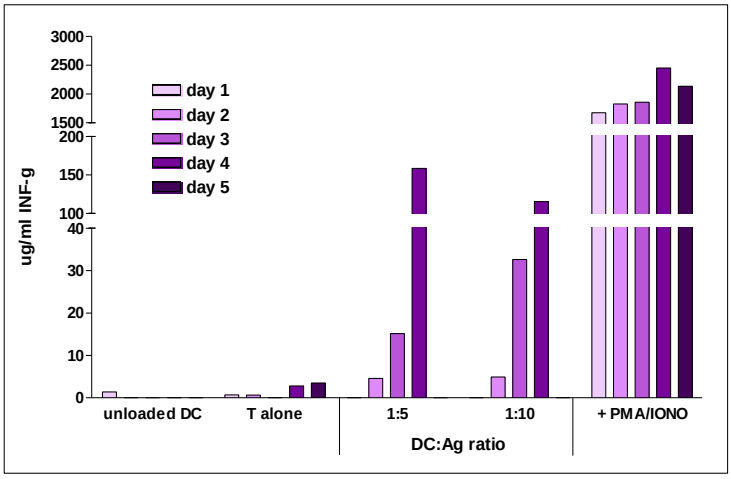

Figure 24. *INFγ production by T-cells after 1:5 and 1:10 antigen loaded DCs stimulation. T alone and unloaded DCs were used as negative control, PMA/IONO was used as positive control. Mean values ±SD are indicated.*

6. Functional Evaluation

Efficient initiation of T-cell dependant immunity is a complex sequence of events that ultimately depends upon simultaneous co-localization of APCs and antigen-specific T lymphocytes. The ability of DCs to migrate to sites of T cells priming is fundamental to their capacity to elicit efficient immune responses

In order to investigate if our antigen loading protocol could affect DCs functionality and to assess the best DCs/ tumour antigen ratio condition we first performed an *in vitro* migration assay in a transwell plate. DC trafficking is known to be tightly regulated by specific chemokines: MIP1α and MIP1β, ligands for CCR1 and CCR6 respectively, are expressed in the peripheral tissues and induce immature DCs migration; MIP3β and 6Ckine are specifically expressed by lymph nodes and determine CCR7-mediated *in vivo* migration of mature DCs. Thus, for our assay we used medium alone, MIP1α and MIP1β as negative controls and compared to MIP3β and 6Ckine in their ability to trigger 1:5 and 1:10 antigen loaded DCs chemotaxis.

In both antigen pulsing conditions migration toward medium alone was absent, toward MIP1α and MIP1β was weak. On the contrary, MIP3β and 6Ckine attracted antigen loaded DCs (Figure 25).

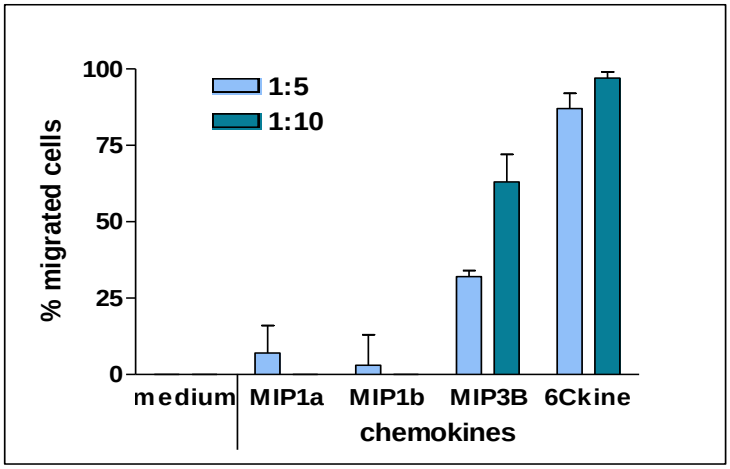

Figure 25. *Percentage of in vitro migrated DCs. Mean values ±SD are indicated.*

After cell counting, migrated DCs were analyzed by flow cytometry for the expression of CCR7 (Figure 26). MIP1α and MIP1β were both able of attracting a small percentage of $CCR7^{low}$ DCs. In contrast, MIP3β and 6Ckine were able to attract high amount of $CCR7^{high}$ DCs.

These data suggest that tumour antigens-pulsing led to DCs specific maturation, with DCs displaying high amounts of CCR7, responsible of *in vitro* DCs migration toward MIP3β and 6Ckine in a transwell assay.

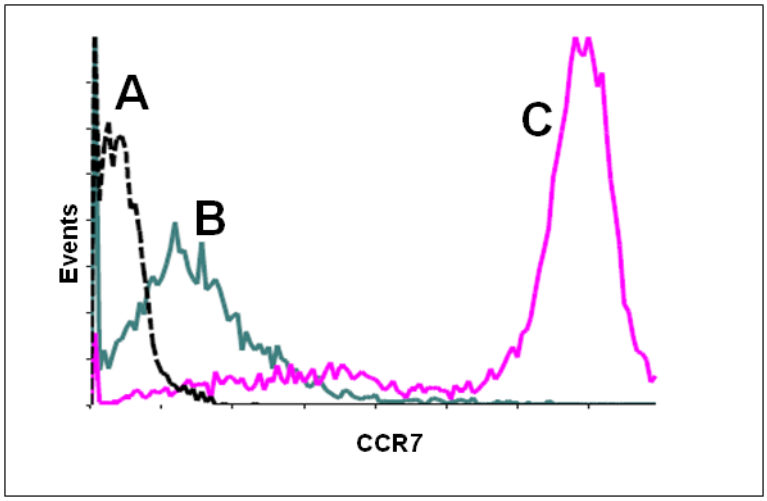

Figure 26. *Exemplificative CCR/ overlay plot.* ***A*** *CCR7 isotype control;* ***B*** *CCR7 on DCs migrated towars MIP1α;* ***C*** *CCR7 on DCs migrated toward MIP3β.*

7. T Cells Proliferation

We then investigated the ability of tumour lysate-pulsed DCs to prime syngenic T cell *in vitro* as measured by tumour-specific proliferative response. [^{3}H]thymidine proliferation assay was performed after 7 days of T lymphocytes and antigen-pulsed DCs co-cultures with proper controls. In our first studies we used splenic T cells from wild-type animals, but no signal were detected (data not shown), probably due to the lack of primed T cells. For the following experiments, T cells from the spleen of MMTV-v-Ha-Ras bearing neoplastic lesions were used and proliferation was analyzed by CFSE assay.
Both 1:5 and 1:10 DC: Antigen ratio conditions were used, with unoaded DCs as negative control and T lymphocytes stimulated with PMA and Ionomycine as positive controls. In both conditions antigen-loaded DCs triggered a T cells proliferation, demonstrating that *in vitro* antigen-loaded DCs maintain their ability to activate T cells. In particular, CFSE assay (Figure 27) showed that 1:5 DC: Antigen ratio condition is able to stimulate 79% T lymphocytes proliferation, with a proliferation index of 2,93. Similarly, 1:10 DC: Antigen ratio condition led to 76.8% T lymphocytes proliferation, with a proliferation index of 2,87. No proliferation was observed in co-cultures with unloaded DCs. Thus, BM-DCs are functionally active, as they are able to elicit a T lymphocytes proliferative response.

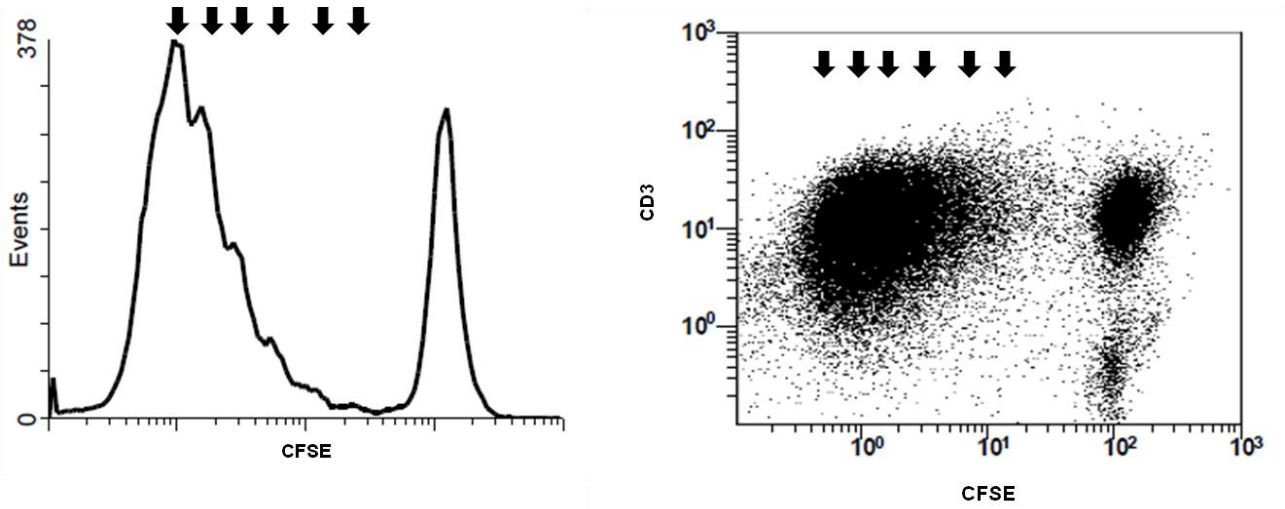

Figure 27. *CFSE assay of 1:5 antigen-pulsed DCs. On the right CFSE histogram, on the left CD3/ CFSE dot plot. Cell divisions are shown (black arrows).*

8. Cytokines Production

We then studied the kinetics of cytokine production by 1:5 antigen-pulsed DCs and T lymphocytes co-cultures over time. Anti-tumour immunity induced by DCs vaccination is dependant on IFN-γ *in vivo*. Therefore, we investigated the influence of antigen-pulsed DCs on the induction of IFN-γ production by flow cytometry (Figure 28) and ELISA (Figure 29). Flow cytometric analysis showed that high amounts of IFN-γ

were produced by CD3+ lymphocytes on day 1 of co-culture with antigen-loaded DCs. Such data suggested that primed T lymphocytes extracted from spleens of tumour-bearing mice could be activated once triggered by DCs *in vitro*. Moreover, IFN-γ production after antigen-loaded DCs stimulation increased over time, with a small decrease only on day 7 probably due to T cells death.
Of note, stimulated T cells promoted a Th1 specific response that could be able to eradicate tumour *in vivo*. Indeed, in ELISA IL-4 levels (Figure 30) were undetectable in each condition examined and low levels of IL-10 were found (Figure 31), except for unloaded DCs in co-culture with T lymphocytes. In that condition IL10 increased over time, suggesting a role of IL-10 in inducing tolerance. However, the lack of IL-10 in all other conditions is a desirable element for the success of a protocol in which cell activation against tumour is critical. Indeed, Th2 cells interrupt the expression of tumour immunity since IL-4 and IL-10 inhibit the generation of Th1 from precursors and modulate the competence of antigen-presenting cells to activate this lymphocyte subpopulation [202].

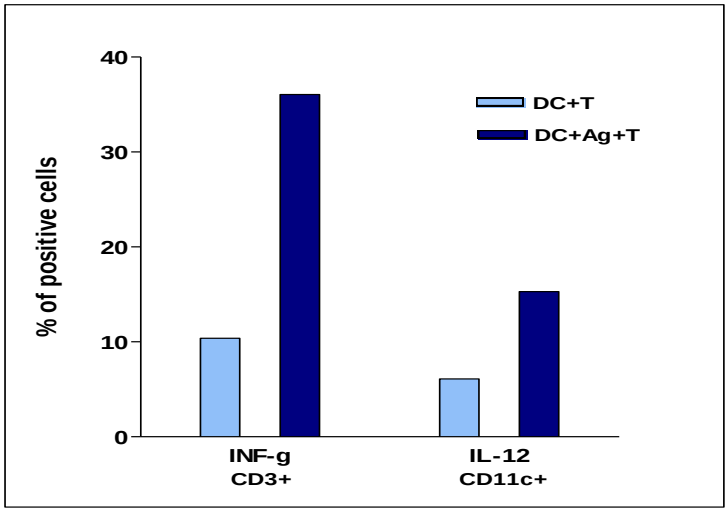

Figure 28. *Intracellular cytokines production by flow cytometry. Co-cultures with T lymphocytes, both with 1:5 antigen-pulsed (blue) or unpulsed (light blue) DCs, were evaluated for the production of IFN-γ on CD3 cells and IL-12 on CD11c^{+} cells.*

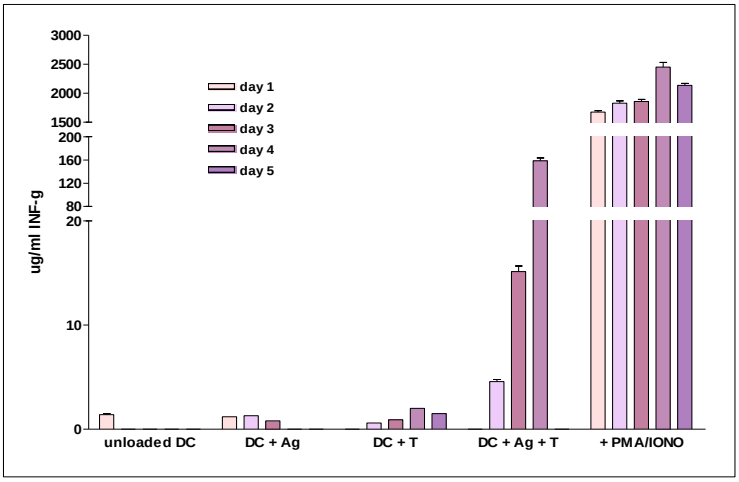

Figure 29. *IFN-γ production by ELISA over time. 1:5 antigen-pulsed or unpulsed DCs, alone or in co-culture with T lymphocytes were evaluated. PMA/IONO was used as positive control. Mean values ±SD are indicated.*

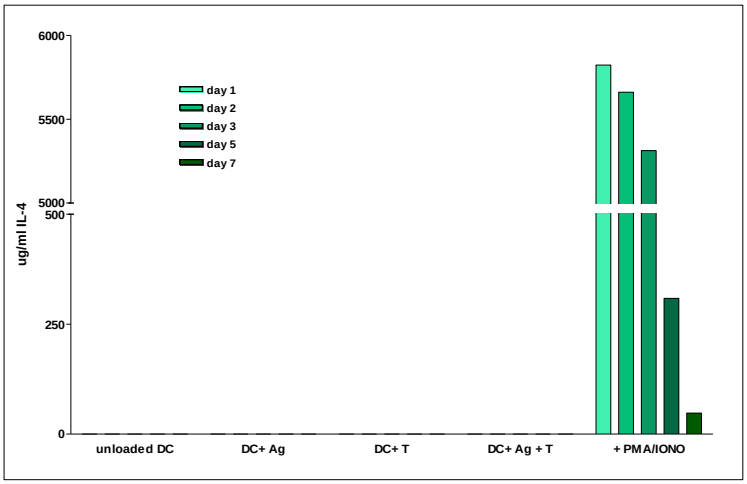

Figure 30. *IL-4 production by ELISA over time. 1:5 antigen-pulsed or unpulsed DCs, alone or in co-culture with T lymphocytes were evaluated. PMA/IONO was used as positive control. Mean values are indicated.*

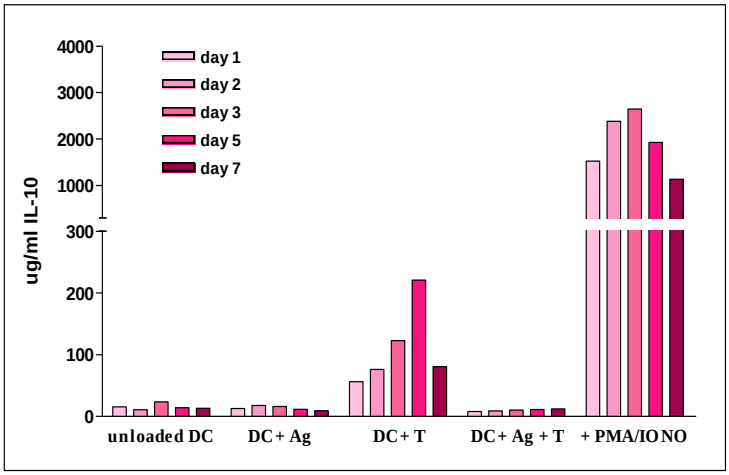

Figure 31. *IL-10 production by ELISA over time. 1:5 antigen-pulsed or unpulsed DCs, alone or in co-culture with T lymphocytes were evaluated. PMA/IONO was used as positive control. Mean values are indicated.*

A major attribute of mature DCs is the synthesis and release of cytokines with important modulatory functions in inflammation and T cell differentiation. Especially, IL-12 production is an important marker for DCs maturation for cancer-therapy and can be used as a tool for selecting adjuvant inducing Th1-dominant immune state. We therefore, tested whether tumour lysate and T lymphocytes presence may regulate the production of IL-12 in DCs. Intracellular staining of IL-12 (Figure 28) and IL-10 (data not shown) revealed that DCs expressed high amounts of IL-12 especially on day 1 of culture. The production remained steady the other days of culture until day 5. After that, our results showed a decrease in IL-12 presence that could be due to cell exhaustion or cell death [203]. When supernatants were analyzed by ELISA, IL-12p40 and IL-12p70 showed result difficult to interpret, as no significant production was highlighted in any of the conditions analyzed (Figure 32).

As already told, IL-10 production in ELISA was detectable only in unloaded DCs co-cultures with T lymphocytes, with an increase over time until day 5; low and steady production of IL-10 was observed in the other conditions. The percentage of IL-10 produced by antigen-loaded DCs measured by flow cytometry was low in the early days of culture and lightly increased between day 5 and 7 (data not shown).

Taken together, these results suggest that BM-DCs are properly matured and are able to elicit a specific and efficient T cells response *in vitro*, and could be then used *in vivo* to trigger an efficient anti-tumour immune response.

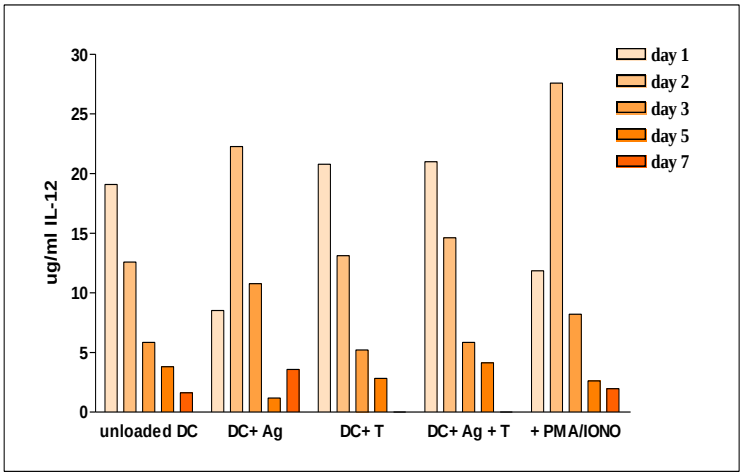

Figure 32. *IL-12 production by ELISA over time. 1:5 antigen-pulsed or unpulsed DCs, alone or in co-culture with T lymphocytes were evaluated. Mean values are indicated.*

9. In vivo MRI

To investigate the ability of BM-DCs to migrate *in vivo* to the draining lymph nodes, we injected MNPs-labelled antigen-loaded DCs into the footpad of syngenic MMTV-v-Ha-Ras mice bearing neoplastic lesions. This mouse model bears the same breast tumour lesions we lysed and used to load DCs.
The day before cell administration, the sites of injection were pre-treated with TNF-α to create an inflammatory microenvironment that could enhance DCs migration. The injection site was chosen depending on the localization of the tumour mass in the animal model: for lesions occurring in the rostral mammary glands, we injected DCs into the footpads of anterior limbs, expecting DCs to migrate towards the proper and accessory axillary lymph nodes; for lesions involving the caudal mammary glands the injection was performed into the footpads of posterior limbs, expecting DCs to migrate towards the popliteal and subiliac lymph nodes.
DCs labelled for 16 hours with 200 µg Iron Endorem®/ ml of culture and loaded with 1:5 and 1:10 DC: Antigen ratio for 24 hours were injected together with a second dose of TNF-α. Mice were then visualized by Magnetic Resonance Imaging. Acquisitions were performed after 4, 24 and 48 hours post-injection using MSME and FLASH sequences. MSME sequences showed images describing the Iron content with a good anatomy resolution, because of the correction of the magnetic field local deformation. FLASH sequences exalted such deformations thanks to the signal enhancement provoked by the presence of Iron, but provided a less defined image as far as the anatomical information is concerned.
Labelled DCs could be easily detected in the lymph nodes at the side of injection as regions of hypointensity (Figure 33). No such regions were observed in the uninjected side control.
As positive control, MNPs alone were injected into the footpads and found in the lymph node thanks to lymphatic draining (data not shown).
Both 1:5 and 1:10 antigen loaded DCs migrated to the lymph nodes (Figure 34 and Figure 35).
1:5 antigen loaded DCs were injected in the anterior footpad of tumour bearing mice. MRI images showed a T2 reduction in the accessory axillary lymph node 24 hours post-injection (Figure 34A) and an even more marked reduction after 48 hours (Figure 34B). MRI images revealed the presence of Iron in the accessory axillary lymph node but failed to show the proper axillary lymph node, where DCs were also expected because both lymph nodes drain from the anterior limb. A reason for this discrepancy can be found in the section scans: proper axillary lymph nodes were very elongated and close to the chest [204]. Moreover, in the axial sections the observation is difficult because of the little node section. Thus, coronal and sagittal sections will be registered in future experiments.

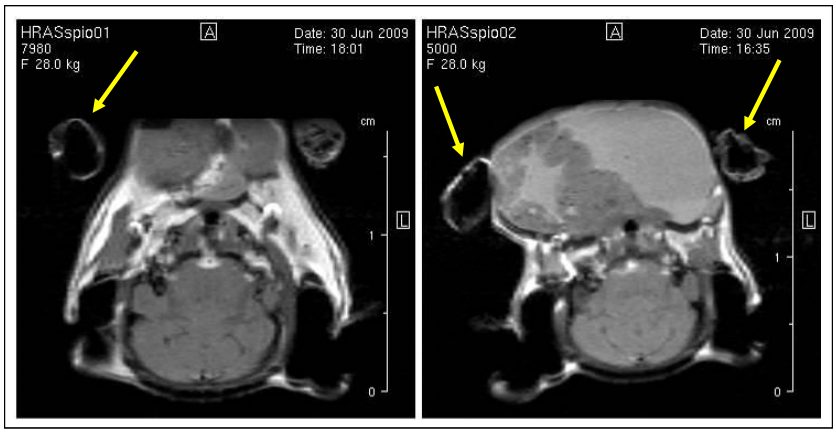

Figure 33. *MRI MSME sequence of mouse anterior footpad. Injection (yellow arrows) in the right limb only (left image) and in both limbs (right image).*

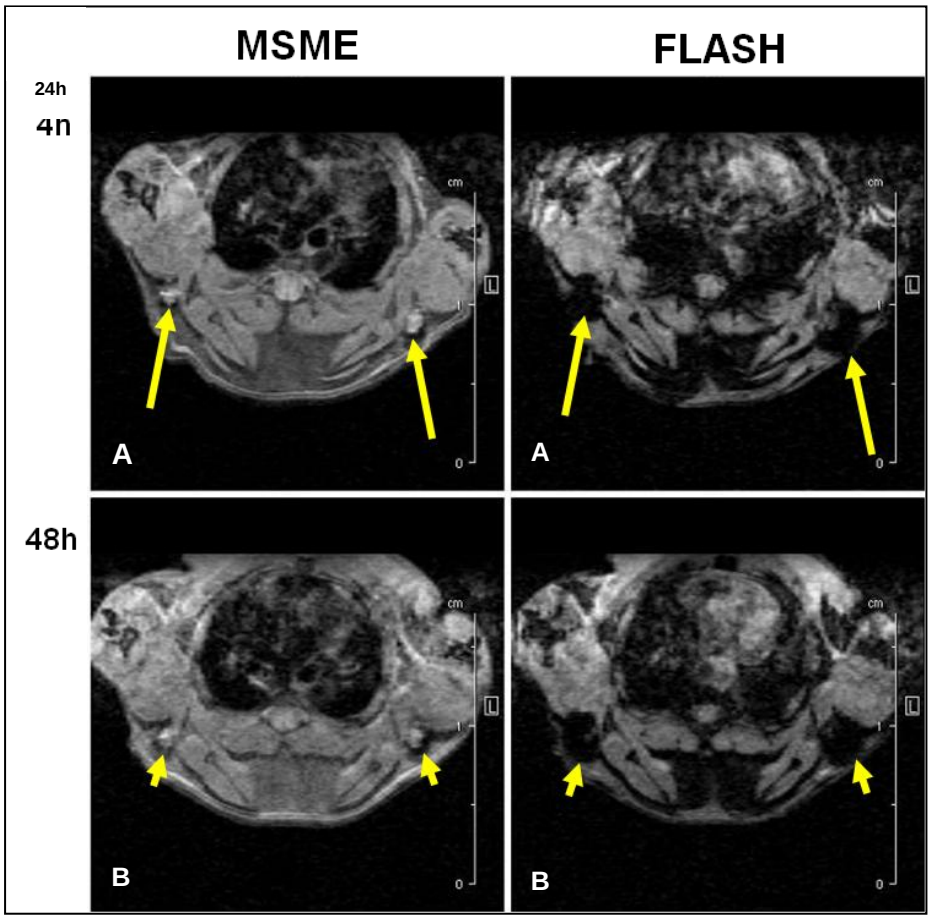

Figure 34*. MRI of axillary lymph nodes. 1:5 antigen loaded DCs were injected in both the anterior footpads. Iron was detectable in the axillary lymph nodes 24 hours (panel A) and 48 hours (panel B) from DCs administration. MSME sequence (right panel) and FLASH sequence (left panel).*

1:5 and 1:10 antigen loaded DCs were also injected in the right posterior footpad. 4 hours post-injection, a T2 decrease was determined, visible both in MSME and FLASH sequences (Figure 35A). 1:10 antigen loaded DCs produced a visible signal only in the FLASH sequence (Figure 35B). Thus, FLASH sequences have greater sensitivity in the T2 reduction detection and moreover, tumoral antigen quantity used to load DCs can affect the speed or the number of migrating cells. Animals were studied for 48h and images showed that signal intensity did not decrease in all the acquisitions (data not shown).

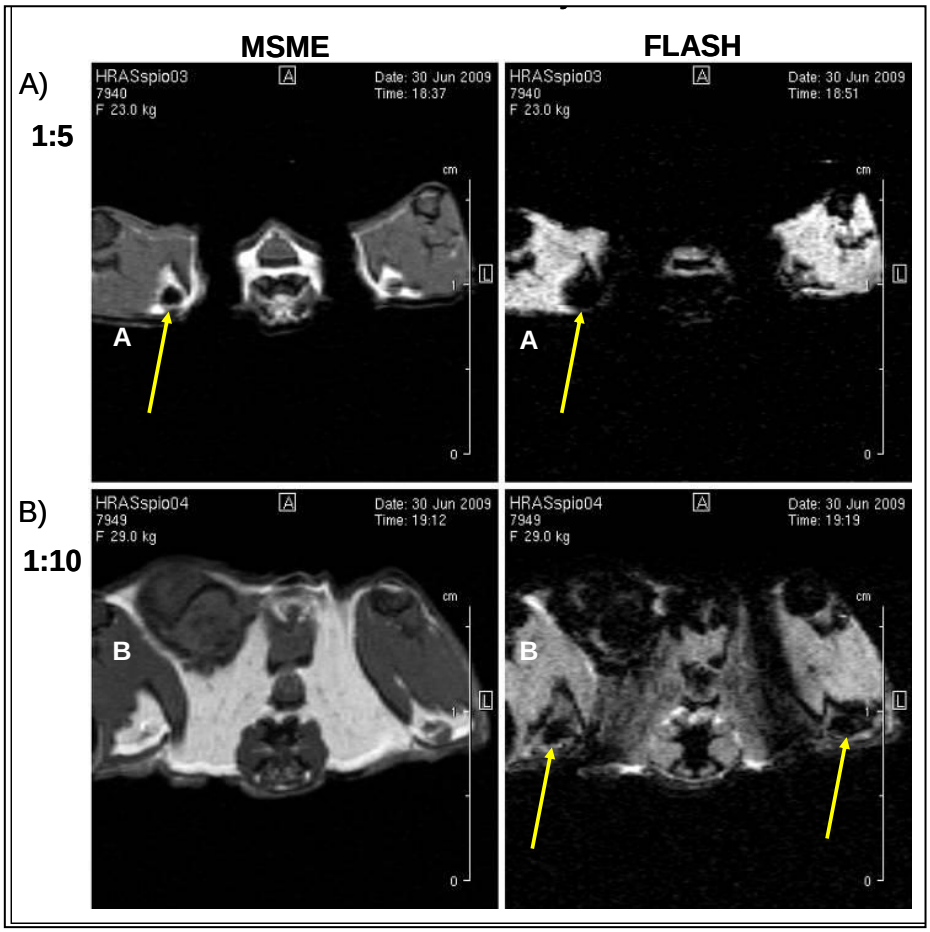

Figure 35. *MRI of popliteal lymph nodes. MSME sequence (left panels) and FLASH sequence (right panels). Panel A: 1:5 antigen loaded DCs were injected in the right posterior footpad. Iron in the popliteal lymph nodes was detectable 4 hours post-injection (yellow arrows). Panel B: 1:10 antigen loaded DCs were injected in both posterior footpads. Only the FLASH sequence exalted the T2 decrement in both popliteal lymph nodes 4 hours post-injection.*

Results obtained by MRI showed different signal intensity over time, depending on the injection site. Indeed, 4 hours post-injection the presence of Iron in the popliteal lymph node is clear, but it appeared later in the axillary nodes and is clearly visible at 24 and 48 hours post injection. The differences observed in the migration time of labeled-DCs with different injection sites can be easily explained if considering the distance between the injection site and the nodes. Axillary lymph nodes are indeed farther than popliteal from the injected footpads and T2 reduction can be observed in popliteal nodes earlier than in axillary.
MRI study of the subiliac lymph node, which is the second lymphnodal station in the posterior limb, showed that labelled and injected DCs did not migrate to that node. These data seem to confirm the hypothesis by which two different DCs populations are involved in antigen presentation: a first migratory population presenting the antigen to a second DC population residing within the node, responsible to present such antigen to T cells [16, 17].
48 hours after cell administration lymph nodes were collected and evaluated for Iron content by specific Perl's staining (Figure 36). In cortical and paracortical regions of the omolateral lymph node to dendritic cells injection site Iron labelled cells could be observed, while no Iron was detectable in the control lymph node, contralateral to the injection side.

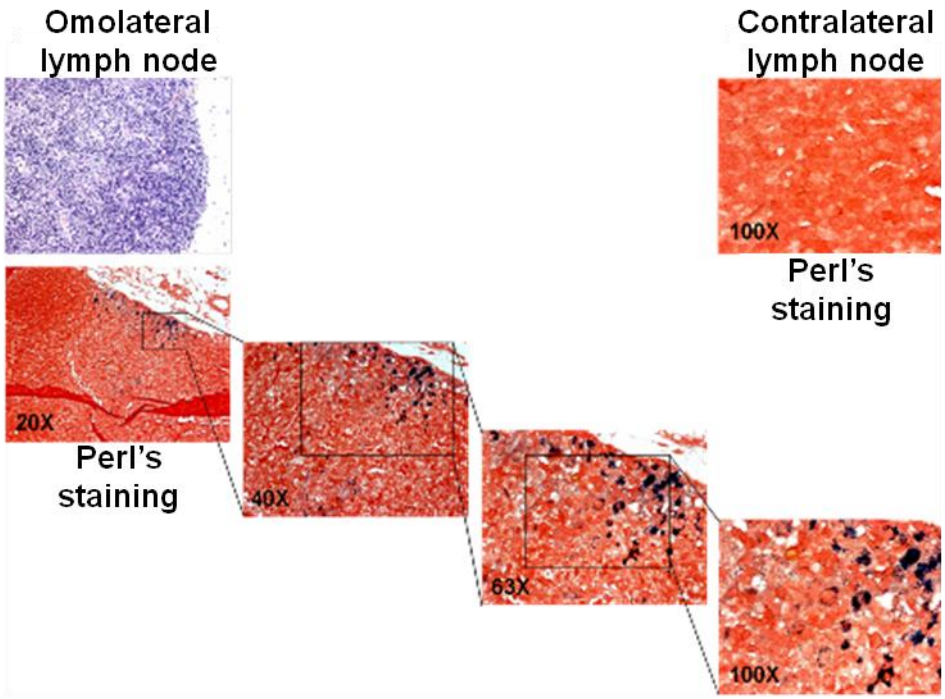

Figure 36. *Histological analysis of collected lymph nodes with consecutive optical enlargement of Perl's staining. In the control lymph node no Iron can be observed.*

Immunohistochemistry assay was also performed on the adjacent sections. The Iron-containing cells revealed by Perl's staining correlated with CD208 expression (Figure 37C), specific for DCs, but didn't correlate with the macrophage marker (Figure 37A). Hematoxylin staining (Figure 37B) clearly shows that Iron appeared inside cells that are not macrophages. Contrast pattern caused by MNPs labelling didn't appear due to random interstitial deposition of Iron-oxide particles but rather to intracellular uptake particles, mainly found in DCs. Thus, MNPs labelled and antigen loaded DCs could migrate *in vivo* from the injection site to the draining lymph nodes.

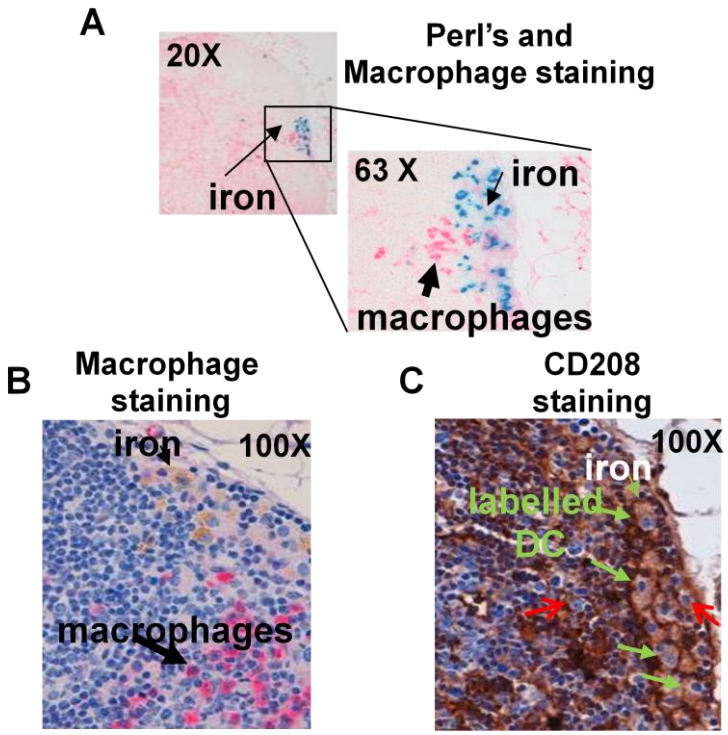

Figure 37. A *Perl's (thin arrows) and macrophage staining (thick arrows)* ***B*** *Macrophage staining and Haematossiline; iron showed as brown spots* ***C*** *DCs are stained with anti CD208: Iron (light brown spots) is within DCs (green arrows); resident unlabelled DCs (red arrows).*

10. DC labelling with ^{111}Indium-oxine

^{111}In-Oxine cell labelling allowed to follow cell distribution by SPET. For ^{111}In-Oxine has 69 hours half-life, to obtain images with good resolution we decided to perform the imaging 24 and 48 hours post-injection.
A dose-response study was carried out in order to evaluate the effect of ^{111}In-Oxine labelling on antigen loaded DCs. The conditions examined were 30-60-150 µCi every $2x10^6$ cells and corresponded to 80%, 83% and 75% labelling efficiency respectively. After cell counting, we concluded that DCs viability was not affected by ^{111}In-Oxine labelling procedures (data not shown). As no significant differences could be observed in labelling efficiency, 30 µCi was chosen as optimal labeling dose, as reported in literature [188].
Thus, cell labelling with ^{111}In-Oxine could be used for *in vivo* imaging of DCs migration by means of nuclear techniques and exploiting the higher sensitivity of SPET in respect to MRI.

11. In vivo SPET imaging

To investigate the ability of BM-DCs to migrate *in vivo* to the draining lymph node, we injected 1:5 and 1:10 antigen-loaded DCs labelled with 30 µCi of ^{111}In-Oxine in presence of TNF-α in the anterior limb of syngenic MMTV-v-Ha-Ras mice bearing neoplastic lesions. Cells were injected into the limb and not into the footpad of mice as in MRI in order to reduce background noise. As for MRI, the day before cell administration the sites of injection were pre-treated with TNF-α to enhance DCs migration.
Migration of DCs was observed for both loading conditions 4 hours post-injection. The signal remained clearly detectable for 24 hours (Figure 38) in the accessory and proper axillary lymph nodes, integrating the data derived by MRI. After 48 hours the signal at the lymph node was not detectable anymore, probably due to radioactive decay. Ineed, the same problem was found at the injection site, where the radioactive signal was higher at 4 and 24 hours but decreased at 48 hours.

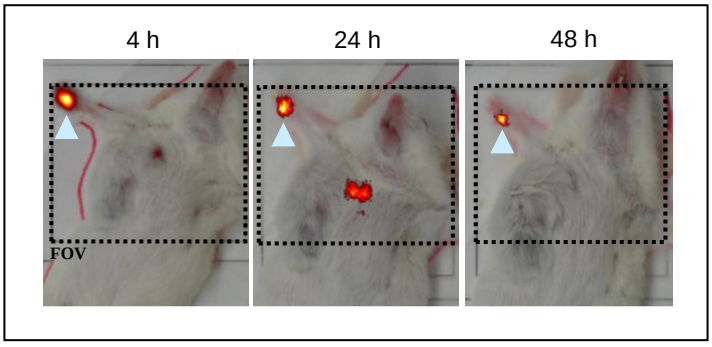

Figure 38. *SPECT imaging of antigen loaded DCs labelled with ^{111}In-Oxine in proper and accessory axillary lymph nodes. DCs distribution 4, 24 and 48 hours post-injection. Site of injection (light blue arrows).*

Cells were injected also in the posterior limbs (Figure 39). SPET images showed a clear signal at popliteal lymph nodes for 48 hours. In this occasion, the injection site was shielded with lead to allow the detection of the node signal, as the injection site signal, higher and close to the lymph node, would have hidden it.

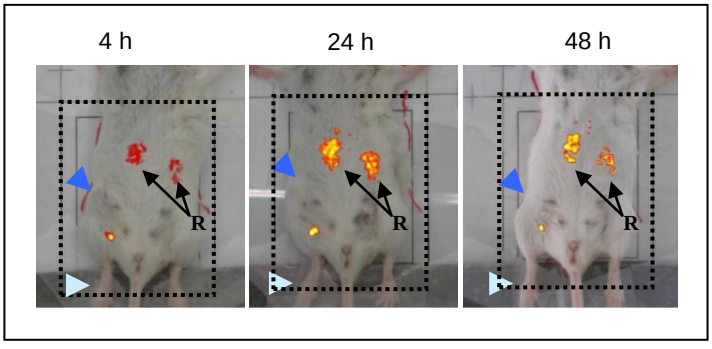

Figure 39. *Popliteal lymph node SPET imaging 4, 24 and 48 hours post-injection. Injection site (light blue arrows) were shielded with lead, inguinal lymph node are shown (blue arrows). R=kidneys, where free ^{111}In.*

Free ^{111}In-Oxine was injected in the posterior limb as control (Figure 40). Free ^{111}In did not localize in the lymph nodes but spread in the abdomen. Furthermore, 48 hours post-injection signals were not detectable anymore. This site too was shielded with lead.

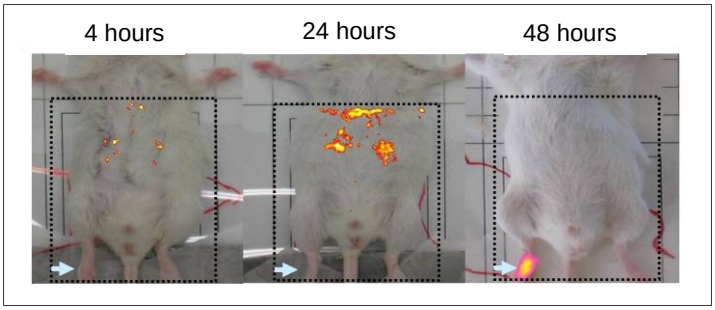

Figure 40. *Free ^{111}In-Oxine injected alone 4, 24 and 48 hours post-injection. Injection site (light blue arrows) were shielded with lead.*

The pictures were taken with a digital camera separated from the γ-camera and were overlaid with the photon emission map. This shrewdness permitted to overcome the lack of anatomical information, the intrinsic limit of SPET. SPET images fail to localize exactly the source of the emitted photon and indeed the emission map resulted to be only a bi-dimensional projection of a three-dimensional mouse model. For this reason, the identification of lymph nodes was derived from the comparison between our acquisition and the descriptive image realized in literature [204].
A confirmation of the presence of radioactivity in the lymph nodes came from the *ex vivo* analysis of the collected organs (Figure 41). A significant increase of the radioactivity in the omolateral organs of the injection side was found, while only a small level of activity was visible in the contralateral side, that could be due to the biodistribution of free ^{111}In. Then, the observation of higher levels of radioactivity in the omolateral lymph nodes led us to hypothesize that it could be due to specific DCs migration.
In SPET analysis, as in MRI, no inguinal signal was detectable both *in vivo* (Figure 38) and *in vitro* (Figure 41).

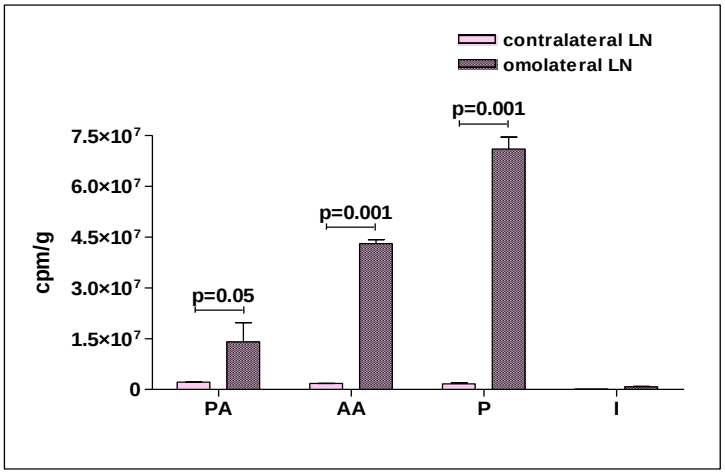

Figure 41. *Lymph nodes (LNs) ex vivo analysis with gamma counter. PA= Proper Axillary; AA= accessory axillary; P=Popliteal; I=Inguinal lymph nodes. Mean values ±SD are indicated.*

Cell labelling with ^{111}In-Oxine produced very low backgrounds in non target tissues, due to a very low redistribution of unbounded radionuclide. Furthermore this technique revealed the great sensitivity of the prototypical sensor provided by the Politecnico of Milan (Professor Carlo Fiorini).

Conclusions

Much attention has currently focused on the biology of dendritic cells in view of their possible clinical use as cellular adjuvants in the treatment of tumours. DCs are professional antigen-presenting cells playing key roles as immune sentinels and initiators of T-cell responses. Their decisive role in inducing both immunity and tolerance has boosted research to understand and exploit their unique immune-modulatory capacity in immunotherapy. Since several studies on animal models using DCs have shown encouraging responses, many preclinical and clinical studies in tumour treatment are underway. Vaccines prime the immune system, establishing an antigen-specific memory that mitigates infection when exposure occurs and precludes disease occurrence. Most efforts to develop cancer vaccines have focused on the treatment of established cancers, targeting tumour associated antigens to elicit a specific immune response. However, cancer vaccination strategies used after the appearance of malignant lesions generally have been unsuccessful in inducing tumour regression and improving survival. One of the critical factors shown to influence the efficacy of DCs immunotherapy has been the preparation and differentiation of DCs used. In this study we demonstrated that high quality myeloid immature DCs can be yielded after 6 days of culture and once pulsed with tumour antigens, DCs were shown to display a mature phenotype and functionally active features. Of note, our vaccine does not take into account a specific antigen associated to the tumour but a whole tumour lysate, able to elicit a potent and broad immune response. Indeed, *in vitro* generated DCs pulsed with such lysate could trigger a specific lymphocyte response and direct a Th1 subset development. Furthermore, the use of tumour lysate could be used in any kind of solid tumours.

Moreover, detailed information regarding cellular migration, fate and how DCs interact with other cells in the secondary lymphoid tissue of the host, remain a subject of intensive study. Thus, we decided to track DCs migration by imaging techniques. Recent advances in the field of molecular imaging have provided a bridge to fill the gap in the knowledge of the molecular mechanisms underlying cell mediated treatments through *in vivo* cell visualization. Non-invasive, imaging-based techniques allow to highlight the localization, distribution and migration of administered cells in a living model. Cells must be labelled to provide sufficient contrast for *in vivo* detection by imaging instruments. This can be performed following direct or indirect protocols. The direct labelling methodology is based on the use of contrast agents, such as paramagnetic nanoparticles and fluorescent or radioactive molecules that a-specifically enter the cell membrane and label cells; the indirect strategy uses genes coding for reporter proteins. In our study we performed direct labelling of DCs using dextran-coated Iron nanoparticles named Endorem®, which are FDA approved contrast agents. We demonstrated that Iron effectively labels cells *in vitro* and that the labelling procedure is efficient and safe, as it does not harm DCs immunological functions.

Furthermore, we radioisotope-labelled DCs with ^{111}In-oxine and demonstrated that such tracer is safe and is visualized efficiently by SPET. In this regard, we proved that the prototypical sensor provided by the Politecnico of Milan, Professor Carlo Fiorini has great sensitivity, as it is able to image the axillary lymph nodes, even though in a bi-dimensional perspective only, and to integrate the information deriving from MRI studies. The data reported allow us to validate our labelling protocols as an efficient strategy to *in vivo* follow DCs that are systemically administered in a mammary tumour mouse models.

The evaluation of the efficacy of cell-mediated treatments will be analyzed in future experiments, as well as proper scheduling of treatment and the potential use of adjuvants.

Bibliography

[1] Banchereau J, Steinman RM, Dendritic cells and the control of immunity, *Nature,* Vol.392, n. 6673, 1998, pp. 245–52.

[2] Mellman I, Steinman RM, "Dendritic cells: Specialized and regulated antigen processing machines", *Cell,* Vol. 106, n.3, 2001, pp. 255–8.

[3] Banchereau J, Steinman RM, "Dendritic cells and the control of immunity", *Nature,* Vol. 392, n.6673, 1998, pp. 245–52.

[4] Zenke M, Hieronymus T, "Towards an understanding of the transcription factor network of dendritic cell development", *Trends of Immunol*ogy, Vol.27, n.3, 2006, pp.140–5

[5] Sozzani S, "Dendritic cell trafficking: more than just chemokines", *Cytokine Growth Factor Review* Vol. 16, n. 6, 2005, pp. 581-92.

[6] Guermonprez P, Valladeau J, Zitvogel L, Thery C, Amigorena S, "Antigen presentation and T cell stimulation by dendritic cells", *Annual Reviw of Immunology* Vol 20, 2002, pp. 621–67.

[7] Villadangos JA, Heath WR, "Life cycle, migration and antigen presenting functions of spleen and lymph node dendritic cells: limitations of the Langherhans cell paradigm", *Seminars in Immunology,* Vol.17, n. 4, 2005, pp. 262-72.

[8] McWilliam AS, Nelson D, Thomas JA, Holt PG, "Rapid dendritic cell recruitment is a hallmark of the acute inflammatory response at mucosal surfaces", *Journal of Experimental Medicine,* Vol. 179, n. 4, 1994, pp. 1331–6.

[9] McWilliam AS, Napoli S, Marsh AM, Pemper FL, Nelson DJ, Pimm CL, et al, "Dendritic cells are recruited into the airway epithelium during the inflammatory response to a broad spectrum of stimuli", *Journal of Experimental Medicine,* Vol. 184, n. 6, 1996, pp. 2429-32.

[10] Stumbles PA, Strickland DH, Pimm CL, Proksch SF, Marsh AM, McWilliam AS, Bosco A, Tobagus I, Thomas JA, Napoli S, Proudfoot AE, Wells TN, Holt PG, " Regulation of dendritic cell recruitment into resting and inflamed airway epithelium: use of alternative chemokine receptors as a function of inducing stimulus" *Journal of Immunology,* Vol.167, n.1, 2001, pp. 228–34.

[11] Reis e Sousa C, "Dendritic cells in a mature age", *Nature*, Vol. 6, n.6, 2006, pp.476-483.

[12] Kubach J, Becker C, Schmitt E, Steinbrink K, Huter E, Tuettenberg A, Jonuleit H, "Dendritic cells: Sentinels of immunity and tolerance", *International Journal of Hematology*, Vol.81, n. 3, 2005, pp. 197-203.

[13] Ardavin C, "Origin, precursors and differentiation of mouse dendritic cells", *Nature Reviews Immunology*, Vol.3, n. 7, 2003, pp.582-90.

[14] Steinman R M, Banchereau J, "Taking dendritic cells into medicine", *Nature*, Vol. 449, n. 7161, 2007, pp. 419-426.

[15] Bousso P, "T cell activation by Dendritic Cells in the lymph node: lessons from the movie", *Nature Reviews Immunology*, Vol. 8, n. 9, 2008, pp. 675-684.

[16] Allan RS, Waithman J, Bedoui S, Jones CM, Villadangos JA, Zhan Y, Lew AM, Shortman K, Heath WR, Carbone FR, "Migratory Dendritic Cells Transfer Antigen to a Lymph Node-Resident Dendritic Cell Population for Efficient CTL Priming", *Immunity*, Vol. 25, n. 1, 2006, pp. 153-162.

[17] Pham W, Kobukai S, Hotta C, Gore JC. "Dendritic cells; therapy and imaging", *Expert Opinion in Biology and Therapy*, Vol. 9, no. 5, 2009, pp. 539-564.

[18] Itano AA, McSorley SJ, Reinhardt RL, Ehst BD, Ingulli E, Rudensky AY, Jenkins MK, "Distinct dendritic cell populations sequentially present antigen to CD4 T cells and stimulate different aspects of cell-mediated immunity", *Immunity*, Vol.19, n.1, 2003, pp. 47-57.

[19] Randolph GJ, Ochando J, Partida-Sanchez S, "Migration of dendritic cell subsets and their precursors", *Annual Review of Immunology*, Vol. 26, 2008, pp. 293-316.

[20] Shortman K, Liu YJ, "Mouse and human dendritic cell subtypes", *Nature Reviews of Immunology*, Vol. 2, n.3, 2002, pp.151–61.

[21] Kissenpfennig A, Henri S, Dubois B, Laplace-Builhè C, Perrin P, Romani N, Tripp CH, Douillard P, Leserman L, Kaiserlian D, Saeland S, Davoust J, Malissen B, "Dynamics and function of Langerhans cells in vivo: dermal dendritic cells colonize lymph node areas distinct from slower migrating Langerhans cells", *Immunity*, Vol. 22, n. 5, 2005, pp. 643-54.

[22] Vremec D, Shortman K, "Dendritic cell subtypes in mouse lymphoid organs: cross-correlation of surface markers, changes with incubation, and differences among thymus, spleen, and lymph nodes", *Journal of Immunology*, Vol. 159, n. 2, 1997, pp. 565-73.

[23] Shortman K, Naik SH, "Steady-state and inflammatory dendritic-cell development", *Nature Reviews of Immunology*, Vol. 7, n. 1, 2007, pp. 19-30.

[24] Liu YJ, "IPC: professional type 1 interferon-producing cells and plasmacytoid dendritic cell precursors", *Annual Reviews of Immunology*, Vol. 23, 2005, pp. 275-306.

[25] Cella M, Jarrossay D, Facchetti F, Alebardi O, Nakajima H, Lanzavecchia A, Colonna M, "Plasmacytoid monocytes migrate to inflamed lymph nodes and produce large amounts of type I interferon", *Nature Medicine*, Vol. 5, n. 8, 1999, pp. 919–923.

[26] Farkas L, Beiske K, Lund-Johansen F, Brandtzaeg P, Jahnsen F L, “Plasmacytoid dendritic cells (natural interferon-{{alpha}} ⁄ {beta}-producing cells) accumulate in cutaneous lupus erythematosus lesions”, *American Journal of Pathology*, Vol. 159, n. 1, 2001, pp. 237–243.

[27] Soumelis V, Liu YJ, “From plasmacytoid to dendritic cell: Morphological and functional switches during plasmacytoid pre-dendritic cell differentiation”, *European Journal of Immunology* 2006;36:2286–92.

[28] Asselin-Paturel C, Trinchieri G, “Production of type I interferons: plasmacytoid dendritic cells and beyond”, *Journal of Experimantal Medicine*, Vol. 202, n. 4, 2005, pp. 461–5.

[29] Hadeiba H, Sato T, Habtezion A, Oderup C, Pan J, Butcher EC, “CCR9 expression defines tolerogenic plasmacytoid dendritic cells able to suppress acute graftversus-host disease”, *Nature Immunology*, Vol. 9, n. 1, 2008, pp. 1253–60.

[30] Van Nierop K, de Groot C, “Human follicular dendritic cells: function, origin and development”, *Seminar of Immunology*, Vol. 14, n. 4, 2002, pp. 251-7.

[31] Steinman RM, Swanson J, “The endocytic activity of dendritic cells”, *Journal of Experimental Medicine*, Vol. 182, n. 2, 1995, pp. 182:283-88.

[32] Sallusto F, Cella M, Danieli C, Lanzavecchia A, “Dendritic cells use macropinocytosis and the mannose receptor to concentrate macromolecules in the major histocompatibility complex class II compartment: downregulation by cytokines and bacterial products”, *Journal of Experimental Medicine*, Vol. 182, n. 2, 1995, pp. 389-400.

[33] Inaba K, Inaba M, Naito M, Steinman RM, “Dendritic cell progenitors phagocytose particulates, including bacillus Calmette-Guerin organisms, and sensitize mice to mycobacterial antigens in vivo”, *Journal of Experimental Medicine*, Vol. 178, n.2 ,1993, pp.479-488.

[34] Albert ML, Sauter B, Bhardwaj N, “Dendritic cells acquire antigen from apoptotic cells and induce class I.restricted CTLs”, *Nature*, Vol. 392, n.6671, 1998, pp. 86-89.

[35] Swanson JA, Watts C, “Macropinocytosis”, *Trends in Cell Biology*, Vol. 5, n. 11, 1995, pp. 424–428.

[36] Ackerman AL, Kritsis C, Tampe R, Cresswell P, “Early phagosomes in dendritic cells form a cellular compartment sufficient for cross presentation of exogenous antigens”, *PNAS USA*, Vol.100, n.22, 2003, pp. 12889–94.

[37] Steinman RM, “Some interfaces of dendritic cell biology”, *APMIS*, Vol.111, n.7-8 , 2003, pp.675–97.

[38] Schiller M, Metze D, Luger T A, Grabbe S, Gunzer M, “Immune response modifiers – mode of action”, *Experimental Dermatology*, Vol. 15, n. 5,2006, pp. 331–341.

[39] Ardavın C, Amigorena S, Reis e Sousa C, “Dendritic cells: immunobiology and cancer immunotherapy”, *Immunity*, Vol. 20, n. 1, 2004, pp. 17–23.

[40] Mazzoni A, Segal DM, “Controlling the Toll road to dendritic cell polarization”, *Journal of Leukocyte Biology*, Vol. 75, n. 5, 2004, pp. 721–730.

[41] Reis e Sousa C, Germain RN, “Analysis of adjuvant function by direct visualization of antigen presentation in vivo endotoxin promotes accumulation of antigen-bearing dendritic cells in the T cell areas of lymphoid tissue”, *Journal of Immunology*, Vol.162, n.11, 1999, pp. 6552-6661.

[42] Mahnke K, Guo M, Lee S, Sepulveda H, Swain SL, Nussenzweig M, Steinman RM, “The dendritic cell receptor for endocytosis, DEC-205, can recycle and enhance antigen presentation via major histocompatibility complex class II-positive lysosomal compartments”, *Journal of Cell Biology*, Vol. 151, n. 3, 2000, pp. 673–684.

[43] Geijtenbeek TB, Torensma R, van Vliet SJ, van Duijnhoven GCF, Adema GJ, van Kooyk Y, Figdor CG , “Identification of DC-SIGN, a novel dendritic cell-specific ICAM-3 receptor that supports primary immune responses”, *Cell*, Vol. 100, n. 5, 2000,pp. 575–585.

[44] Esposite-Farese ME, Sautes C, de la Salle H, Latour S, Bieber T, de la Salle C, Ohlmann P, Fridman WH, Cazenave JP, TeillaudJL, “Membrane and soluble Fc gamma RII/RIII modulate the antigen-presenting capacity of murine dendritic epidermal Langerhans cells for IgG-complexed antigens”, *Journal of Immunology*, Vol. 155, n. 4, 1995, pp. 1725–1736.

[45] Amigorena S, “Fc gamma receptors and cross-presentation in dendritic cells”, *Journal of Experimental Medicine*, Vol. 195, n. 1, 2002, F1–3.

[46] Bajtay Z, Csomor E, Sandor N, Erdei A, “Expression and role of Fc and complement-receptors on human dendritic cells”, *Immunology Letters*, Vol. 104, n. 1-2, 2006, pp. 46–52.

[47] Morelli AE, Larregina AT, Shufesky WJ, Zahorchak AF, Logar AJ, Papworth G, Wang Z, Watkins SC, Falo LD Jr, Thomson AW, “Internalization of circulating apoptotic cells by splenic marginal zone dendritic cells: dependence on complement receptors and effect on cytokine production”, *Blood*, Vol. 101, n.2, 2003, pp. 611–620.

[48] Harshyne LA, Zimmer MI, Watkins SC, Barratt-Boyes SM, “A role for class A scavenger receptor in dendritic cell nibbling from live cells”, *Journal of Immunology*, Vol. 170, n. 5, 2003, pp. 2302–2309.

[49] Albert ML, Pearce SF, Francisco LM, Sauter B, Roy P, Silverstein RL, Bhardwaj N, “Immature dendritic cells phagocytose apoptotic cells via a_vb_5 and CD36, and cross-present antigens to cytotoxic T lymphocytes”, *Journal of Experimental Medicine*, Vol. 188, n. 7, 1998, pp. 1359–1368.

[50] Delneste Y, Magistrelli G, Gauchat J, Haeuw J, Aubry J, Nakamura K, Kawakami-Honda N, Goetsch L, Sawamura T, Bonnefoy J, Jeannin P, "Involvement of LOX-1 in dendritic cell-mediated antigen cross-presentation", *Immunity*, Vol. 17, n. 3, 2002,pp. 353–362.

[51] Newman SL, Holly A, "Candida albicans is phagocytosed, killed, and processed for antigen presentation by human dendritic cells", *Infection and Immunity*, Vol. 69, n. 11, 2001, pp. 6813–6822.

[52] Shimaoka T, Nakayama T, Kume N, Takahashi S, Yamaguchi J, Minami M, Hayashida K, Kita T, Ohsumi J, Yoshie O, Yonehara S, "Cutting edge: SR-PSOX/CXC chemokine ligand 16 mediates bacterial phagocytosis by APCs through its chemokine domain", *Journal of Immunology*, Vol. 171, n. 4, 2003, pp. 1647–1651.

[53] Vermeulen M, Giordano M, Trevani AS, Sedlik C, Gamberale R, Fernandez-Calotti P, Salamone G, Raiden S, Sanjurjo J, Geffner JR, "Acidosis improves uptake of antigens and MHC class I-restricted presentation by dendritic cells", *Journal of Immunology*, Vol. 172, n. 5, 2004, pp. 3196–3204.

[54] Rutault K, Alderman C, Chain BM, Katz DR, "Reactive oxygen species activate human peripheral blood dendritic cells", *Free Radical Biology & Medicine*, Vol. 26, n. 1-2, 1999, pp. 232–238.

[55] Basu S, Srivastava PK, "Fever-like temperature induces maturation of dendritic cells through induction of hsp90", *International Immunology*, Vol. 15, n.9, 2003, pp. 1053–1061.

[56] Moody DB, Briken V, Cheng TY, Roura-Mir C, Guy MR, Geho DH, Tykocinski ML, Besra GS, Porcelli SA, "Lipid length controls antigen entry into endosomal and nonendosomal pathways for CD1b presentation", *Nature Immunology* 2002;3:435-42.

[57] Trombetta ES, Mellman I, "Cell biology of antigen processing in vitro and in vivo", *Annual Reviews of Immunology*, Vol.23, 2005, 975–1028.

[58] Porcelli SA, Modlin RL, "The CD1 system: antigen-presenting molecules for T cell recognition of lipids and glycolipids" *Annual Reviews of Immunology*, Vol. 17, 1999, pp. 297–329.

[59] Inaba K, Turley S, Iyoda T, Yamaide F, Shimoyama S, Reis e Sousa C, Germain RN, Mellman I, Steinman RM, "The formation of immunogenic major histocompatibility complex class II-peptide ligands in lysosomal compartments of dendritic cells is regulated by inflammatory stimuli", *Journal of Experimental Medicine,* Vol. 191, 2000, pp. 927–936.

[60] Saeki H, Moore AM, Brown MJ, Hwang ST, "Cutting edge: secondary lymphoid-tissue chemokine (SLC) and CC chemokine receptor 7 (CCR7) participate in the emigration pathway of mature dendritic cells from the skin to regional lymph nodes", *Journal of Immunology*, Vol. 162, n. 5, 1999, pp. 2472 -2475.

[61] Willimann K, Legler DF, Loetscher M, Roos RS, Delgado MB, Clark-Lewis I, Baggiolini M, Moser B , "The chemokine SLC is expressed in T cell areas of lymph nodes and mucosal lymphoid tissues and attracts activated T cells via CCR7", *European Journal of Immunology*, Vol. 28, n. 2, 1998, pp. 2025 -34.

[62] Martin-Fontecha A, Sebastiani S, Hopken UE, Uguccioni M, Lipp M, LAnzavecchia A, Sallusto F, "Regulation of dendritic cell migration to the draining lymph node: impact on T lymphocyte traffic and priming", *Journal of Experimental Medicine*, Vol. 198, n. 4, 2003, pp. 615 -621.

[63] Ohl L, Mohaupt M, Czeloth N, Hintzen G, Kiafard Z, Zwirner J, Blankestein T, Henning G, Foster R, "CCR7 governs skin dendritic cell migration under infl ammatory and steady-state conditions", *Immunity*, Vol. 21, n. 2, 2004, pp. 279 -288.

[64] Randolph Randolph GJ, Angeli V, Swartz MA, "Dendritic-cell trafficking to lymph nodes through lymphatic vessels", *Nature Reviews. Immunology*, Vol. 5, 2005, pp. 617-628.

[65] Grayson MH, Ramos MS, Rohlfi NG MM, Kitchens R, Wang HD, Gould A, Agapov E, Hiltzamn MJ, "Controls for lung dendritic cell maturation and migration during respiratory viral infection", *Journal of Immunology*, Vol. 179, n. 3, 2007, pp. 1438 -1448.

[66] Qu C, Edwards EW, Tacke F, Angeli V, Llodrà J, Sanchez-Schmitz G, Garin A, Haque NS, Peters W, van Roojen N, Sanchez-Torres C, Bromberg J, Charo IF, Jung S, Lira SA, Randolph GJ, "Role of CCR8 and other chemokine pathways in the migration of monocyte-derived dendritic cells to lymph nodes", *Journal of Experimental Medicine*, Vol. 200, n. 10, 2004, pp. 1231 -1241.

[67] Yoneyama H, Matsuno K, Zhang Y, Nishiwaki T, Kitabatake M, Ueha S, Narumi S, Morikawa S, Ezaki T, Lu B, Gerard C, Ishikawa S, Matsushima K, "Evidence for recruitment of plasmacytoid dendritic cell precursors to inflamed lymph nodes through high endothelial venules", *International Immunology*, Vol. 16, n. 7, 2004, 915 -28.

[68] De La Rosa RG, Longo N, Rodriguez-Fernandez JL, Puig-Kroger A, Pineda A, Corbì AL, Sanchez-Mateos P, "Migration of human blood dendritic cells across endothelial cell monolayers: adhesion molecules and chemokines involved in subset-specifi c transmigration", *Journal of Leukocyte Biology*, Vol. 73, n. 5, 2003, pp. 639 -649.

[69] Rodriguez-Fernandez JL, Corbi AL, "Adhesion molecules in human dendritic cells", *Current Opinions in Investigational Drugs*, Vol. 6, n. 11, 2005, pp. 1103 -1111.

[70] Price AA, Cumberbatch M, Kimber I, Ager A, "Alpha 6 integrins are required for Langerhans cell migration from the epidermis", *Journal of Experimental Medicine,* Vol. 186, n. 10, 1997, pp. 1725 -1735.

[71] Ma J, Wang JH, Guo YJ, Sy MS, Bigby M, "*In vivo* treatment with anti-ICAM-1 and anti-LFA-1 antibodies inhibits contact sensitization-induced migration of epidermal Langerhans cells to regional lymph nodes", *Cellular Immunology*, Vol. 158, n. 2, 1994, pp. 389 -399.

[72] Weiss JM, Sleeman J, Renkl AC, Dittmar H, Termeer CC, Taxis S, Howells N, Hofmann M, Kohler G, Schopf E, Ponta H, Herrlich P, Simon JC, "An essential role for CD44 variant isoforms in epidermal Langerhans cell and blood dendritic cell function", *Journal of Cellular Biology*, Vol. 137, n. 5, 1997, pp. 1137 - 1147.

[73] Averbeck M, Gebhardt C, Anderegg U, Termeer C, Sleeman JP, Simon JC, "Switch in syndecan-1 and syndecan-4 expression controls maturation associated dendritic cell motility", *Experimental Dermatology*, Vol. 16, n. 7, 2007, pp. 580 -589.

[74] Kapsenberg ML, "Dendritic-cell control of pathogen-driven T-cell polarization", *Nature Reviews of Immunology*, Vol.3, n. 12, 2003, pp. 984–993.

[75] Lanzavecchia A, Sallusto F, "Regulation of T cell Immunity by Dendritic Cells", *Cell*, Vol. 106, 2001, pp. 263-366.

[76] Lanzavecchia A, Sallusto F, "Antigen decoding by T lymphocytes: from synapses to fate determination", *Nature Immunology*, Vol. 2, 2001, pp. 487-492.

[77] Lanzavecchia A, Sallusto F, "Dynamics of T lymphocyte responses: intermediates, effectors, and memory cells", *Science*, Vol. 290, 2000, pp. 92-9

[78] Reis e Sousa C, "Activation of dendritic cells: translating innate into adaptative immunity", *Current Opinions in Immunology*, Vol. 16, n. 1, 2004, pp. 21–25.

[79] Amsen D, Blander JM, Lee GR, Tanigaki K, Honjo T, Flavell RA, "Instruction of distinct CD4 T helper fates by different notch ligands on antigen-presenting cells", *Cell*, Vol. 117, n. 4, 2004, pp. 515–26.

[80] Weaver CT, Harrington LE, Mangan PR, Gavrieli M, Murphy KM, "Th17: an effector CD4 T cell lineage with regulatory T Cell ties", *Immunity*, Vol.24, n. 6, 2006, pp. 677–688.

[81] Rudner XL, Happel KI, Young EA, Shellito JE, "Interleukin-23 (IL-23)-IL-17 cytokine axis in murine pneumocystis carinii infection". *Infectious Immunology*, Vol. 75, n. 6, 2007, pp. 3055–3061.

[82]Cua D J, Sherlock J, Chen Y, Murphy CA, Joyce B, Seymour B, Lucian L, To W, Kwan S, Churakova T, Zurawski S, Wiekowski M, Lira SA, Gorman D, Kastelein RA, Sedgwick JD, "Interleukin-23 rather than interleukin-12 is the critical cytokine for autoimmune inflammation of the brain", *Nature*, Vol. 421, n. 6924, 2003, pp. 744–748.

[83] Steinman RM, Hawiger D, Nussenzweig MC, "Tolerogenic dendritic cells", *Annual Reviews in Immunolgy*, Vol. 21, 2003, pp. 685–711.

[84] Brocker T, "The role of dendritic cells in T cell selection and survival", *Journal of Leukocyte Biology,* Vol. 66, 1999, pp. 331–335.

[85]Mahnke K, Schmitt E, Bonifaz L, Enk AH, Jonuleit H, "Immature, but not inactive: The tolerogenic function of immature dendritic cells", *Immunology & Cell Biology*, Vol. 80, n. 5, 2002, pp. 477–483 .

[86] Roncarolo MG, Levings MK, Traversari C, "Differentiation of T regulatory cells by immature dendritic cells", *Journal of Exprimental Medicine*, Vol. 193, n. 2, 2001, pp. F5–10.

[87] Yamazaki S, Inaba K, Tarbell KV, Steinman RM, "Dendritic cells expand antigenspecific Foxp3+ CD25+ CD4+regulatory T cells including suppressors of alloreactivity" *Immunology Reviews*, Vol. 212, 2006, pp. 314–329.

[88] Jonuleit H, Schmitt E, Schuler G, Knop J, Enk AH, "Induction of interleukin 10-producing, nonproliferating CD4 T cells with regulatory properties by repetitive stimulation with allogeneic immature human dendritic cells", *Journal of Exprimental Medicine*, Vol. 192, n. 9, 2000, pp. 1213–1222.

[89] Green EA, Gorelik L, McGregor CM, Tran EH, Flavell RA, "CD4+CD25+ T regulatory cells control anti islet CD8+ T cells through TGF-beta-TGF-beta receptor interactions in type 1 diabetes" *PNAS USA*, Vol. 100, n. 19, 2003, pp. 10878-10883.

[90] Asseman C, Mauze S, Leach MW, Coffman RL, Powrie F, "An essential role for interleukin 10 in the function of T regulatory cells that inhibit intestinal inflammation", *Journal of Exprimental Medicine*, Vol. 190, n. 7, 1999, pp. 995-1004.

[91] Paust L, Lu L, McCarty N, Cantor H, "Engagement of B7 on effector T cells by regulatory T cells prevents autoimmune disease", *PNAS USA*, Vol. 101, n. 28, 2004, pp. 10398-10403.

[92] Fontenot JD, Rudensky AY, "A well adapted regulatory contrivance: regulatory T cell development and the forkhead family transcriptional factor Foxp3", *Nature Immunology*, Vol. 6, n. 4, 2005, pp. 331-337.

[93] Ehrlich P, "Uber den jetzigen Stand der Karzinomforschung", *Nederland Tijdschr Geneeskd*, Vol. 5, 1909, pp. 273–90.

[94] Burnet M, "Cancer; a biological approach. I. The processes of control", *British Medical Journal*, 1957, pp. 779–86.

[95] Thomas L, Lawrence HS, **Cellular and humoral aspects of the hypersensitive states**, New York: Hoeber-Harper, 1959.

[96] Novellino L, Castelli C, Parmiani G, "A listing of human tumor antigens recognized by T cells: March 2004 update", *Cancer Immunology & Immunotherapies*, Vol. 54, n. 3, 2005, pp.187–207.

[97] Jager E, Chen YT, Drijfhout JW, Karbach J, Ringhoffer M, Jager D, Arand M, Wada H, Noguchi Y, Stockert E, Old LJ, Knuth A, "Simultaneous humoral and cellular immune response against cancer-testis antigen NY-ESO-1: definition of human histocompatibility leukocyte antigen (HLA)-A2-binding peptide epitopes", *Journal of Exprimental Medicine*, Vol. 187, n.2, 1998, pp. 265–270.

[98] Shankaran V, Ikeda H, Bruce AT, White JM, Swanson PE, Old LJ, Schreiber RD, "IFNγ and lymphocytes prevent primary tumour development and shape tumour immunogenicity", *Nature*, Vol. 401, n. 6832, 2001, pp. 1107–1111.

[99]Dunn GP, Bruce AT, Ikeda H, Old LJ, Schreiber RD, "Cancer immunoediting: from immunosurveillance to tumor escape", *Nature Immunology*, VOl. 3, n. 11, 2002, pp. 991–998.

[100] Nauts HC, "Bacteria and cancer – antagonisms and benefits", *Cancer Surveillance*, Vol. 8, n. 4, 1989, pp. 713 -723.

[101] Jaffee EM, Pardoll DM, "Murine tumor antigens: is it worth the search?", *Current Opinions in Immunology*, Vol. 8. N. 5, 1996, pp. 622 -627.

[102] Papac DI, Briggs JB, Chin ET, Jones AJ, "A high-throughput microscale method to release N-linked oligosaccharides from glycoproteins for matrix-assisted laser desorption/ionization time-of-flight mass spectrometric analysis", *Glycobiology*, Vol. 8, n. 5, 1998, pp. 445 -454.

[103] McCann J, "Can skin cancers be minimized or prevented in organ transplant patients?", *Journal of National Cancer Institute*, Vol. 91, n.11, 1999, pp. 911 -913.

[104] Rosenberg SA, Yannelli JR, Yang JC, et al, "Treatment of patients with metastatic melanoma with autologous tumor-infiltrating lymphocytes and interleukin 2", *Journal of National Cancer Institute*, Vol. 86, n. 15, 1994, pp. 1159 -66.

[105] Weiden PL, Sullivan KM, Flournoy N, et al, "Antileukemic effect of chronic graft-versus-host disease: contribution to improved survival after allogeneic marrow transplantation", *New England Journal of Medicine*, Vol. 304, n. 25, 1981, pp. 1529 -1533.

[106] Van Pel A, Boon T, "Protection against a nonimmunogenic mouse leukemia by an immunogenic variant obtained by mutagenesis", *PNAS USA*, Vol. 79, n. 15, 1982, pp. 4718 -4722.

[107] Steinman RM, Banchereau J, "Taking dendritic cells into medicine", *Nature,* Vol. 449, n. 7161, 2007, pp. 419–26.

[108] Zitvogel L, Apetoh L, Ghiringhelli F, Kroemer G, "Immunological aspects of cancer chemiotherapy." *Nature Reviews Immunology*, Vol. 8, n. 7, 2008, pp. 59-73.

[109] Koebel CM, Vermi W, Swann JB, Zerafa N, Rodig SJ, Old LJ, Smith MJ, Schreiber RD, "Adaptive immunity maintains occult cancer in equilibrium state", *Nature*, Vol. 450, n. 7171, 2007, pp. 903-907.

[110] Apetoh L, Ghiringhelli F, Tesniere A, Obeid M, Ortiz C, Criollo A, Mignot G, Maiuri MC, Ullrich E, Saulnier P, Yang H, Amigorena S, Ryffel B, Barrat FJ, Saftig P, Levi F, Lidereau R, Nogues C, Mira JP, Chompret A, Joulin V, Clavel-Chapelon F, Bourhis J, André F, Delaloge S, Tursz T, Kroemer G, Zitvogel L, "Toll-like receptor 4-dependent contribution of the immune system to anticancer chemotherapy and radiotherapy", *Nature Medicine*, Vol. 13, n. 9, 2007, pp. 1050-1059.

[111] van der Bruggen P, Traversari C, Chomez P, Lurquin C, De Plaen E, Van den Eynde BJ, Knuth A, Boon T, "A gene encoding an antigen recognized by cytolytic T lymphocytes on a human melanoma", *Science*, Vol. 254, n. 5038, 1991, pp. 1643 -1647.

[112] Van Den Eynde BJ, Van Der Bruggen P, "T cell defi ned tumor antigens", *Current Opinion in Immunology*, Vol. 9, n. 5, 1997, pp. 684 -693.

[113] Boon T, Van Der BP, "Human tumor antigens recognized by T lymphocytes", *Journal of Experimental Medicine*, Vol. 183, n. 3, 1996, pp. 725 -729.

[114] Old LJ, Chen YT, "New paths in human cancer serology", *Journal of Experimental Medicine*, Vol. 187, n. 8, 1998, pp. 1163 -1167.

[115] Brasseur F, Marchand M, Vanwijck R, Hérin M, Lethé B, Chomez P, Boon T, "Human gene MAGE-1, which codes for a tumor-rejection antigen, is expressed by some breast tumors", *International Journal of Cancer*, Vol. 52, n. 5, 1992, pp. 839 -841.

[116] Wood LD, Parsons DW, Jones S, Lin J, Sjöblom T, Leary RJ, Shen D, Boca SM, Barber T, Ptak J, Silliman N, Szabo S, Dezso Z, Ustyanksky V, Nikolskaya T, Nikolsky Y, Karchin R, Wilson PA, Kaminker JS, Zhang Z, Croshaw R, Willis J, Dawson D, Shipitsin M, Willson JK, Sukumar S, Polyak K, Park BH, Pethiyagoda CL, Pant PV, Ballinger DG, Sparks AB, Hartigan J, Smith DR, Suh E, Papadopoulos N, Buckhaults P, Markowitz SD, Parmigiani G, Kinzler KW, Velculescu VE, Vogelstein B, "The genomic landscapes of human breast and colorectal cancers", *Science*, Vol 318, n. 5853, 2007, pp.1108–1113.

[117] Glazer CA, Smith IM, Ochs MF, Begum S, Westra W, Chang SS, Sun W, Bhan S, Khan Z, Ahrendt S, Califano JA, "Integrative discovery of epigenetically derepressed cancer testis antigens in NSCLC", PLoS *ONE*, Vol. 4, n. 12, 2009, e8189.

[118] *Goodell V, Waisman J, Salazar LG, de la Rosa C, Link J, Coveler AL, Childs JS, Fintak PA, Higgins DM, Disis ML, "Level of HER-2/neu protein expression in breast cancer may affect the development of endogenous HER-2/neu-specific immunity",* Molecular Cancer Therapeutics*, Vol. 7, n. 3, 2008, pp. 449–454.*

[119] Nelson PT, Zhang PJ, Spagnoli GC, Tomaszewski JE, Pasha TL, Frosina D, Caballero OL, Simpson AJ, Old LJ, Jungbluth AA, "Cancer/testis (CT) antigens are expressed in fetal ovary", *Cancer Immunology*, Vol. 7, 2007, pp. 1.

[120] Chomez P, De Backer O, Bertrand M, De Plaen E, Boon T, Lucas S, "An overview of the MAGE gene family with the identification of all human members of the family", *Cancer Research*, Vol. 61, n. 14, 2001, pp. 5544 -51.

[121] Miyagawa N, Kono K, Mimura K, Omata H, Sugai H, Fujii H, "A newly identifi ed MAGE-3-derived, HLA-A24-restricted peptide is naturally processed and presented as a CTL epitope on MAGE-3-expressing gastrointestinal cancer cells", *Oncology*, Vol. 70, n. 1, 2006, pp. 54 -62.

[122] Wölfel T, Hauer M, Schneider J, Serrano M, Wölfel C, Klehmann-Hieb E, De Plaen E, Hankeln T, Meyer zum Büschenfelde KH, Beach D, "A p16INK4a-insensitive CDK4 mutant targeted by cytolytic T lymphocytes in a human melanoma", *Science*, Vol. 269, n. 5228, 1995, pp. 1281 -1284.

[123] Mandruzzato S, Stroobant V, Demotte N, Van Der BP, "A human CTL recognizes a caspase-8-derived peptide on autologous HLA-B * 3503 molecules and two unrelated peptides on allogeneic HLA-B * 3501 molecules", *Journal of Immunology*, Vol. 164, n. 8, 2000, pp. 4130 -4134.

[124] Coulie PG, Brichard V, Van Pel A, Wölfel T, Schneider J, Traversari C, Mattei S, De Plaen E, Lurquin C, Szikora JP, Renauld JC, Boon T, "A new gene coding for a differentiation antigen recognized by autologous cytolytic T lymphocytes on HLA-A2 melanomas", *Journal of Experimental Medicine*, Vol. 180, n. 1, 1994, pp. 35 -42.

[125] Kawakami Y, Eliyahu S, Delgado CH, Robbins PF, Rivoltini L, Topalian SL, Miki T, Rosenberg SA, "Cloning of the gene coding for a shared human melanoma antigen recognized by autologous T cells infiltrating into tumor", *PNAS USA*, Vol 91, n. 9, 1994, pp. 3515 -3519.

[126] Robbins PF, el-Gamil M, Li YF, Topalian SL, Rivoltini L, Sakaguchi K, Appella E, Kawakami Y, Rosenberg SA, "Cloning of a new gene encoding an antigen recognized by melanoma-specific HLA-A24-restricted tumor-infiltrating lymphocytes", *Journal of Immunology*, Vol 154, n. 11, 1995, pp. 5944 -5950.

[127] Dunn GP, Koebel CM, Schreiber RD, "Interferons, immunity and cancer immunoediting", *Nature Reviews of Immunology*, Vol. 6, n. 11, 2006, pp. 836–848.

[128] Zitvogel L, Tesniere A, Kroemer G, "Cancer despite immunosurveillance: immunoselection and immunosubversion", *Nature Reviews of Immunology*, Vol. 6, n. 10, 2006, pp. 715–727.

[129] Yu H, Kortylewski M, Pardoll D, "Crosstalk between cancer and immune cells: role of STAT3 in the tumour microenvironment", *Nature Reviews of Immunology*, Vol. 7, n. 1, 2007, pp. 41–51.

[130] Figdor CG, de Vries IJ, Lesterhuis WJ, Melief CJ, "Dendritic cell immunotherapy: mapping the way", *Nature Medicine*, VOl. 10, n. 5, 2004, pp. 475–80.

[131] Disis ML, Bernhard H and. Jaffee EM, "Use of tumour-responsive T cells as cancer treatment", *Lancet*, Vol 373, n. 9664, 2009, pp. 673–683.

[132] Rosenberg SA, Yang JC and Restifo NP, "Cancer immunotherapy: moving beyond current vaccines", *Nature Medicine*, Vol. 10, n. 9, 2004, pp. 909–915.

[133] Galon J, Costes A, Sanchez-Cabo F, Kirilovsky A, Mlecnik B, Lagorce-Pagès C, Tosolini M, Camus M, Berger A, Wind P, Zinzindohoué F, Bruneval P, Cugnenc PH, Trajanoski Z, Fridman WH, Pagès F, "Type, density, and location of immune cells within human colorectal tumors predict clinical outcome", *Science*, Vol. 313, n. 5795, 2003, pp. 1960–1964.

[134] Wei WZ, Jacob JB, Zielinski JF, Flynn JC, Shim KD, Alsharabi G, Giraldo AA, Kong YC, "Concurrent induction of antitumor immunity and autoimmune thyroiditis in CD4+ CD25 +regulatory T cell-depleted mice", *Cancer Research*, Vol. 65, n. 18, 2003, pp. 8471–8478.

[135] Phan GQ, Yang JC, Sherry RM, Hwu P, Topalian SL, Schwartzentruber DJ, Restifo NP, Haworth LR, Seipp CA, Freezer LJ, Morton KE, Mavroukakis SA, Duray PH, Steinberg SM, Allison JP, Davis TA, Rosenberg SA, "Cancer regression and autoimmunity induced by cytotoxic T lymphocyte-associated antigen 4 blockade in patients with metastatic melanoma", *PNAS USA*, Vol. 100, n. 14, 2003, pp. 8372–8377.

[136] Gilboa E., Nair SK. and Lyerly HK, "Immunotherapy of cancer with dendritic-cellbased vaccines", *Cancer Immunology & Immunotherapies*, Vol. 46, n. 2, 1998, pp. 82–87.

[137] Nestle FO, Banchereau J, Hart D, "Dendritic cells: On the move from bench to bedside", *Nature Medicine*, Vol. 7, n. 7, 2001, pp. 761–765.

[138] Mackensen A, Herbst B, Chen JL, Köhler G, Noppen C, Herr W, Spagnoli GC, Cerundolo V, Lindemann A,*"* Phase I study in melanoma patients of a vaccine with peptidepulsed dendritic cells generated *in vitro* from CD34+ hematopoietic progenitor cells", *International Journal of Cancer,* Vol. 86, n. 17, 2000, pp. 385–392.

[139] Banchereau J, Palucka AK, Dhodapkar M, Burkeholder S, Taquet N, Rolland A, Taquet S, Coquery S, Wittkowski KM, Bhardwaj N, Pineiro L, Steinman R, Fay J, " Immune and clinical responses in patients

with metastatic melanoma to CD34+ progenitor-derived dendritic cell vaccine" *Cancer* Research, Vol. 61, n. 17, 2001, pp. 6451–6458.

[140] Dhodapkar MV, Steinman RM, Sapp M, Desai H, Fossella C, Krasovsky J, Donahoe SM, Dunbar PR, Cerundolo V, Nixon DF, Bhardwaj N, "Rapid generation of broad T-cell immunity in humans after a single injection of mature dendritic cells", *Journal of Clinical Investigation*, Vol. 104, n. 2, 1999, pp. 173–180.

[141] de Vries IJ, Lesterhuis WJ, Scharenborg NM, Engelen LP, Ruiter DJ, Gerritsen MJ, Croockewit S, Britten CM, Torensma R, Adema GJ, Figdor CG, Punt CJ, " Maturation of dendritic cells is a prerequisite for inducing immune responses in advanced melanoma patients", *Clinical Cancer Research* , Vol. 9, n. 14, 2003; pp. 5091–5100.

[142]Dhodapkar MV, Krasovsky J, Steinman RM, Bhardwaj N, "Mature dendritic cells boost functionally superior CD8+ T-cell in humans without foreign helper epitopes", *Journal of Clinical Investigation*, Vol. 105, n. 6, 2000, R9–R14.

[143] De Vries IJ, Krooshoop DJ, Scharenborg NM, Lesterhuis WJ, Diepstra JH, Van Muijen GN, Strijk SP, Ruers TJ, Boerman OC, Oyen WJ, Adema GJ, Punt CJ, Figdor CG, "Effective migration of antigen-pulsed dendritic cells to lymph nodes in melanoma patients is determined by their maturation state" *Cancer Research*, VOl. 63, n. 1, 2003, pp. 12–17.

[144] Guardino AE, Rajapaksa R, Ong KH, Sheehan K, Levy R, "Production of myeloid dendritic cells (DC) pulsed with tumor-specific idiotype protein for vaccination of patients with multiple myeloma", *Cytotherapy,* Vol. 8, n. 3, 2006, pp. 277- 89.

[145] Nestle FO, Alijagic S, Gilliet M, Sun Y, Grabbe S, Dummer R, Burg G, Schadendorf D, "Vaccination of melanoma patients with peptide- or tumor lysate-pulsed dendritic cells", *Nature Medicine*, Vol. 4, n. 3, 1998, pp. 328-332.

[146] So-Rosillo R, Small EJ, "Sipuleucel-T (APC8015) for prostate cancer", *Expert Review* of *Anticancer Therapy*, Vol. 6, n. 9, 2006, pp. 1163 -1167.

[147] Small EJ, Schelhammer PF, Higano CS, et al, "Results of a placebo-controlled phase III trial of immunotherapy with APC8015 for patients with hormone refractory prostate cancer (HRPC)", ASCO Annual Meeting Proceedings. *Journal of Clinical Oncology*, Vol. 23, 16S Suppl: 4500.

[148] Haigh PI, Difronzo LA, Gammon G, Morton DL, "Vaccine therapy for patients with melanoma", *Oncology* (Williston Park), Vol. 13, n. 11, 1999, pp. 1561–1574.

[149] Shumway NM, Ibrahim N, Ponniah S, Peoples GE, Murray JL, "Therapeutic breast cancer vaccines: a new strategy for early-stage disease", *BioDrugs*, Vol. 23, n. 5, 2009, pp. 277–287.

[150] Fearnley DB, LF Whyte, SA Carnoutsos, AH Cook, DN Hart, "Monitoring human blood dendritic cell numbers in normal individuals and in stem cell transplantation", *Blood*, Vol. 93, 2, 1999, pp. 728-736.

[151] Freudenthal PS, Steinman RM, "The distinct surface of human blood dendritic cells, as observed after an improved isolation method", *PNAS USA*, VOl. 187, n. 19, 1990, pp. 7698-7702.

[152] Mehta-Damani A, Markowicz S, Engleman EG, "Generation of antigen specific CD4+ T cell lines from naïve precursors" *European Journal of Immunology*, Vol. 25, n. 5, 1995, pp. 1206-1211.

[153] Mehta-Damani A, Markowicz S, Engleman EG, "Generation of antigenspecific CD8+ CTLs from naïve precursors", *Journal of Immunology,* vol. 153, n. 3, 1994, pp. 996-1003.

[154] Romani N, S Gruner, D Brang, E Kampgen, A Lenz, B Trockenbacher, G Konwalinka, PO Fritsch, RM Steinman, G Schuler, "Proliferating dendritic cell progenitors in human blood", *Journal of Experimental Immunology,* VOl. 180, n. 1, 1994, pp. 83-93.

[155] Sallusto F, Lanzavecchia A, "Efficient presentation of soluble antigen by cultured human dendritic cells is maintained by granulocyte/macrophage colony-stimulating factor plus interleukin 4 and downregulated by tumor necrosis factor alpha", *Journal of Experimental Immunology*, Vol. 179, n.4, 1994, pp. 1109-1118.

[156] Mortarini R, A Anichini, M Di Nicola, S Siena, M Bregni, F Belli, A Molla, AM Gianni, G Parmiani, "Autologous dendritic cells derived from CD34+ progenitors and from monocytes are not functionally equivalent antigen-presenting cells in the induction of melan-A/Mart-1(27-35)-specific CTLs from peripheral blood lymphocytes of melanoma patients with low frequency of CTL precursors". *Cancer Research*, Vol. 57, n. 24, 1997, pp. 5534-5541.

[157] Lutz MB, Kukutsch N, Ogilvie ALJ, Rößner S, Koch F, Romani N, Schuler G, "An advanced culture method for generating large quantities of highly pure dendritic cells from mouse bone marrow", *Journal of Immunological Methods*, Vol. 223, 1999, pp. 77-92.

[158] Copier J, Dalgleish A, "Overview of tumor cell-based vaccines", *International Reviews in Immunology*, Vol. 25, n. 5-6, 2006, pp. 297 -319.

[159] Chang AE, Redman BG, Whitfield JR, Nickoloff BJ, Braun TM, Lee PP, Geiger JD, Mulé JJ, "A Phase I trial of tumor lysate-pulsed dendritic cells in the treatment of advanced cancer", *Clinical Cancer Research*, Vol. 8, n. 4, 2002, pp. 1021-32.

[160] Saito K, Dai Y, Ohtsuka K, "Enhanced expression of heat shock proteins in gradually dying cells and their release from necrotically dead cells", *Experimental Cell Research*, Vol. 310, n. 1, 2005, pp.229-236.

[161] Srivastava PK, “Immunotherapy for human cancer using heat shock protein–peptide complexes”, *Current Oncology Report*, Vol. 7, n. 2, 2005, pp.104-108.

[162] Brichard VG, Gerard C, “Melanoma vaccines: achievements and perspectives”, Forum (Genova); Vol. 13, n. 2, 2003, pp. 144 -54.

[163] Velders MP, Markiewicz MA, Eiben GL, Kast WM, “CD4+ T cell matters in tumor immunity”, *International* Reviews of *Immunology*, Vol. 22, n. 2, 2003, pp. 113–140.

[164] Mitchell MS, “Cancer vaccines, a critical review – Part II”, Curr Opin Investig *Drugs*, Vol. 3, n. 1, 2002, pp. 150 -158.

[165] Delluc S, Tourneur L, Fradelizi D, Rubio MT, Marchiol-Fournigault C, Chiocchia G, Buzyn A, “DC-based vaccine loaded with acid-eluted peptides in acute myeloid leukemia: the importance of choosing the best elution method”, Cancer *Immunology & Immunotherapies*, Vol. 56, n. 1, 2007, pp. 1–12.

[166] Vari F, Hart DN, “Loading DCs with Ag”, *Cytotherapy*, Vol. 6, n. 2, 2004, pp. 111–121.

[167] Van Tendeloo VF, Ponsaerts P, Lardon F, Nijs G, Lenjou M, Van Broeckhoven C, Van Bockstaele DR, Berneman ZN, “Highly effcient gene delivery by mRNA electroporation in human hematopoietic cells: superiority to lipofection and passivepulsing of mRNA and to electroporation of plasmid cDNA for tumor antigen loading of dendritic cells”, *Blood*, Vol. 98, n. 1, 2001, pp. 49–56.

[168] Hege KM, Jooss K, Pardoll D, “GM-CSF gene-modifed cancer cell immunotherapies: of mice and men”, *International* Reviews of *Immunology*, Vol. 25, n. 5-6, 2006, pp. 321 -52.

[169] Eggert AA, Schreurs MW, Boerman OC, et al, “Biodistribution and vaccine effi ciency of murine dendritic cells are dependent on the route of administration”, *Cancer Research*, Vol. 59, n. 14, 1999, pp. 3340 -5.

[170] Yoneyama H, Matsuno K, Zhang Y, et al, “Evidence for recruitment of plasmacytoid dendritic cell precursors to infl amed lymph nodes through high endothelial venules”, *International Immunology*, Vol. 16, n. 7, 2004, pp. 915 -28.

[171] Bedrosian I, Mick R, Xu S, et al, “Intranodal administration of peptide-pulsed mature dendritic cell vaccines results in superior CD8+ T-cell function in melanoma patients”, *Journal of Clinical Oncology*, Vol. 21, n. 20, 2003, pp. 3826 -35.

[172] Trakatelli M, Toungouz M, Blocklet D, Dodoo Y, Gordower L, Laporte M, Vereecken P, Sales F, Mortier L, Mazouz N, Lambermont M, Goldman S, Coulie P, Goldman M, Velu T, “A new dendritic cell vaccine generated with interleukin-3 and interferon- α induces CD8+ T cell responses against NA17-A2 tumor peptide in melanoma patients”, *Cancer Immunology & Immunotherapies*, Vol. 55, n. 4, 2006, pp. 469 -74.

[173] Ridolfi R, Riccobon A, Galassi R, Giorgetti G, Petrini M, Fiammenghi L, Stefanelli M, Ridolfi L, Moretti A, Migliori G, Fiorentini G, “Evaluation of in vivo labelled dendritic cell migration in cancer patients”, *Journal of Translational Medicine*, Vol. 2, n. 1, 2004, 27.

[174] Quillien V, Moisan A, Carsin A, Lesimple T, Lefeuvre C, Adamski H, Bertho N, Devillers A, Leberre C, Toujas L, “Biodistribution of radiolabelled human dendritic cells injected by various routes”, *European Journal of Nuclear Medicine & Molecular Imaging*, Vol. 32, n. 7, 2005, pp. 731 -41.

[175] Mackensen A, Krause T, Blum U, Uhrmeister P, Mertelsmann R, Lindemann A, “Homing of intravenously and intralymphatically injected human dendritic cells generated in vitro from CD34+ hematopoietic progenitor cells”, *Cancer Immunology & Immunotherapies*, Vol. 48, n. 2-3, 1999, pp. 118 -122.

[176] North RJ, “The murine antitumor immune response and its therapeutic manipulation”, *Advances in Immunology*, VOl. 35, 1984, pp. 89–155.

[177] Ma J, Urba WJ, Si L, Wang Y, Fox BA, Hu HM, “ Anti-tumor T cell response and protective immunity in mice that received sublethal irradiation and immune reconstitution”, *European Journal of Immunology*, Vol. 33, n. 8, 2003, pp. 2123–2132.

[178] Santini SM, Lapenta C, Logozzi M, Parlato S, Spada M, Di Pucchio T, Belardelli F, “Type I interferon as a powerful adjuvant for monocyte-derived dendritic cell development and activity in vitro and in Hu-PBL-SCID mice”, *Journal of Experimental Medicine,* Vol. 191, n. 10, 2000, pp. 1777–1788.

[179] Marrack P, Kappler J, and Mitchell T, “Type I interferons keep activated T cells alive”, *Journal of Experimental Medicine*, Vol. 189, 1990, pp. 521–530.

[180] Stockfleth E, Trefzer U, Garcia-Bartels C, Wegner T, Schmook T, Sterry W, “The use of Toll-like receptor-7 agonist in the treatment of basal cell carcinoma: an overview”, *British Journal of Dermatology*, Vol. 149, 2003, pp. 53-6.

[181] Callahan R, Smith GH, “MMTV-induced mammary tumorigenesis: gene discovery, progression to malignancy and cellular pathways”, *Oncogene*, Vol. 19, n. 8, 2000, pp.992-1001.

[182] Bos JL, “ras oncogenes in human cancer: a review”, *Cancer Research*, Vol. 49, n. 17, 1989, pp. 4682–4689.

[183] Sinn E, Muller W, Pattengale P, Tepler I, Wallace R, Leder P, “Coexpression of MMTV/v-Ha-ras and MMTV/c-myc genes in transgenic mice: synergistic action of oncogenes in vivo”, *Cell*, Vol. 49, n. 4, 1987, pp. 465-475.

[184] Bulte JW, Kraitchman DL, “Iron oxide MR contrast agents for molecular and cellular imaging”, *NMR Biomedicine*, Vol. 17, n. 7, 2004, pp. 484–499.

[185] Lewis JS, Achilefu S, Garbow JR, Laforest R, Welch MJ, “Small animal imaging. Current technology and perspectives for oncological imaging”, *European Journal of Cancer*, Vol. 16, 2002, pp. 2173–2188.

[186] Cahalan MD, Parker I, Wei SH, Miller MJ, “Two-photon tissue imaging: seeing the immune system in a fresh light”, *Nature Reviews in Immunology*, Vol. 2, n. 11, 2002, pp. 872-880.

[187] Morawski AM, Lanza GA, Wickline SA, “Targeted contrast agents for magnetic resonance imaging and ultrasound”, *Current Opinion in Biotechnology*, Vol. 16, n. 1, 2005, pp. 89–92.

[188] de Vries IJ, Lesterhuis WJ, Barentsz JO, Verdijk P, van Krieken JH, Boerman OC, Oyen WJ, Bonenkamp JJ, Boezeman JB, Adema GJ, Bulte JW, Scheenen TW, Punt CJ, Heerschap A, Figdor CG, “Magnetic resonance tracking of DC in melanoma patients for monitoring of cellular therapy”, *Nature Biotechnology*, Vol. 23, no. 11, 2005, pp. 1407-1413.

[189] Lecchi M, Ottobrini L, Martelli C, Del Sole A, Lucignani G, “Instrumentation and probes for molecular and cellular imaging”, *Quarterly Journal of Nuclear Medicine and Molecular Imaging*, Vol. 51, 2007, pp. 111-26.

[190] Kupiec-Weglinski JW, Austyn JM, Morris PJ, “Migration pattern of dendritic cells in the mouse. Traffic from the blood, and T cell-dependent and –independent entry to lymphoid tissue”, *Journal of Experimental Medicine*, Vol. 167, 1988, pp. 632-645.

[191] Morse MA, Coleman RE, Akabani G, Niehaus N, Coleman D, Lyerly HK, “Migration of human dendritic cells after injection in patients with metastatic malignancies”, *Cancer Research*, Vol. 59, n. 1, 1999, pp. 56-8.

[192] Baumjohann D, Lutz MB, “Non-invasive imaging of dendritic cell migration in vivo*” Immunobiology*, Vol. 211, 2006, pp. 587–597.

[193] Awasthi S, Awasthi V, Magee DM, Coalson JJ, “Efficacy of antigen 2/proline-rich antigen cDNA-transfected dendritic cells in immunization of mice against Coccidioides posadasii”, *Journal of Immunology*, Vol. 175, n. 6, 2005, pp. 3900-3906.

[194] Olasz EB, Lang L, Seidel J, Green MV, Eckelman WC, Katz SI, “Fluorine-18 labeled mouse bone marrow-derived dendritic cells can be detected in vivo by high resolution projection imaging”, *Journal of Immunological Methods*, Vol. 260, n. 2002; 260, 137-48.

[195] Dodd SJ, Williams M, Suhan JP, Williams DS, Koretsky AP, Ho C, “Detection of single mammalian cells by high-resolution magnetic resonance imaging”, *Biophysical Journal* Vol. 76, 1999, pp. 103-109

[196] Kobukai S, Baheza R, Cobb JG, Virostko J, Xie J, Gillman A, Koktysh D, Kerns D, Does M, Gore JC, Pham W, “Magnetic nanoparticles for imaging dendritic cells”, *Magnetic Resonance Medicine*, Vol. 63, n. 5, 2010, pp. 1383-90.

[197] Baumjohann D, Hess A, Budinsky L, Brune K, Schuler G, Lutz MB, “In vivo magnetic resonance imaging of dendritic cell migration into the draining lymph nodes of mice”, *European Journal of Immunology*, Vol. 36, 2006, pp. 2544-2555.

[198] Quillien V, Moisan A, Carsin A, Lesimple T, Lefeuvre C, Adamski H, Bertho N, Devillers A, Leberre C, Toujas L, “Biodistribution of radiolabelled human dendritic cells injected by various routes”, *European Journal of Nuclear Medicine and Molecular Imaging* Vol. 32, no. 7, 2005, pp. 731-41.

[199] Lanzavecchia A, Sallusto F, “The instructive role of dendritic cells on T cell responses: lineages, plasticity and kinetics”, *Current Opinion in Immunology*, Vol. 13, 2001, pp. 291-298.

[200] Verdijk P, Scheenen TWJ, Lesterhuis WJ, Gambarota G, Veltien AA, Walczak P, Scharenborg NM, Bulte JWM, Punt CJA, Heerschap A, Figdor CG, de Vries IJM, “Sensitivity of magnetic resonance imaging of dendritic cells for in vivo tracking of cellular cancer vaccines”, International Journal of Cancer, Vol. 120, 2006, pp. 978–984.

[201] Qiu J, Li GW, Sui YF, Song HP, Si SY, Ge W, “Heat-shocked tumor cell lysate-pulsed dendritic cells induce effective anti-tumor immune response in vivo”, *World Journal of Gastroenterology,* Vol. 12, no. 3, 2006, pp. 473-478.

[202] Langenkamp a, Messi M, Lanzavecchia A, Sallusto F, “Kinetics of dendritic cell activation: impact on priming of Th1, Th2 and nonpolarized T cells”, *Nature*, Vol. 1, n. 4, 2000, pp. 311-316.

[203] Bernhard H, Disis ML, Heimfeld S, “Generation of immunostimulatory dendritic cells from human CD34+ hematopoietic progenitor cells of the bone marrow and peripheral blood”, *Cancer Research*, Vol. 55, 1995, pp. 1099-104.

[204] Van den Broeck, Derore A, Simoens P, “Anatomy and nomenclature of murine lymph nodes: Descriptive study and nomenclatory standardization in BALB/cAnNCrl mice”, *Journal of Immunological Methods*, Vol. 312, 2006, pp. 12–19.